UNIVERSIDAD MIGUEL HERNÁNDEZ DE ELCHE

DEPARTMENT OF SCIENCE OF MATERIALS, OPTICS AND ELECTRONIC TECHNOLOGY

Realistic Acoustic Prediction Models to Efficiently Design Higher Layer Protocols in Underwater Wireless Sensor Networks

Thesis submitted in partial fulfillment of the requirements for the degree of Doctor of Philosophy in Computer Science

By

Jesús Antonio Llor Sirvent

Ph.D. Advisors:

Manuel Pérez Malumbres

Milica Stojanovic

Elche, Spain 2012

D. MANUEL PÉREZ MALUMBRES, Catedrático de Universidad de la Universidad Miguel Hernández y Ms. MILICA STOJANOVIC, Associate Professor at Northeastern University and Visiting Scientist at Massachusetts Institute of Technology,

CERTIFICAN:

Que la presente memoria *Realistic Acoustic Prediction Models to Efficiently Design Higher Layer Protocols in Underwater Wireless Sensor Networks,* ha sido realizada bajo su dirección, en el Departamento de Ciencia de Materiales, Óptica y Tecnología Electrónica de la Universidad Miguel Hernández, por el Ingeniero D. JESÚS ANTONIO LLOR SIRVENT, y constituye su tesis para optar al grado de Doctor.

Para que conste en complimiento de la legislación vigente, autorizan la presentación de la referida tesis doctoral ante la Comisión de Doctorado de la Universidad Miguel Hernández, firmando el presente certificado.

D. MANUEL PÉREZ MALUMBRES, Catedrático de Universidad de la Universidad Miguel Hernández and Ms. MILICA STOJANOVIC, Associate Professor at Northeastern University and Visiting Scientist at Massachusetts Institute of Technology,

CERTIFY:

That the present thesis, *Underwater Wireless Sensor Network: Realistic Acoustic Prediction Models for Network Planning*, has been written under their supervision, at the Department of Science of Materials, Optics and Electric Technology of the Miguel Hernández University of Elche, by the Engineer D. JESÚS ANTONIO LLOR SIRVENT, and that represents his thesis to apply for the degree of Doctor of Philosophy.

In compliance with current regulations, they authorize the presentation of this thesis to the Ph.D. Commission at the Miguel Hernández University by signing this certification.

Elche, 30 de Marzo de 2012

Fdo. Manuel Pérez Malumbres　　　　Fdo. Milica Stojanovic

Dña. JULIA ARIAS RODRIGUEZ, Profesora Titular de Universidad de la Universidad Miguel Hernández y directora del Departamento de Ciencia de Materiales, Óptica y Tecnología Electrónica de la Universidad Miguel Hernández,

CERTIFICA:

Que la presente memoria *Realistic Acoustic Prediction Models to Efficiently Design Higher Layer Protocols in Underwater Wireless Sensor Networks*, realizada bajo la dirección de D. MANUEL PÉREZ MALUMBRES y Ms. MILICA STOJANOVIC, en el Departamento de Ciencia de Materiales, Óptica y Tecnología Electrónica de la Universidad Miguel Hernández, por el Ingeniero D. JESÚS ANTONIO LLOR SIRVENT, constituye su tesis para optar al grado de Doctor.

Para que conste en complimiento de la legislación vigente, autoriza la presentación de la referida tesis doctoral ante la Comisión de Doctorado de la Universidad Miguel Hernández, firmando el presente certificado.

D. JULIA ARIAS RODRÍGUEZ, Profesora Titular de Universidad Miguel Hernández University and Director of the Department of Science of Materials, Optics and Electric Technology of Miguel Hernández University of Elche,

CERTIFIES:

That the present thesis, *Underwater Wireless Sensor Network: Realistic Acoustic Prediction Models for Network Planning,* has been written under the supervision of D. MANUEL PÉREZ MALUMBRES y Ms. MILICA STOJANOVIC, at the Department of Science of Materials, Optics and Electric Technology of the Miguel Hernández University of Elche, by the Engineer D. JESÚS ANTONIO LLOR SIRVENT, and that represents his thesis to apply for the degree of Doctor of Philosophy

In compliance with current regulations, they authorize the presentation of this thesis to the Ph.D. Commission at the Miguel Hernández University by signing this certification.

Elche, 30 de Marzo de 2012

Fdo. Julia Arias Rodríguez

For my love, Angela.

Acknowledgments

There are many things in my life that have led me into a career in research, many turns and changes in the directions that finally brought me to Elche to the Miguel Hernandez University where I began my Ph.D. program.

I would like to thank all the people who have encouraged me to excel here and the ones who have traveled the path alongside me.

First of all, I would like to thank my parents for cheering me at the beginning of studying, and for providing me all the necessary material to develop my skills, including my first computer that aroused my interest in the computing world.

During my student years in elementary school, high school and the university, I have learned important things from many teachers and professors in many subjects, but I would like to highlight Professor Juan Manuel Garcia Chamizo for believing that I was able to become a scientist and lending me his time for my preparation to apply for grants.

I am very grateful to have shared during my Ph.D. preparation in Elche all the experiences with my research group partners (GATCOM), where I was accepted like one more right upon my arrival: Dr. Otoniel Lopez, Miguel Martinez Rach, Pablo Piñol, Dr. Hector Migallon and Dr. Vicente Galiano. Additionally, a special mention for my office partner, Adrian Cendrán, the group's laboratory assistant.

During 2010, I performed a six-month stay at Northeastern University in Boston under the supervision of MIT Scientist and IEEE Fellow Professor Milica Stojanovic; special thanks to her and the group at ECE Lab for accepting me and letting me experience one of the most wonderful times of my life.

This thesis has not been an isolated job. I would like to thank my Director, Professor Manuel Malumbres, for guiding me along the way these years, supporting me and making things much easier, for trusting me from the very first day and encouraging me right up until the last one; I will never forget these years.

I do not want to forget my undergraduate friends Pedro and Alex because there is strength in numbers and together we progressed faster than we would have ever done alone.

I also want to thank my family members; my father Jesús, my mother Paqui and my brother Jaime, who made receiving a good education possible, and allowing me to have the chance to decide what I wanted to do in life. Thanks to my girlfriend Angela, because she has always been at my side and has shared both the good and the trying moments, both close or many miles away.

Finally, I offer my regards to all the people I have met throughout my Ph.D. adventure, many friends and colleagues who go unmentioned but who have supported me all this time; the G group, the ZOO people, all the people at San Francisco Church in Elda. Thanks to everyone …

Jesus Llor
Elche, 2012

Abstract

The study of Underwater Wireless Sensor Networks (UWSNs) as a research field has grown significantly in recent years, offering a multitude of proposals for resolving communication between nodes and protocols for information exchange networks. Acoustics has been used by nature for many millennia to communicate as a language in underwater environments; for instance, dolphins and whales are able to use it for sending information between their groups.

Wireless sensor networks have been proposed for deployment in underwater environments where many applications, such as aquiculture, pollution monitoring, offshore exploration, etc., could benefit from this technology. Despite having a very similar functionality, Underwater Wireless Sensor Networks exhibit several architectural differences with respect to terrestrial ones, which are mainly due to transmission medium characteristics (sea water) and the signal employed to transmit data (acoustic ultrasound signals).

Then, the design of appropriate network architecture for UWSNs is seriously made difficult by the communication systems conditions and, as a consequence, what is valid for terrestrial WSNs is perhaps not valid for UWSNs. So, a general review of the overall network architecture is required in order to supply appropriate network service for the demanding applications in such a trying submarine communication environment.

Propagation conditions in an underwater acoustic channel are known to vary in time, causing the received signal strength to deviate from the nominal value predicted by a Deterministic Propagation Model (DPM). To facilitate large-scale system design under such conditions (for instance power allocation), we develop a Statistical Propagation Model (SPM) in which the transmission loss is treated as a random variable.

By repetitive computation of an acoustic field using a ray tracing tool (DPM) for a set of varying environmental conditions (surface height, wave activity, small displacements of a transmitter and a receiver around nominal locations), an ensemble of transmission losses is compiled which is then used to infer the statistical model parameters.

A reasonable agreement is found with log-normal distribution, whose mean obeys a log-distance increase, and whose variance appears to be constant for a certain range of inter-node distances in a given deployment location. A statistical prediction model is deemed useful for higher-level system planning where simulation is needed to assess the performance of candidate network protocols under various resource allocation policies, i.e. to determine the transmitting power and bandwidth allocation necessary to achieve a desired level of performance (connectivity, throughput, reliability, etc.).

Resumen

Las tecnologías de redes inalámbricas han experimentado un considerable desarrollo en los últimos quince años, no sólo en las áreas de la estandarización sino también en el despliegue y la comercialización de dispositivos, servicios y aplicaciones. Entre esta cantidad de productos inalámbricos, las redes de sensores inalámbricos están demostrando un auge increíble, siendo una de las áreas tecnológicas con el mayor desarrollo científico e industrial. Recientemente, se han propuesto redes de sensores inalámbricos para su despliegue en ambientes subacuáticos, donde aplicaciones como la acuicultura, la monitorización de la contaminación marina y la explotación del litoral podrían beneficiarse de esta tecnología.

A pesar de tener una funcionalidad muy similar, las redes de sensores inalámbricas subacuáticas (Underwater Wireless Sensor Networks UWSNs) exhiben varias diferencias arquitectónicas con respecto a las terrestres, que son debidas a las características del medio de transmisión (agua de mar) y a la señal empleada para transmitir los datos (señales acústicas).

Básicamente, una UWSN está formada por varios nodos que cooperan entre sí para establecer y mantener la red a través del uso de enlaces acústicos bidireccionales. Cada nodo puede enviar o recibir mensajes desde o hacia otros nodos de la red, y también remitir mensajes a los destinatarios alejados en caso de redes multisalto (multi-hop). La manera más común de enviar datos en ambientes subacuáticos es por medio de señales acústicas, como lo hacen los delfines y las ballenas para comunicarse.

El principal objetivo de esta tesis ha sido el estudio de modelos de propagación realistas y su implementación en un simulador desarrollando las principales capas del modelo OSI. Para ello se ha utilizado la plataforma OPNET como base del simulador, una conexión con el programa MATLAB para conectar con bases de datos globales del NOAA (National Oceanographic and Atmospheric Association) y del GEBCO (General Bathymetry Chart of the Oceans) para a continuación llamar a la herramienta de trazado de rayos Bellhop. Además se han implementado prolocolos MAC y Routing. Todo ello con el fin de obtener un modelo de canal que se ajuste lo más fielmente posible a la realidad del medio acuático.

Para obtener un modelo acústico realista y computacionalmente abordable por los ordenadores de hoy en día se ha realizado un modelo estadístico basado en un Modelo de Propagación Determinista (DPM) en el que se calcula la intensidad de la señal recibida, obteniendo un valor nominal y una desviación estándar alrededor de este valor. Estos experimentos se realizan cambiando un conjunto de condiciones ambientales (altura de la superficie, actividad de las olas, pequeños desplazamientos de emisor y receptor alrededor de una zona), como resultado un conjunto de valores de atenuación de la señal es compilado y procesado de modo que se pueda inferir los parámetros del modelo estadístico de propagación (SPM).

Estudios recientes apuntan a que la variación de la señal obedece a una distribución log-normal, cuya media responde a un aumento respecto a la distancia del nodo emisor, y cuya variación parece ser constante para un cierto rango de distancias entre nodos en una ubicación de implementación dado. Un modelo de predicción estadístico se considera útil para la planificación de diseño de capas de nivel superior, donde la simulación es necesaria para evaluar el rendimiento de protocolos de red en las diferentes políticas de asignación de recursos, es decir, para determinar la potencia de transmisión y la asignación de ancho de banda necesario para alcanzar un nivel de rendimiento deseado (conectividad, fiabilidad, escalabilidad, etc.).

Contents

List of Figures

List of Tables

Chapter 1
Motivation, Objectives and Organization of the Thesis

In this chapter, wireless acoustic underwater networks are introduced, showing the applications of this emerging technology. Also, we introduce the proposed research goals and the structure of this document.

1.1 Introduction & Motivation

The study of Underwater Wireless Sensor Networks (UWSN) as a research field has grown significantly in recent years, offering a multitude of proposals to resolve communication between nodes and protocols for information exchange networks. Acoustics has been used by nature for many millennia to communicate as a language in the underwater environment; for instance, dolphins and whales are able to use it to send information between their groups. The first reference to underwater sound propagation can be found in what Leonardo Da Vinci wrote in 1490: "If you cause your ship to stop and place the head of a long tube in the water and place the outer extremity to your ear, you will hear ships at a great distance from you".

Years later, in 1826, the first scientific studies were done by picking real data measures [11]. The physicist Jean-Daniel Colladon and his partner Charles-Francois Sturm, a mathematician, made the first recorded attempt at Lake Geneva, Switzerland, to find out the speed of sound in water.

After experimenting with an underwater bell and ignition from gunpowder on a first boat, the sound of the bell and flash from the gunpowder were observed 10 miles away on a second boat. With this collection of data of the time between the gunpowder flash and the reception of the sound reaching the second boat, they were able to establish a pretty accurate value for the speed of sound in water, tested by this empirical method.

In the early XX century, in 1906, the first sonar type was developed for military purposes by Lewis Nixon; there was great interest in this technology during

World War I so as to be able to detect submarines. It was in 1915, when the "echo location to detect submarines", was released by physicist Paul Langévin and engineer Constantine Chilowski, a device capable of detecting submarines using the piezoelectric properties of quartz. It was not useful during the war as it arrived too late, but it established the roots for upcoming designs for sonar devices.

The first targets where the development of underwater sound technology was involved were to determine the distance to shore or to other ships. After experimenting, researchers quickly discovered that by pointing the sound device down towards the seafloor, the depth could also be collected with sufficient precision. Then, by picking a lot of values it was used for new purposes, like measuring ocean relief (bathymetry), seafloor shape registering, searching for geological resources (oil, gas, etc.), detecting and tracking fish banks, submarine archaeology, etc.

The main underwater acoustic applications were mainly used for seafloor exploration, fishing with sonar devices. In the 1990s, researchers became aware of a new feature applicable to underwater communications; multipoint connections could be capable of translating the networked communication technology to the underwater environment. One of the earliest deployments was the Autonomous Oceanographic Surveillance Network (AOSN), supported by the US Office of Naval Research (ONR) [13]. It calls for a system of moorings, surface buoys, underwater sensor nodes and Autonomous Underwater Vehicles (AUVs) to coordinate their sampling via an acoustic telemetry network.

Meanwhile, sensor network technology in the terrestrial environment have experienced considerable development in the past fifteen years, and not only in standardization areas but also in market deployment of several devices, services and applications. Among these wireless products, wireless sensor networks are exhibiting an incredible boom, being one of the technological areas with the greatest scientific and industrial development growth.

The interest and opportunity for working on wireless sensor network (WSN) technologies is endorsed by (a) technological indicators like the ones published by MIT (Massachusetts Institute of Technology) in 2003 [61], where wireless sensor network technology was defined as one of the 10 technologies that will change the world, and (b) economic and market forecasts published by different economic magazines like [45], where investment in WSN ZigBee technology was estimated to be over 3.5 Billion dollars during 2007.

Recently, wireless sensor networks have been proposed for deployment in underwater environments where many applications, such as aquiculture, pollution monitoring, offshore exploration, etc., could benefit from this technology [12]. Despite having a very similar functionality, Underwater Wireless Sensor Networks (UWSNs) exhibit several architectural differences with respect to terrestrial ones, which are mainly due to the transmission medium characteristics (sea water) and the signal employed to transmit data (acoustic ultrasound signals) [4].

Then, the design of appropriate network architecture for UWSNs is seriously made difficult by the communication systems conditions and, as a consequence, what works for terrestrial WSNs might not be not valid for UWSNs. So, a general review of the overall network architecture is required in order to supply appropriate network service for the demanding applications in such a trying submarine communication environment

Major challenges in the design of underwater acoustic networks are:

- Battery power is limited and batteries cannot normally be recharged because solar energy cannot be exploited.
- The available bandwidth is severely limited.
- The channel suffers from long and variable propagation delays, multi-path and fading problems.
- Bit error rates are typically very high.
- Underwater sensors are prone to frequent failures because of fouling, corrosion, etc.

The drawbacks found in the development of UWSN motivates the need to describe the characteristics of the underwater environment affecting the transmission, propagation speed of sound, ocean waves effect, especially in shallow water, the influence of the nodes depth, the seafloor and obstacles in the area. In this thesis, we aim tackle these concerns by modeling the acoustic channel. It is necessary to create a realistic prediction model and incorporate it in a framework that by accurately defining the underwater environment allows, evaluating the performance of higher layer protocols with reliable results.

In this manner, we can design a cross layer framework to adapt in the closest approach to underwater scenarios to obtain not only the best performance of the network resources (throughput, delay, collisions…) but to also achieve energy efficient consumption which is a critical factor in the design of wireless sensors.

1.2 Thesis Objectives

The main purpose of this research is to develop a simulation framework to be able to evaluate underwater wireless sensor networks with a realistic approach, so that the results can be inferred into real scenario networks with the same performance. The specific objectives are detailed as follows:

- Study the state of the art in UWSNs, the means of transmission in the underwater channel, the model layers: physical, network, routing and application.
- Analyze the behavior of underwater physical parameters in the channel response.
- Analyze acoustic propagation models in underwater network scenarios.
- Develop a realistic simulation framework that includes results found in previous studies.
- Performance evaluation of higher layer protocols under the proposed simulation framework.

1.3 Organization of the Thesis

After the introduction and motivation of this work and the definition of its main objectives, the remainder of the document is organized as follows:

In Chapter 2, we study the state of art and the main issues in the design of efficient underwater wireless sensor networks. Following a bottom-to-top approach, we will review the network architecture, highlighting some critical design parameters at each of the different network layers, and how to overcome the limitations and problems introduced by UWSN environments.

Chapter 3 introduces the simulator framework for underwater acoustic networks and explains the development and steps it follows to work a solution out. Some test examples are presented to validate its results and verify its correct operation.

Afterwards, in Chapter 4, along with the study of a deterministic prediction model, we propose a statistical sound propagation model (prediction model) that agrees with two major requirements of protocol modeling, accuracy and reduced complexity. The capability to allocate the power required to transmit a signal is one of the major features of this model.

Later, in Chapter 5, the evaluation of higher layer protocols comes up with the importance of using a proper propagation model and precise definition of the environment to validate these protocols.

Finally, Chapter 6 presents the conclusions and publications related to the Thesis.

Chapter 2
Underwater Wireless Sensor Networks

This chapter provides a description of the state of the art in the field of underwater communications. We begin with a description of wireless sensor networks, and we define underwater sensor networks to establish the research scenario. Then a whole revision of the different layers of the OSI model is done, highlighting the most outstanding and recent developments in each one of them.

Before taking a closer look at UWSN a brief summary of the wireless sensor networks is introduced.

In the 1990s, the networks transformed the way people and organizations exchange information and coordinate their activities. The latest technological discoveries have brought to reality the development of distributed mechanisms, small, cheap, with light consumption, and moreover capable of processing information and transmitting wirelessly. The availability of micro sensors and wireless communications allows developing networks of sensors for a wide range of applications.

A challenge to overcome is the variability of this new environment. While a good distributed system is developed with reliability as a main feature, these new applications present a level of randomness beyond the usual.

Sensor networks can be considered an autonomous network, built by small intelligent nodes where they self-organize and manage the network and collaborate and work together to measure a physical parameter of the environment such as the temperature, the pressure, the humidity, pollution, etc. At the same time, they process the information and make it travel through the network until a sink node where it is stored or delivered through a wide area network (WAN) connection towards the control data center.

A wireless sensor network (WSN) consists of a number of nodes that are distributed throughout the network scenario to get measures of the environmental parameters to be monitored. Node positioning does not need to be predetermined and can assume a random deployment. Furthermore, it can be defined that nodes are static, or with low, medium or high mobility, depending on the particular application and the network purpose.

Therefore, typical ad-hoc network discovery techniques are required for the network's construction. However, WSNs are not exactly ad-hoc networks, so these techniques can be the starting point but it is necessary to go one step further, to answer a more detailed problem. The main differences with ad-hoc networks are:

- The number of nodes in a WSN can be several times bigger (thousands of nodes). And in a given area, the number of nodes can be very high (high density).
- A node has limited resources and is susceptible to failures. Only by getting all the nodes to cooperate and coordinate can the network work properly.
- A sensor node typically uses broadcast communication with its environment neighbors while the majority of ad-hoc networks are based on point-to-point communications.
- A sensor node has limited both processing power and memory capacity, and it uses battery power to operate.
- The sensor nodes usually do not have a global identifier, as is an IP address, because of the computational and memory overhead that this feature introduces in a network with a high number of sensor nodes.

As an overview, WSN consists of a high number of devices that are densely spread over an area. It is based in a multi-hop ad-hoc network, able to provide communication among two network nodes without relying on external infrastructure. One of the distinctive features is the type of information generated and how it is generated. Usually, we consider two occurrences: (a) In the first one, the network notifies about a happening fact; (b) or the user requests information about what is happening. In the second possibility, the usual thing in a WSN is that the user is interested in not focusing on the current state of one of the nodes in question, but about the state of one parameter within a specific area (for instance, the area under study that has reached a certain threshold). Because of this, there is a need for introducing a new notion, information collection. If all the nodes that are over a threshold transmit to the user, the network will probably get busy and disable (thousands of nodes with low processing capability) [2]. So, is necessary developing processing techniques to manage the information in traffic. In this way, the information is processed and added as it travels through the network to the destination, thereby reducing the network traffic load

2.1 Why Acoustic Sensor Networks

Basically, an UWSN is formed by the cooperation between several nodes that establish and maintain a network through the use of bidirectional acoustic links. Every node is able to send/receive messages to/from other nodes in the network, and also to forward messages to remote destinations in the case of multi-hop networks. The most common way to send data in underwater environments is by means of acoustic signals, just like dolphins and whales do for communicating between themselves. Radio frequency signals have serious problems propagating in sea water, being operative for radio-frequency only at very short ranges (up to 10 meters) and with low-bandwidth modems (tens of Kbps) [47].When using optical signals, the light is strongly scattered and absorbed in underwater scenarios, so only in very clear water conditions (often very deep) does the range extend to 100 meters with high bandwidth modems (several Mbps) and blue-green wavelengths.

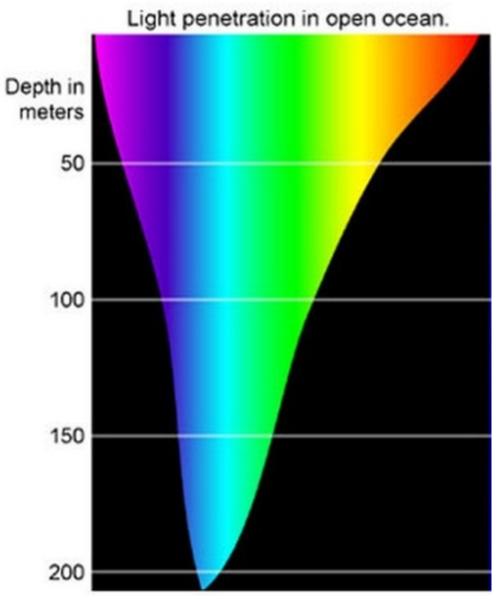

Figure 2.1 This diagram offers a basic illustration of the depth at which different colors of light penetrate ocean waters. Water absorbs warm colors like reds and oranges and scatters cooler colors

Since acoustic signals are mainly used in UWSNs, it is necessary to take into account the main aspects involved in the propagation of acoustic signals in underwater environments, including: (a) the underwater sound propagation speed is around 1500 m/s (5 orders of magnitude slower than radio signals), with communication links prone to large and variable propagation delays and relatively large motion-induced Doppler effects; (b) phase and magnitude fluctuations lead to higher bit error rates compared with radio channels' behavior, with mandatory use of forward error correction codes (FEC); (c) as the frequency increases, the attenuation observed in the acoustic channel also increases, and this is a serious bandwidth constraint; (d) multipath interference in underwater acoustic communications is severe due mainly to surface waves or vessel activity, and this is a serious problem for attaining good bandwidth efficiency.

2.2 Acoustic Wave Theory Propagation

The theory of sound propagation is that according to the description by Urick [60], a regular molecular movement in an elastic substance that propagates to adjacent particles. A sound wave can be considered the mechanical energy transmitted by the source from particle to particle, propagated through the ocean at the speed of sound. There are many environmental factors that have an impact on acoustic transmission in underwater acoustic communication [53]:

- Both the surface and seafloor affect the transmission. The sea surface produces an almost perfect reflection of the acoustic waves due to different impedance from the terrestrial to underwater ambient. However, surface waves are not flat. Moreover, the shape and sediments of the seabed are also variable.

- The sea is not a homogenous environment; its temperature and salinity depend on the location in the world, the season and depth.

- The sea is not an isotropic environment due to seawater pressure and density.

Moreover, there are also other problems to take into consideration when making an underwater transmission, such as sounds produced by marine organisms, ships, surface noise, rain noise, and noise due to hydrostatic pressure changes.

One of the main factors is the speed of sound; depending on the changes in salinity, temperature and pressure, the value will range from 1450 to 1540 m/s.

2.2.1 Sound Speed Propagation

The propagation of sound under water depends on the characteristics of the column of water passing through the sound; and any environment change can make sound travel by another route, or another speed, producing delays, taking also into account that the path and the absorption of the sound wave depends on the signal frequency.

The formula proposed in [60] describes the speed of sound propagation:

$$C = 1449 + 4.6\,t + 0.055t^2 + 0.003\,t^3 + (1.39 - 0.012)(S - 35) + 0.017d \qquad (2\text{-}1)$$

Where:

t: water temperature (in degrees Celsius).
S: water salinity (in parts per million).
d: node depth (in meters).

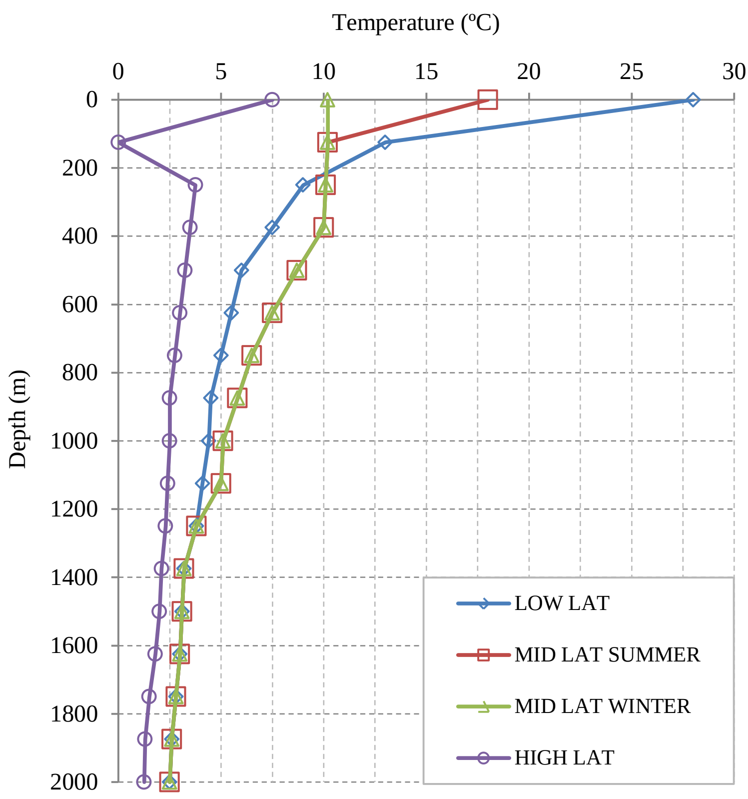

Figure 2.2 Temperature variation depending on latitude and season

Depth (m)	Salinity (ppm)
0	37.45
50	36.02
100	35.34
500	35.11
1000	34.90
1500	34.05

Table 2.1 Salinity depending on the water depth

2.2.2 Transmission Loss

The transmission loss (TL) is defined as the decrease in sound intensity through the path from of sender to receiver. Diverse empirical expressions have been developed to measure transmission loss. Thorp's formula defines the signal transmission loss as:

$$\propto = \frac{0.11\, f^2}{1+f^2} + \frac{44\, f^2}{4100+f^2}\,[\mathrm{db/Km}]$$

$$SS \; = 20\log r \qquad (2\text{-}2)$$

$$TL = SS + \propto \mathrm{x}\; 10^{-3}$$

Where f is frequency in kHz, r is the range in meters; SS is the spherical spreading factor and α is the attenuation factor. A more accurate expression for the attenuation factor was then presented, the one proposed in Thorp's formula in [6] :

$$\propto = \frac{0.11\, f^2}{1+f^2} + \frac{44\, f^2}{4100+f^2} + \; 2.75 \;\mathrm{x}\; 10^{-4} f^2 + \; 0.003 \qquad (2\text{-}3)$$

Since acoustic signals are mainly used in UWSNs, it is necessary to take into account the main aspects involved in the propagation of acoustic signals in underwater environments, including: (a) the underwater propagation speed of sound is around 1500 m/s (5 orders of magnitude slower than the speed of light), and so communication links will suffer from large and variable propagation delays and relatively large motion-induced Doppler effects; (b) phase and magnitude fluctuations lead to higher bit error rates compared with radio channels' behavior; this makes the use of forward error correction codes necessary; (c) as the frequency increases, the attenuation observed in the acoustic channel also increases, which is a serious bandwidth constraint; (d) multipath interference in underwater acoustic communications is severe due mainly to surface waves or vessel activity, which are an important issue for attaining good bandwidth efficiency.

2.2.3 Noise

Several works in the literature propose models for an acoustic underwater link, taking into account environment parameters like salinity degree, temperature, depth, environmental interference, etc. Other physical aspects in the ocean like noise in the medium [10], wind, thermal noise, turbulence and ship noise are included in these formulas, depending on the frequency and these factors:

$$\begin{aligned} 10\log N_t(f) &= 17 - 30\log f \\ 10\log N_s(f) &= 40 + 20\,(s - 0.5) + 26\log f \\ 10\log N_w(f) &= 50 + 7.5\,w^{\frac{1}{2}} + 20\log f - 40\log(f + 0.4) \\ 10\log N_{th}(f) &= -15 + 20\log f \end{aligned} \qquad (2\text{-}4)$$

Where N_t is the noise due to turbulence, N_s is the noise due to shipping, N_w is the noise due to wind, and N_{th} represents thermal noise. The overall noise power spectral density for a given frequency f is then:

$$N(f) = N_t(f) + N_s(f) + N_w(f) + N_{th}(f) \qquad (2\text{-}5)$$

While underwater networking research has followed the traditional layered approach so far, it is an increasingly accepted opinion in the wireless networking community that improved network efficiency, especially in critical environments, can be obtained with a cross-layer design approach. These techniques will entail a joint design of different network functionalities, from modem design to MAC and routing, from channel coding and modulation to source compression and transport layer, with the objective of overcoming the shortcomings of a layered approach that lacks information sharing across protocol layers, forcing the network to operate in a suboptimal mode. Hence, for the sake of clarity, we present the challenges associated with underwater sensor networks following the traditional layered approach, we believe that the underwater environment particularly requires cross-layer design solutions that enable more efficient use of the scarce resources available.

However, although we advocate integrating functionalities to improve network performance and avoid duplication of functions by means of cross-layer design, it is important to consider ease of design by following a modular design approach.

This also allows improving and upgrading particular functionalities without the need of re-designing the entire communication system.

2.3 Propagation Delay Models

Simulating UWSN communications requires modeling the acoustic wave's propagation while a node tries to transmit data to another. There are several models proposed in the literature, from the simplest ones based on the sound propagation theory, to more elaborate and complex models based on the physics of acoustic sound propagation. In this section, we will describe several acoustic propagation models that represent different approaches to the same problem but with different degrees of complexity/accuracy. We will present them in order of increasing complexity, so for each approach we will know how propagation acoustics are predicted and what parameters are taken into account for that purpose.

2.3.1 Urick Description and Thorp's Formula

The theory of sound propagation is according to the description by Urick [60], a regular molecular movement in an elastic substance that propagates to adjacent particles. A sound wave can be considered the mechanical energy that is transmitted by the source from particle to particle, being propagated through the ocean at the speed of sound. The empirical formula presented by Thorp [6] is defined as the sound intensity decrease through the path between the source and destination nodes. The absorption coefficient factor α depends on the sound frequency f. The proposed acoustic attenuation expression is represented as follows:

$$A(d,f) = d^k \, \alpha(f)^d \qquad (2\text{-}6)$$

Where:

d: Distance

k: Geometry (k = 1: Cylindrical, k = 2: Spherical)

In the same set of formulas, the definition for power spectral density to calculate the noise in the receiver nodes is also available (See [6] for more details).

2.3.2 Monterrey Miami Parabolic Equation

The Monterey-Miami Parabolic Equation model [50] is used to predict underwater acoustic propagation using a parabolic equation, which is closer to the Helmholtz equation (wave equation) [58]; this equation is based on Fourier analysis. The sound pressure is calculated in small incremental changes in range and depth, forming a grid. It incorporates randomness and wave motion to the approximation using a dynamic propagation loss calculation. The authors show that small changes in depth and node distances can lead to big differences in the path loss as a result of the ocean wave motion impact on acoustic propagation (more details in [66]). The propagation loss formula based on the MMPE model is the following one:

$$PL(t) = m(f, s, d_A, d_B) + w(t) + e() \tag{2-7}$$

Where:

PL(t): propagation loss while transmitting from node A to node B.
m(): propagation loss without random and periodic components; obtained from regression using MMPE data.
f: frequency of transmitted acoustic signals (in kHz).
$\boldsymbol{d_A}$: sender's depth (in meters).
$\boldsymbol{d_B}$: receiver's depth (in meters).
r: horizontal distance between A and B nodes, called range in the MMPE model (in meters).
s: Euclidean distance between A and B nodes (in meters).
w(t): periodic function to approximate signal loss due to wave movement.
e(): signal loss due to random noise or error.

The *m()* function represents the propagation loss provided by the MMPE model. According to the data's logarithmic nature, a nonlinear regression is the best option for providing an approach to the model based on the coefficients supplied by the preliminary model. The proposed expression to calculate this function is the following one:

$$m(f, s, d_A, d_B) = log\left(\left|\frac{\left(\frac{s}{0.914}\right)^{A0} (d_A)^{A9} s^{A7} ((d_A - d_b)^2)^{A10}}{(s * d_B)^{10\ A5}}\right|\right) \tag{2-8}$$

$$+\left(f^2\left(\frac{A1}{1+f^2}+\frac{40}{4100+f^2}+0.00275\right)+0.003\right)*\left(\frac{s}{914}\right)$$
$$+A6*d_B+A8*s$$

The *w()* function considers the movement of a particle that will oscillate around its location in a sinusoidal way [62]. That movement is represented as circular oscillations that reduce their radius as the depth of the particle increases. The length of that radius is dependent on the wave energy and is related to the wave height. Common waves have hundreds of meters of wave length and have an effect up to 50 meters of depth.

For the calculation of the effects of the wave, we will consider:

$$w(t)=h\left(l_w,d_Bt,h_{w,}T_w\right)E(t,T_w) \quad (2\text{-}9)$$

Where:
w(t): periodic function to approximate the lost signal by the wave movement.
h(): scale factor function.
$\boldsymbol{l_W}$: ocean wave length (meters).
$\boldsymbol{d_B}$: depth of the receiver node.
$\boldsymbol{h_W}$: wave height (meters).
$\boldsymbol{T_W}$: wave period (seconds).
E(): function of wave effects in nodes.

This function contains the elements that resembled the node movement, first calculating the scale factor *h()* and then the wave effect in a particular phase of the movement. The scale factor calculation is as follows:

$$h\left(l_w,d_B,t,h_{w,}T_w\right)=\frac{\left(h_w\left(1-\left(\frac{2d_B}{l_w}\right)\right)\right)}{0.5}*\left|sin\left(\frac{2\pi(mod\ T_w)}{T_w}\right)\right| \quad (2\text{-}10)$$

The *e()* function represents a random term to explain background noise. As the number of sound sources is large and undetermined, this random noise follows a Gaussian distribution and is modeled to have a maximum 20 dB at the furthest distance. This function is calculated by the following equation:

$$e()=20\left(\frac{s}{s_{max}}\right)R_N \quad (2\text{-}11)$$

Where:
e(): random noise function.
s: distance between the sender and receiver (in meters).
s_{max}: maximum distance (transmission range).
h_w: wave height (in meters).
R_N: random number, Gaussian distribution centered in 0 and with variance 1.

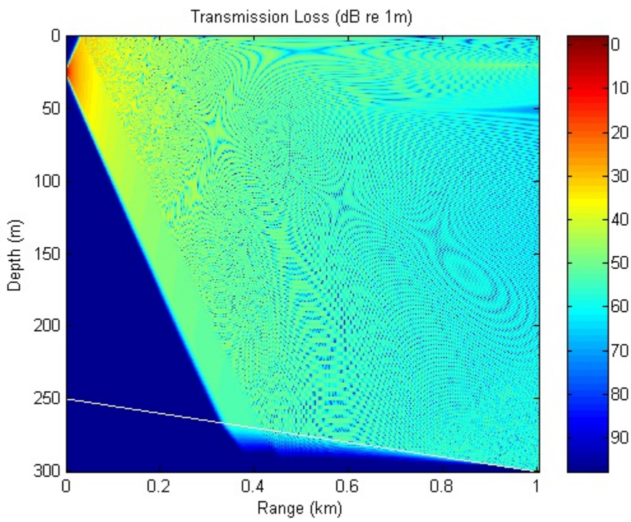

Figure 2.3 MMPE Transmission Loss (db).

2.3.3 Bellhop Ray Tracing Tool

Bellhop Ray Tracing requires the solution of ray equations to determine the ray coordinates of the acoustic signal propagation. Amplitude and acoustic pressure require the solution of dynamic ray equations, which are described in detail in [40]. This tool is integrated with empirical data updated from world databases that measure the sound speed profile (SSP), bathymetry and floor sediment such as the General Bathymetric Chart of the Oceans (GEBCO) and National Oceanic and Atmospheric Administration (NOAA) [18], [33]. The ocean wave motion is also included to calculate the rays' trajectories; so taking into account the type of sediments and the sound speed profile (SSP), this propagation model shows a behavior that it is very close to experimental studies for acoustic propagation in underwater environments (more details can be found in [40], [24]).

For a system with cylindrical symmetry, the ray equations can be written as:

$$\frac{dr}{ds} = c\xi(s) \quad , \quad \frac{d\xi}{ds} = -\frac{1}{c^2}\frac{\vartheta c}{\vartheta r}$$
$$\frac{dz}{ds} = c\zeta(s) \quad , \quad \frac{d\zeta}{ds} = -\frac{1}{c^2}\frac{\partial c}{\partial z} \qquad (2\text{-}12)$$

Where *r(s)* and *z(s)* represent the ray coordinates in cylindrical coordinates and s is the arclength along the ray; the pair *c(s) [ξ (s),ζ(s)]* represents the tangent versor along the ray. Initial conditions for and *r(s)*, and *z(s)*, *ξ(s)* and *ζ(s)* are:

$$r(0) = r_s \quad , \quad z(0) = z_s \quad \xi(0) = \frac{\cos\theta_s}{c_s}, \quad \zeta(0) = \frac{\sin\theta_s}{c_s} \qquad (2\text{-}13)$$

where θ_s represents the launching angle, (r_s, z_s) is the source position, and c_s is the sound speed at the source position. The coordinates are sufficient to obtain the ray travel time:

$$\tau = \int_{\Gamma} \frac{ds}{c(s)} \qquad (2\text{-}14)$$

Which is calculated along the curve [*r(s)*, *z(s)*].

Figure 2.4 shows the ray trajectories drawn by Bellhop to calculate the acoustic signal travel and thus obtain the attenuation at different points on the scenario.

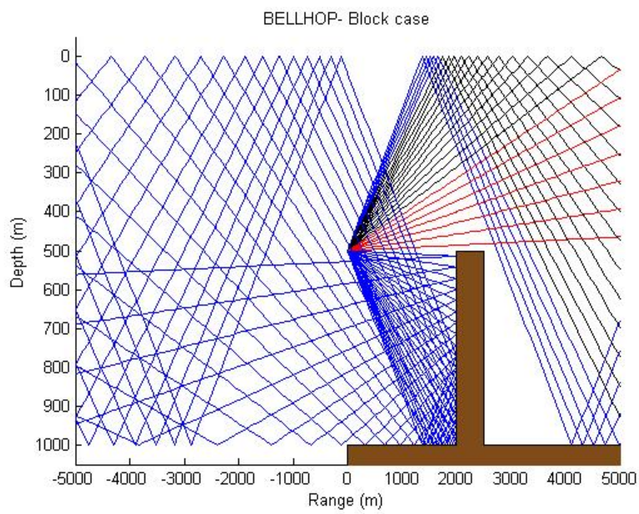

Figure 2.4 Bellhop ray trace

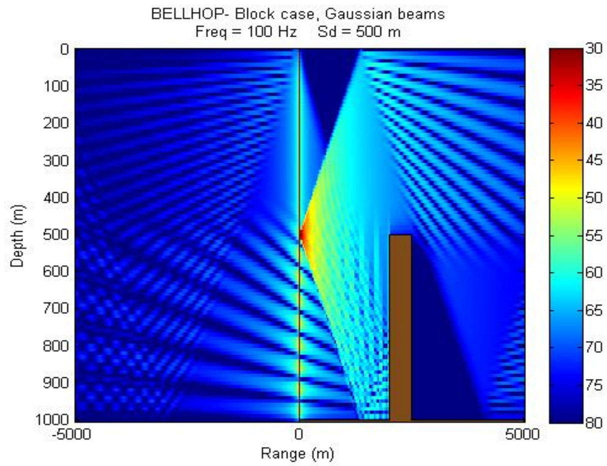

Figure 2.5 Bellhop pressure

Bellhop ray is one of the main tools used in simulation and its veracity towards real data scenario deployment has been tested in several works in different locations, confirming that if a correct definition of the environment is done, the results provided by bellhop are pretty fair to the empirical data collected during experiments.

Some of these studies, including both Bellhop and real data collection scenarios modeling, can be found in [23] where an experiment was realized on the south coast of Portugal, east of Vilamoura, in June 2010. In [5], [20], [37] and [38] to validate the Bellhop model, real measures were done in underwater scenarios located at Pianosa Island in Italy. In [19], the region of Calabria in Italy, a comparison between Bellhop and real measurements were done to evaluate MAC protocols. In [49], a theoretical study of signal propagation in underwater scenarios was found in full agreement with Bellhop simulations and with results obtained from experimental tests performed in the town of Setubal, approximately 50 km south of Lisbon, Portugal.

All the propagation models presented here have been implemented, validated and tested, and some of these results appear next to new experiments and results in subsequent chapters.

2.4 Physical Layer

Due to drawbacks found in the underwater environment, when transmitting acoustic signals (time-varying, multipath, Doppler Effect, etc.), commercial solutions have faced the issue mainly on the use of non-coherent modulation that offers low throughput performance. By the way, the combination of phase coherent modulation and the process for exploiting the spatial multipath diversity offer a more efficient usage of the acoustic channel. These improvements are about to appear in the latest product release in underwater sensor networks; this fact will mean a step forward in the evolution of the amount of data that can be transmitted, and thus an improvement in the network communication performance.

The techniques used to mitigate the effect of multipath can be classified in relation to a couple of aspects: first the signal design, the way in which modulation/detection is implemented; and second, the transmitter receiver/structure, the array processing method election and the equalization method.

Many of the standing systems operate on the vertical or on very short range channels, however current development deployments try to put the eye on the harshly spread horizontal shallow water channels. In the next section we introduce the main signal processing methods [54].

2.4.1 Non-Coherent Modulation

In the early 1990s, many difficulties were found in underwater acoustic channel transmission, so development was focused on non-coherent frequency shift keying (FSK) modulation, because it depends on energy detection. Another reason is that it does no phase tracking, which becomes a hard task when doppler-spread affects the underwater acoustic channel. The goodness of using FSK in the development of underwater networks comes when the multipath does not have an effect on communication, thanks to the time guard insertion in between consecutive pulses. In this way, the ocean wave effects and their variation throughout the communication as the signal travel bouncing between the surface and bottom is cancelled when each subsequent pulse is received.

Likewise, dynamic frequency guards are used to adjust the transmission to the doppler spread in the channel between frequency tones. Nevertheless, solving these matters with low energy power requirement schemes has a direct inversely proportional impact on the bandwidth usage. With such a low performance, this strategy cannot be applied to the deployment of networks where tremendous amounts of communication are established between nodes where data rate requirements are larger.

2.4.2 Coherent Modulation

In order to reach the specifications in terms of throughput that an underwater sensor network requires, coherent modulation techniques have been introduced in recent years. Since digital processing has become a feasible task, full coherent modulation schemes, for instance phase shift keying (PSK) and quadrature amplitude modulation (QAM), have become real solutions to equalize the channel taking advantage of the inter-symbol interference (ISI), despite trying to ignore it or cancel its effect.

Decision-Feedback Equalizers (DFEs) [15] are used to track the complex slow varying channel response in order to provide high throughput when the channel is slowly varying. In contrast, if the channel is varying faster, DFE requires a combination with a Phase Locked Loop (PLL) [55] [16], PLL does estimation and balances for the phase offset in a quick, stable way. The acoustic channel complexity and the time varying impulse responses will lead to the use of Decision-Feedback Equalization and Phase-Locked Loop.

If the system requires an in-between solution within incoherent and full coherent schemes in terms of bandwidth usage, the answer is Differential Phase Shift Keying (DPSK), which encodes the information in relation to previous symbols rather than to an arbitrary fixed reference in the signal phase and may be referred to as a partially coherent modulation. In this way, the mix relieves carrier phase-tracking requirements, despite the fact that there is an increment chance for error over PSK at the same data rate. Table 2.2 compares the progression from non-coherent schemes to coherent ones in time [3].

Type	Year	Rate [kbps]	Band [kHz]	Range (km)[a]
FSK	1984	1-2	5	3_s
PSK	1989	500	125	0.06_d
FSK	1991	1.25	10	2_d
PSK	1993	0.3-0.5	0.3-1	200_d-90_s
PSK	1994	0.02	20	0.9_s
FSK	1997	0.6-2.4	5	10_d-5_s
DPSK	1997	20	10	1_d
PSK	1998	1.67-6.7	2-10	4_d-2_s
16-QAM	2001	40	10	0.3_s

[a] The subscripts *d* and *s* stand for deep and shallow water.

Table 2.2 Evolution of modulation technique

It is remarkable in Table 2.2 that in the first approaches of coherent schemes the achieved bandwidth was very high (bit rate/usage of the bandwidth) towards non-coherent ones; however, they did not overtake incoherent as they had lower performance over long distances in horizontal channels before the inclusion of ISI adjustment through DFE to optimize the channel estimation[56].

Still, the addition of these algorithms to filter the signal is too complex to fit real-time communications because they do not gather real-time constrains. Therefore, methods that are under the optimal filter have to be taken into account, but the limited information provided by the channel impulse response comes up with an error in the estimation, leading to worse performance.

2.4.3 Orthogonal Frequency Division Multiplexing

Another innovative alternative to tackle the issue of underwater communications is the Orthogonal Frequency Division Multiplexing (OFDM) spread spectrum technique that offers worthy efficiency when noise is spread over a larger portion of the available bandwidth. OFDM is also known as multi-carrier modulation, as it transmits signals over multiple sub-carriers simultaneously.

Mainly sub-carriers that involve high SNR are allotted with a higher number of bits, whereas less bits are allotted to sub-carriers experiencing attenuation, according to the concept of bit loading, where the estimation of the channel is required. As the symbol duration for each individual carrier increases, OFDM schemes achieve high spectral efficiency, standing with high performance in harsh multi-path scenarios.

Overall, it is necessary to properly estimate the SNR in the underwater environment to apply the method commented on previously [27]. The way to acquire an accurate enough estimation can be done by performing a high probing rate and/or with large probe packet size, even though it will come up with high overhead, and in the following drain channel capacity and energy.

2.5 Mac Layer

The main task of MAC protocols is to provide efficient and reliable access to the shared physical medium in terms of throughput, delay, error rates and energy consumption. However, due to the different nature of the underwater environment, there are several drawbacks with respect to the suitability of the existing terrestrial MAC solutions for the underwater environment. In fact, channel access control in UWSNs poses additional challenges due to the aforementioned peculiarities in underwater channels [32].

A number of adaptations have been proposed to adopt MACA (Multiple Access with Collision Avoidance) [28], MACAW (Media Access Protocol for Wireless LANs) [7], and FAMA (Floor Acquisition Multiple Access) [17] for underwater networks in [32]. But also new protocols, such as T-Lohi (between handshake and non-handshake) are becoming more popular as they also have a great efficiency in terms of battery use. The performance is one of the main parameters but new alternatives are becoming more popular as they also have a great efficiency in terms of battery use.

Depending on the network deployment and expected traffic pattern, authors have suggested different proposals and techniques, where some of them are just adapted protocols from terrestrial sensor networks. We have organized MAC layer protocols in two groups, depending on the traffic pattern produced by the target applications. The first group represents those MAC protocols that are better fits for managing periodic/continuous traffic patterns and exhibit deterministic channel access behavior. Therefore, the channel access time is bounded to a maximum value and they used to be collision free protocols. The other group of MAC layer protocols is related with random access traffic patterns, where their channel access behavior is non-deterministic, so the channel access is not guaranteed to be granted at a certain period of time due to interferences from neighbor nodes in the form of collisions.

2.5.1 Continuous Traffic

a. CDMA Based

Code Division Multiple Access [57] is robust to frequency selective fading, caused by multipath since it is able to distinguish between signals simultaneously transmitted by multiple devices through codes that spread the user signal over the entire available band. This allows exploiting the time diversity in underwater acoustic channels by leveraging Rake filters [52] at the receiver, so as to compensate for the multipath effect. With this method, CDMA achieves increasing the channel reuse at the same time that it reduces retransmissions of DATA packets, leading to better energy management and throughput improvement.

UW-MAC

In [39], the authors propose a distributed Medium Access Control (MAC) protocol called UW-MAC for UWSNs. UW-MAC is a transmitter based CDMA scheme that incorporates a novel closed-loop distributed algorithm to set the optimal transmit power and code length to minimize the near-far effect. UW-MAC leverages a multi-user detector on resource-rich devices such as surface stations, gateways and vehicles, and a single-user detector on low-end sensors. UW-MAC aims to achieve a threefold objective, i.e., guarantee (a) high network throughput, (b) low access delay, and (c) low energy consumption.

The distributed power and code self-assignment problem to minimize the near-far effect is also formulated, and a low-complexity yet optimal solution is proposed. UW-MAC is the first protocol that leverages CDMA properties to achieve multiple access to the scarce underwater bandwidth, while existing papers analyzed CDMA only from a physical layer perspective. Experiments show that UW-MAC outperforms existing MAC protocols tuned for the underwater environment under all considered network architecture scenarios and simulation settings.

b. TDMA Based

Signals can be deterministically separated in time (Time Division Multiple Access, TDMA). Users take turns accessing the medium so that signals do not overlap in time, and therefore, interference is avoided.

TDMA can be more flexible, but requires synchronization among all users to make sure they access disjointed time slots. Many schemes and protocols are based on such an underlying time-division structure, which, however, needs some coordination and some guard times to compensate for inconsistencies in dealing with propagation delays.

Multi-Cluster

In [46], a Multi-Cluster protocol is proposed for networks with autonomous underwater vehicles. The proposed scheme is based on organizing the network in multiple clusters, each composed of adjacent vehicles. Inside each cluster, TDMA is used with long band guards to overcome the effect of propagation delay in underwater. In this case, TDMA is not highly inefficient since vehicles in the same cluster are close to one another. Hence, the propagation delay effect is limited. Interference among different clusters is avoided by assigning different spreading codes to different clusters. The proposed protocol also sketches some mechanisms to reorganize clusters after node mobility.

2.5.2 Random Access

a. ALOHA Based

The ALOHA protocol [1] is the simplest MAC protocol since it does not care about channel status or packet delivery success. So, it quickly reaches the network saturation point, producing a huge number of collisions. This MAC approach is avoided in other network technologies due its lack of ability to properly order the access to a shared medium. However, ALOHA based protocols do not require handshaking exchange to deliver data frames, being this an interesting feature when signal propagation delays are so high as in underwater acoustic networks.

In Aloha mode, the source node sends its data frames as soon as it receives a packet from the upper-layer protocol. It does not check the medium to see if it is busy and so it does not perform any back-off. The node that receives the data will answer with and acknowledge data frame if there was no problem at the reception such as a collision or packet lost during the transmission (i.e. when there is overlapping of the receiving periods of two or more frames at the destination location, or the receiver was transmitting).

If the source does not receive an ACK, because either the frame was not correctly delivered or the ACK was lost, the sender will timeout, wait a random period (back-off) and retransmit the frame. This protocol follows the stop-and-wait paradigm. That is, the source must receive an acknowledgement for each data frame before the next frame can be sent. In addition, after a successful frame transmission, the sender will perform a back off, even if it has additional frames to send from the same packet or from a new packet.

There are different versions called Aloha-based protocols; in particular for underwater networks two proposals can be found in [9]: Aloha with Collision Avoidance (Aloha-CA) and Aloha with Advance Notification (Aloha AN).

Aloha-CA

Pays close attention to every packet it overhears, picking the information of who are the sender and receiver. With this information, it can easily calculate the busy duration due to the packet at every one of the nodes. Each node will store the information of the monitored packets in a database table with the busy durations of every neighborhood node.

Aloha-AN

This protocol has all the features of Aloha-CA and adds the sending of a small advanced notification packet with the necessary information to let the other nodes build the database tables. The sender will wait after this packet for a lag time before sending the actual data packet. Whenever a node has a packet to transmit, it will check the database table to ensure that the packet does not result in a collision at any other reachable nodes.

b. CSMA Based

CSMA

The Carrier Sense Multiple Access (CSMA) [57] is an evolution of ALOHA that includes a channel-sensing mechanism. This protocol considerably reduces the channel collisions when compared with the ALOHA protocol, without requiring extra signaling.

Before transmitting data, the station listens to the channel to see if it is occupied by someone else's transmission. If the channel is busy, the station waits until it is free; when the station detects an idle channel, it transmits a frame. If a collision occurs, the station waits a random amount of time and begins the sequence again. This protocol is persistent because the station transmits with a 100% probability when the channel is idle.

The propagation delay has a significant effect on the performance of the protocol. There is a small chance that, immediately after a station begins the transmission, another station is ready to send and detect the channel. If the first station signal has not arrived even to the second, the latter detects an idle channel and also starts sending a frame, whereas the result is a collision. The higher the propagation time towards the transmission time, the more influence it has in these kind of collisions, and thus worse protocol performance.

Even if the propagation delay is zero, there will still be a collision. If two stations become ready when a third station is sending a frame, they wait until the end of the transmission and begin to transmit simultaneously, resulting in a collision. This protocol is still much better than the Pure ALOHA, since both stations have the courtesy of withdrawing to interfere under the third season. Naturally, this will lead to better performance than Pure ALOHA.

However, if the channel is already in use, the station does not continually monitor the channel to detect the end of the ongoing transmission. Instead, it waits a random time period and repeats the algorithm. The natural consequence of using this algorithm should lead to better channel utilization and higher delays.

CSMA/CA

The Carrier Sense Multiple Access with Collision Avoidance (CSMA/CA) incorporates a handshaking process to establish the communication channel between two nodes.

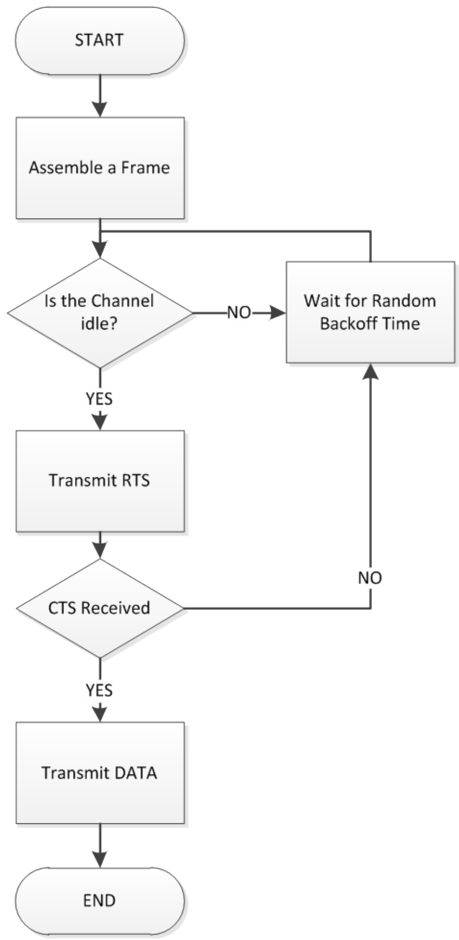

Figure 2.6 CSMA/CA. RTS/CTS exchange scheme

When a node needs to transmit, before sending any data it checks whether the channel is busy; if it is occupied by other transmissions it waits a randomized time. If the channel is idle before sending DATA, it uses request to send (RTS) and clear to send (CTS) control packets to create a tunnel free of collisions at both communication ends. After acquiring the channel, the DATA packet is sent to the destination node.

Finally, the sender waits for an acknowledgment control packet (ACK) that will indicate the successful reception of the data packet. If no ACK is received, then a contention mechanism, typically based on a back-off scheme, randomly delays the packet retransmission. Also, a maximum number of consecutive retransmission attempts are defined. If this maximum is reached, then the packet is discarded.

DACAP

Distance Aware Collision Avoidance Protocol (DACAP) [36] is a handshaking protocol designed for Ad-Hoc Underwater Acoustic Sensor Networks. The protocol includes a power-aware behavior that is intended to reduce power consumption by avoiding/reducing collisions and at the same time achieving good network throughput. It also minimizes the handshake time by using the tolerance to interference of receiver node, especially when the receiver is close to the reception range limits. The network nodes do not need to be synchronized and it supports node mobility (dynamic scenarios).

The improvement introduced by DACAP towards the traditional CSMA/CA mechanism lies in the behavior of the receiving node when it is waiting for a data packet. If it overhears a control message coming from another node, it will send a warning packet (WAR) to this node in order to let it know that there is a transmission already in process. Moreover, after receiving the CTS control packet, the sender node defers the transmission data packet for a defined delay time. The transmission attempt is aborted if by any chance the sender node receives another control or warning message. The delay times are determined according to the distance between the nodes involved in the transmission that can be solved during the handshake by measuring the roundtrip time. Even though when the receiver node sends a warning message, it has no feedback that lets it know if the interfering node cancels its transmission. That is the reason why the receiver keeps listening to the channel after sending the warning message, and thus the defer state is set to a minimum delay time between the CTS and the DATA so that it avoids a collision.

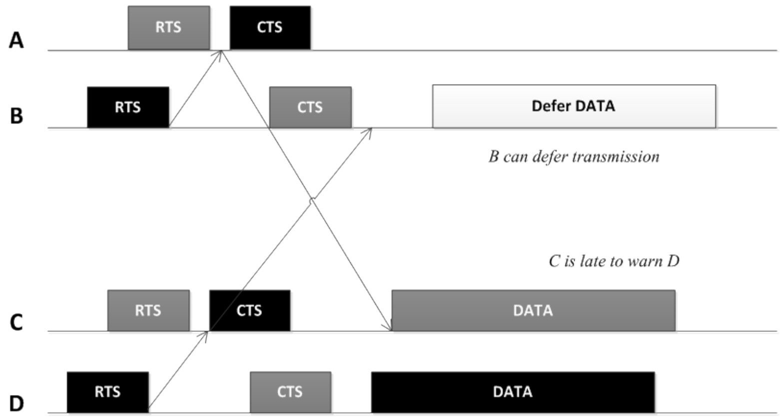

Figure 2.7 Transmission in DACAP

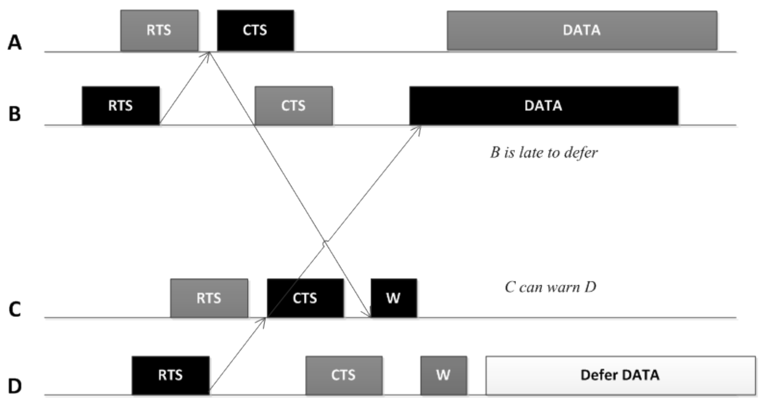

Figure 2.8 Reception in DACAP

The protocol is described in Figure 2.7 and Figure 2.8, explained in the following steps: (a) In Figure 2.8 node C receives a RTS packet from node D: After this event, it sends CTS to the sender and waits for a data packet. If another RTS is received (like the one from node A), the node sends a warning short packet to node D warning that the medium is in use. (b) In Figure 2.7, node B receives a CTS packet from node A : when node B receives this message, it waits for those nodes whose transmissions are still happening to avoid any collisions. If it happens to receive another CTS (like the one from node C) or a warning packet, the current data packet will be deferred for a random back-off time; if the waiting time expires, the transmission proceeds normally.

DACAP is a collision avoidance protocol with an easy scalable adaptation to big networks involving more nodes and a greater area. The protocol is aware of power consumption by avoiding collisions at the same time that maximizes the throughput. It minimizes the handshake time, using the tolerance to interference of the receiver node when this one is close to the limit of the range reception range. It works with a half-duplex communication link; the nodes do not need to be synchronized and it supports mobile nodes.

The throughput with this protocol is several times higher than the one achieved with Slotted FAMA, while offering similar protection to collisions, i.e. energy savings. Although CS-ALOHA offers higher throughput in most cases, it wastes too much power on collisions.

T-Lohi

Tone-Lohi is a contention-based MAC protocol that uses a short packet as a wake up tone to reserve the medium. It is a full distributed reservation process and one of its main features is its power consumption; the nodes will be in an idle mode with low energy requirements until it receives the wake up tone.

The main goals of T-Lohi are to make efficient use of channel utilization, achieve stable throughput, and save as much energy as possible without impacting the performance. This energy conservation is approached in two ways: (a) the reservation to prevent data packet collisions or at least reduce them, (b) and the usage of wake-up tones for the receivers to keep them in low power while in listening mode.

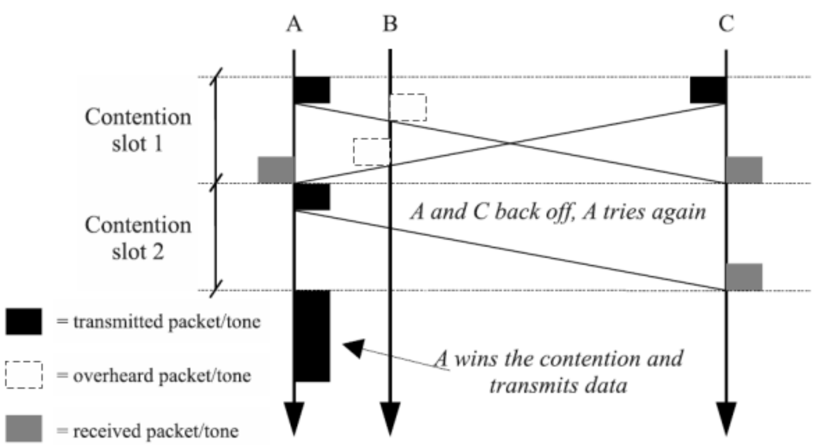

Figure 2.9 T-Lohi Protocol Scheme

With T-Lohi, time is divided in frames; each frame consists of two portions, namely the reservation and data periods. The reservation period is partitioned further into contention rounds.

A tone transmission can take place only at the beginning of a round. Any node that wishes to send a data packet transmits a tone first. If no other tone is received from any neighbor, the node has been successful in reserving the channel, and can start transmitting the data packet.

In the case the node hears other tones during the current contention round, a contention resolution procedure is started, whereby each contender backs off for a random number of rounds, uniformly chosen in the interval $[0,N]$. The node listens to the channel for the whole duration of this backoff (Figure 2.9).

During this phase, if a node is the only one to choose the earliest round to transmit another tone among all contenders, it is called the *winner* and allowed to start data transmissions immediately. If more than one node chooses the earliest contention round simultaneously, they are called *competitors* and continue to contend for channel access by repeating the aforementioned procedure.

If a node hears one or more tones before attempting to access the channel again (i.e., one or more competitors choose a shorter backoff time), it is called a *loser* and exits the contention phase. All losers start listening to channel activity until both the contention and the data transmission phase ends, after which they go back to idle mode.

2.6 Routing Layer

This layer is mainly responsible for routing packets to the proper destinations. Therefore, a routing protocol is required when a packet must go through several hops to reach its destination. It is responsible for finding a route for the packet and making sure it is forwarded through the appropriate path. The way paths are selected for every source destination pair will have a direct impact on the overall network performance.

Most of the routing proposals for UWSN are based on the ones developed for terrestrial ad-hoc and wireless sensor networks. Some of the protocols designed exclusively for underwater wireless networks are:

2.6.1 DBR

The Depth-Based Routing protocol [68] can handle network dynamics efficiently without the assistance of a localization service, it needs only local depth information. It is a greedy algorithm that tries to deliver a packet from a source node to sinks.

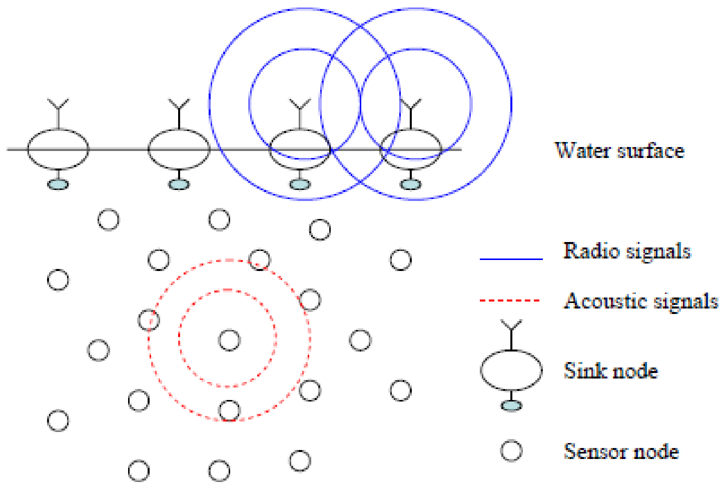

Figure 2.10 Multiple sinks underwater sensor network architecture

The source nodes send the data packets toward the sinks; in this process as the packet hops from one node to another, the depth decreases as it gets closer to the final sink receiver (usually located at the surface). The decision that is taken in each one of the nodes during the transmission is based on its own depth and the depth of the previous sender.

When a node receives a packet, it extracts the information of the depth of the previous node and compares it against its own depth. After comparing, the node will have two behaviors: (a) the node is closer to the surface, $dc < dp$, so it will forward the packet; (b) if the current node depth is greater, $dc > dp$, it will discard the packet as it comes from a node with a better position.

Probably, especially at the beginning of the transmission in the first hops, a lot of receivers of the packet will decide to forward it. To avoid the collisions that these retransmissions would bring and the high power requirements needed in the network, the number of forwarded messages must be controlled.

It can also happen that as it has been using a multiple omnidirectional path algorithm to route the packets, a node receives the same packet several times and in the same way forwards it the same number of times. In order to save energy, a node will know which packets have already been sent so as not to send a packet more than one time.

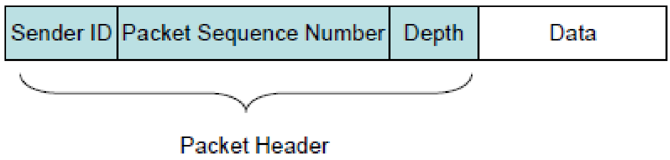

Figure 2.11 DBR packet format

The Packet Header Format will be composed of the following fields:

- Sender ID: the identifier of the source node.
- Packet Sequence Number: a unique sequence number assigned by the source node to the packet. Together with Sender ID, Packet Sequence Number is used to differentiate packets in later data forwarding.
- Depth: the depth information of the last forwarder node, which is updated hop-by-hop when the packet is forwarded.

As mentioned before, there is a need to reduce power consumption, forwarding only the necessary packets. To achieve this, DBR protocol uses Redundant Packet Suppression, which consists of two features for avoiding redundant packets. One is that multiple paths are naturally used to forward packets. The other is that a node may send a packet many times. Although multiple paths in DBR cannot be completely eliminated, a priority queue is created to reduce the number of forwarding nodes, and thus control the number of forwarding paths. To solve the second problem, a packet sent buffer is used in DBR to ensure that a node forwards the same packet only once in a certain time interval.

2.6.2 VBF

Vector-Based Forwarding protocol [65] is an algorithm that allows the nodes to weigh the benefit of forwarding packets and reduce energy consumption by discarding the low benefit packets. One of the main factors in underwater wireless networks is to save power so as not to let nodes run out of batteries, due to not being able to recharge them for long periods. This protocol tries to focus its features in this direction. To aim this target, each packet will include the location information of sender node, destination node and the next hop node in path to destination.

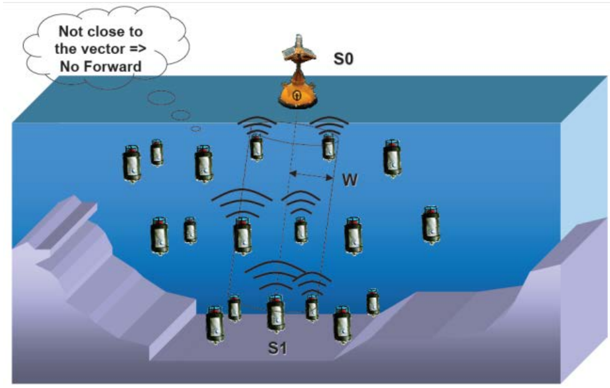

Figure 2.12 High level of VBR of UWSN

To be able to run this protocol, it is assumed that every node has the capacity of measuring the distance and angle of arrival (AOA) of the signal. The route of the packet is computed in the sender and included in the packet. When a node receives a packet, it calculates its relative position towards the target. This works recursively in all nodes during transmission. If the node knows that it is close enough to the routing vector (it will be under the threshold value established for this purpose), it will include its position and forward the packet; in other cases, it drops the packet. In this way, all the packet forwarders in the sensor network form a “routing pipe”: only the sensor nodes in this pipe are eligible for packet forwarding.

Figure 2.12 represents the nodes that are within the routing pipe that forward the packet; *“w”* is the threshold used to measure the pipe width. And the nodes that are out of this path discard the packets. This protocol is scalable to the network size. VBF can effectively accomplish the goals of energy efficiency, high success of data delivery and low end-to-end delay.

2.6.3 FBR

Focus Beam Routing, a location-based routing protocol [26], is presented as a way to find the path between two nodes in a random deployed network. Figure

2.13 shows a simple two-dimensional network to explain the protocol, although it works in the same way in three-dimensional scenarios.

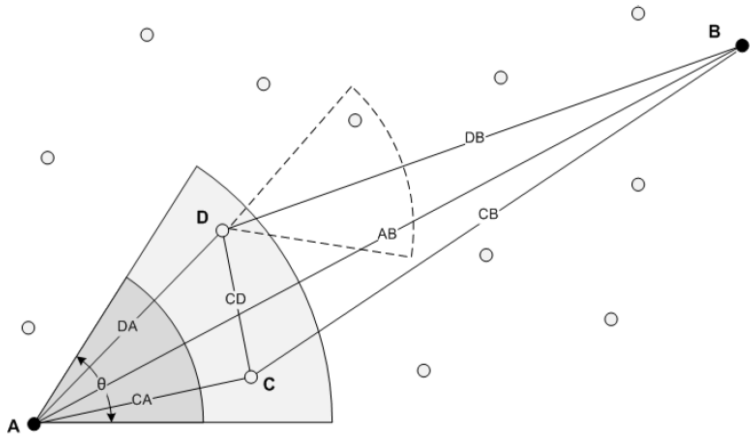

Figure 2.13 Nodes within the transmitter cone θ are candidate relays

Assuming communication between node A and node B, node A will send and Request to Send (RTS) multicast messages to all the reachable neighbors. This packet will include the information for the source (node A) and final receiver (node B). As the protocol works with power levels, the first try is done at the lowest level and it increases if there is a need because it receives no answers within a wait time established for each power level.

This request is a short control packet that contains the source's location (node A) and the final destination (node B). Note that this is in fact a multicast request. The initial transaction is performed at the lowest power level and the power is increased only if necessary. Power control is performed as an integral part of routing and medium access control.

Each power level will have a radius, and in each one a certain number of nodes will be reached. These will be the nodes that receive the RTS and its information that will be used to calculate the relative position to the AB line. This is done to learn if the node is a candidate to be a relay node. Candidate nodes are inside a cone of $\pm\theta/2$ from line AB. Every candidate node will answer to with a Clear to Send (CTS) to the transmitter; the nodes out of the candidate zone will remain silent.

After sending the RTS, the transmitter will wait to receive CTS messages from other nodes, and three possible things can occur: (a) The transmitter receives no answers, the RTS has not reached any neighbor, therefore the transmitter increases the power level and tries again as shown in the example; (b) The transmitter receives one CTS, the sender of this message is selected as a relay for the next hop, sending the DATA message; (c) The transmitter receives more than one CTS message, looking at the location information from the candidates included in the CTS message the node that is closer to the final destination is selected as relay receiving the DATA message. After sending data, the transmitter will wait for an acknowledgement message. This process will continue until we reach the final destination.

Packet collisions can happen but will always involve short packets as the link is safe for data packets which have no risk of collisions. Although the chances of collision are small, if the source node detects a collision, it will detect the signal but will not decode the data information, and it will resend the RTS once again, without increasing the power level.

2.7 Application Layer

Applications in underwater wireless sensor networks have a lot to do with terrestrial sensor networks and thus we can classify them in the same set of categories.

The need to observe and collect data with scientific studies, remote sensing of physical environment conditions such as temperature, salinity, noise, etc., as well as birthrate and population control of sea life, like microorganism, fish and/or mammals. Pollution is nowadays one of the greatest problems: oil spills from ships or broken pipelines can do a lot of harm to marine biological activity, industry and tourist locations. Monitoring ecosystems can help in understanding and predicting the effects from humans, climate and weather in underwater environments. In this manner, we can prevent natural disasters by measuring seismic activity from different remote locations; sensors could alert coastal areas by detecting tsunami or submarine earthquake alarms.

In underwater navigation, the sensors can be placed to make routing, identify hazards on the seafloor, rocks or shoals in shallow water. Assisted navigation sensors can be used to identify hazards on the seabed, locate dangerous rocks or shoals in shallow waters, mooring positions and mapping the areas bathymetry profile. Underwater Autonomous Vehicles (UAVs), or distributed sensors in movement can help monitor the area for surveillance, recognition and intrusion detection. Underwater wireless sensor networks can be used to find oilfields or reservoirs, locate routes for placing connections for intercontinental submarine cables. Also, they could seek out shipwrecks or archaeology or lost sunken cities.

Defense and homeland security involve controlling ships and ports, harbors, the presence of submarines or divers in safe locations, communications, coastal protection monitoring illegal immigration, shipwreck protection from gold hunters, etc.

Scientific usually collect experimental data and later they analyze them in laboratory. The main reason is because it is expensive to get data in situ. In a translation from terrestrial low cost sensor network deployments, many present proposals [22] are based on surface and shallow water exploration, meanwhile the cost of deep water sensing increases exponentially.

2.8 Future Trends

Many advantages can be exploited by using underwater sensor networks, but a lot of research must be done in the upcoming years. Developing this technology will have a great impact on the industry.

It is necessary to improve the physical layer performance in terms of efficiency, building low power acoustic modems that are able to make the best use of the bandwidth, reducing the error rate with forward error correcting coders.

Currently, there is a lot of work related to MAC layer proposals since this is one of the more sensible parts of UWSN architecture. It seems that distributed CDMA-based schemes are the candidates for underwater environments, but it depends on many factors, such as the application and network topology. Also, MAC protocols should be designed by taking energy consumption into account as a main design parameter.

Chapter 3
Underwater Wireless Sensor Network Framework Simulator

3.1 Introduction

Terrestrial wireless sensor networks have been developed over the last two decades. As a result of this research, the physical layer has been modeled and a wide range of MAC protocols, routing protocols and applications have been worked out. But in order to make this possible, standardization and simulation tools are needed for researchers and commercial companies to test and validate the algorithms before implementing them in real hardware prototypes.

The most outstanding simulator tools used in terrestrial networks are Network Simulator 2 and 3 (NS) [8] and OPNET [34]. In these simulators you can find protocol models that are currently used by mobile wireless networks like 802.11, UMTS/3G, Zigbee, etc. Underwater wireless sensor networks are just beginning to appear in the world of simulators, and that is the reason that today there are many proposals but not one is complete.

Many of these simulators are based on terrestrial network models reusing many elements in common; other simulators are specific underwater acoustic programmed in python, c/c++, etc. Even though there is not a definitive proposal, interesting options have been recently presented, for instance the WOSS, from Guerra, Casiri and Zorzi [19] [20], claims to be a global simulator.

3.2 Related Work

Although we can find a lot of simulation tools for underwater networks, we have chosen three of them that we consider the most representative and that also have their code available for testing and comparing results.

3.2.1 AuvNetSim

AUVNetSim [25] is an example of a simulator exclusively programmed in python for underwater wireless networks. Highlights in this simulator are the MAC layer with DACAP protocol [36] and the routing algorithm FBR [26], including power control. But the definition of the channel is too simple, and so different environmental conditions cannot be detailed.

Although this simulator is code available, it is not based on a standard framework, so the results are difficult to compare with new research discoveries. On the other hand, it includes interesting novel proposals in both MAC and routing layers.

3.2.2 Xie Gibson Simulator

Based on the Monterrey Miami Parabolic Equation (MMPE) [66], a propagation model is presented and implemented in OPNET for the physical layer, and Aloha and CSMA protocols for the MAC layer. This simulator stands out because it describes the physical layer with great detail, and it is possible to define a scenario considering more environmental parameters like the effect of waves, and the depth of nodes. The drawback of this model is that before doing network simulations, several propagation model parameters need to be computed as this process is very high time-consuming. Also, the model only works on static scenarios with static conditions across the simulation period.

The code necessary to build this simulator is not available, but the authors include a full description of the implementation as well as the formulas obtained in their study.

3.2.3 WOSS

The world ocean simulator system (WOSS) [19] [20] seems to be one of latest and most complete simulator tools at the present time. It is implemented in the Network Simulator 2 package. It uses world databases that measure the sound speed profile (SSP), bathymetry and floor sediment, such as the General Bathymetric Chart of the Oceans (GEBCO) and National Oceanic and Atmospheric Administration (NOAA). Combining this data with scenario information like latitude, longitude and depth position of the nodes, it creates environmental files that describe the scenario. With this information, the Bellhop ray tracing tool [41] is called giving as a result several files with amplitude, travel times, ray coordinates and the acoustic pressure map information.

The code is available, but this simulator does not include the ocean wave in the definition of the environment, so this effect is not considered in the acoustic transmission.

3.3 Early Simulator Approaches

The path building a simulator framework has not been straight forward. In this section, we explain the attempts, the trial-and-error procedure, the failures and successes that have led to a complete solution framework.

3.3.1 Thorp's Equation

The very first try to incorporate underwater acoustic functionality to the simulation framework was to introduce the formulas developed by Thorp (as mentioned in Section 2.3.1) into the OPNET simulator to describe the sound behavior. The good point on the use of these formulas is that their simplicity lets the simulator work very fast, allowing quick performance evaluation of protocols. By the way, the attenuation formula accuracy is very poor as it is only based on the frequency and the distance from the nodes, leaving apart important physical criteria such as the effect of ocean waves, depth, etc. This is the reason this option was quickly discarded and so the search for a better solution was still in progress.

3.3.2 MMPE

The next step led us to the Monterrey Miami parabolic equation, after implementing and validating the simulator framework toward the Xie & Gibson results. This offered a better description of the attenuation calculation by including the effect of ocean waves, depth of the nodes, the seafloor multipath. Two improvements were added to this proposal:

- Accurate calculation of the propagation speed of sound: Setting the temperature and salinity as a parameter and using the formulas in section 2.3.2, the exact value is calculated and used.

- The effect of noise in the attenuation and thermal noise based on the studies of Harris [21]. Taking into consideration the environmental conditions introduced by Harris, an improvement has been introduced when calculating *e()* in order to reduce the randomness and introduce more realistic noise sources. Based on [21] we propose that the major factors contributing to the underwater environmental noise are ship activity, wind, turbulence and thermal noise. Notice that in the MMPE model, the wind and the turbulence are already considered when introducing the wave effect. So, the ship activity and thermal noise sources are added to the physical layer, and as a consequence, we reduce the high degree of randomness of expression (2-11). Thus, in order to model the environmental noise, we propose the following expression:

$$N(f) = N_t + N_s$$
$$10\ logN_s(f) = 40 + 20\ (ship - 0.5) + 26 \log f - 60 \log(f + 0.03) \quad (3\text{-}1)$$
$$10\ logN_{th}(f) = -15 + 20 \log f$$

Where N_s is the noise due to shipping activity, the ship parameter indicates the noise due to ship activity (ranges from 0 to 1) and N_{th} refers to the thermal noise. Finally, the function *e()* stands as follows:

$$e() = 20 \left(\frac{s}{s_{max}}\right) R_N + N(f) \quad (3\text{-}2)$$

The study of the influence of the physical parameters was done with this framework as follows:

a. Propagation Speed effect

The evaluation to test the influence of the physical parameters in the behavior of the model is done in a scenario with a point-to-point connection among two nodes at a fixed distance of 1250 meters and with the same depth of 40 meters. The remaining parameters are those shown in Table 3.1.

Parameter	Value
Frequency (kHz)	20
Wave height (meters)	4
Wave length (meters)	100
Global load (packets/s)	5
Data packet size (bits)	1024
Data rate (bits/s)	1000

Table 3.1 System parameters

To observe the salinity and temperature influence on the propagation speed, we run several simulations varying those parameters within their operational range. In particular, in this scenario the salinity goes from 32 to 37 ppm and the temperature from 0 to 18 ºC. As a summary of this simulation process, the results for the minimum and maximum values are presented in Table 3.2 and Table 3.3. The *propagation time* is calculated as *distance/propagation speed*, *transmission time* will be equal to *data packet size/data rate* (*1.024 s* in this example) and the *delay* will be the sum of both.

Salinity	Propagation speed	Propagation time	Delay
32	1537 m/s	0.8133 s	1.8373 s
37	1543 m/s	0.8101 s	1.8341 s

Table 3.2 Salinity influence

Temperature	Propagation speed	Propagation time	Delay
0	1450 m/s	0.8620 s	1.886 s
18	1550 m/s	0.806 s	1.830 s

Table 3.3 Temperature influence

As can be seen, even comparing the lowest and highest salinity and temperature values, the effect on the link propagation delay may look small (around 3%), but this could be a determinant factor in the network performance, especially in collision avoidance protocols where knowing if the channel is idle or not is fundamental for a proper operation. Hence, this slight time difference can turn the throughput, delay and collision results upside down.

Many authors have used a fixed value of 1500 m/s, but they can no further justify its usage, and their results are not well validated to implement them in real network scenarios. In the proposed model, these parameters are obtained from global databases to calculate the exact value of the propagation speed at any world location.

b. Depth and Distance effect

We define a point-to-point link among two nodes that keep the same distance. Both nodes move at the same time from the surface to a depth of 60 meters (they always share the same depth). If the connection link is broken, the node re-transmits the message, and thus the delay and throughput are affected. The *reachability* (*number of succeeded transmission/number of attempts*) between the two nodes is shown in Figure 3.1.

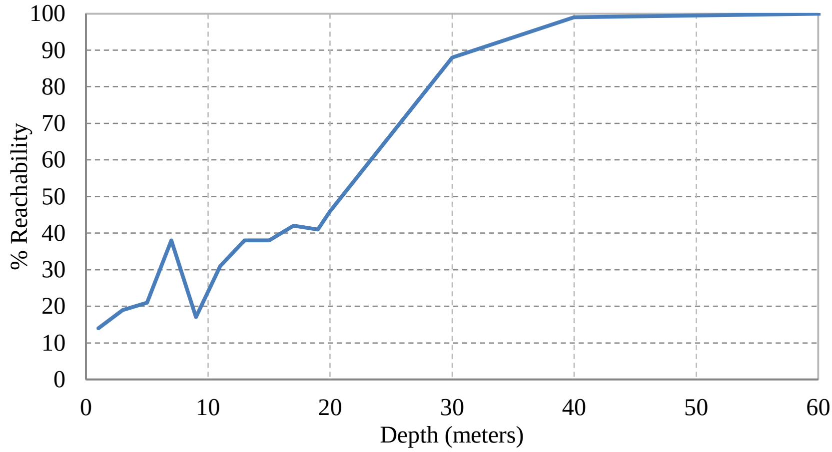

Figure 3.1 Depth effect in reachability

As can be shown, the reachability increases proportionally with the node depth. This behavior is mainly due to the wave effect at low depths, where the propagation multipath caused by surface activity and wave turbulence effects severely impacts the propagation loss. So, there are a lot of packet losses that lead to retransmissions and, as consequence, the network performance is severely hindered.

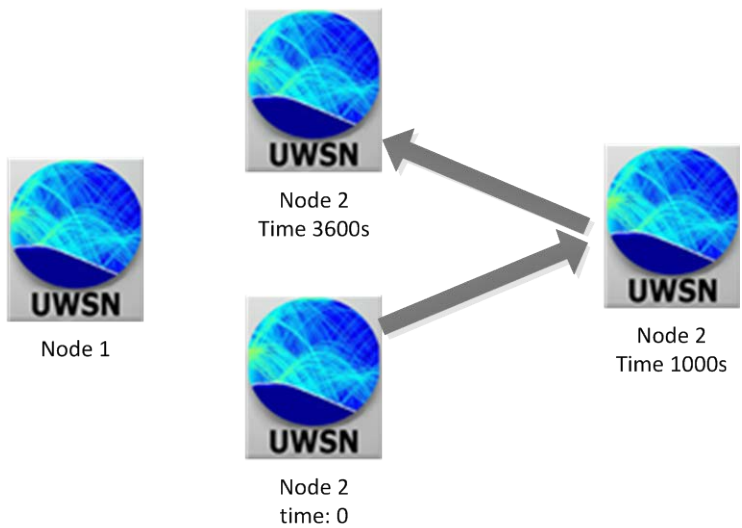

Figure 3.2 Distance effect movement

In Figure 3.2, the distance effect in the reachability limits is displayed by defining a scenario of two nodes fixed at 40 meters and where one node moves away from the other and returns back. In Figure 3.3, the distance curve represents the distance among both nodes as a function of time, while the reachability curve indicates if both nodes are reachable (value of 1500) or not (0).

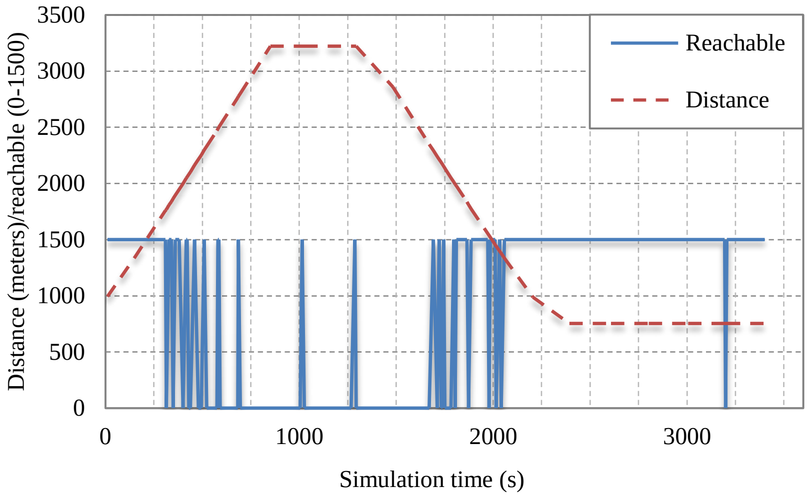

Figure 3.3 Distance effect in reachability

As can be shown, in the present conditions when the distance is above 1400 or 1500 meters, the reachability changes from always to sometimes, and at more than 2200 meters, both nodes are considered unreachable.

c. Wave effect

Combing the possible values of the characteristics in which a wave is modeled (height, length), we evaluate the wave effect by using a range from 0, which represents the minimum values of height (0.5), length (50) and period (1), to 100 that represents the highest values of height (5), length (150), and period (8). In table 6, we show the values that represent the wave activity.

In Table 3.4, we show the delay of a point-to-point link of 1400 meters where both nodes are at the same depth (30 meters) and the packet time generation was set to 20 seconds. The end-to-end delay remains constant up to 50% of wave activity (no effect), but above 50% the delay significantly increases due to the need of retransmission.

Height	Length	Period	%	Delay
0.5	50	1	0	2.11
2	75	2	25	2.11
3	100	4	50	2.11
4	125	6	75	6.38
5	150	8	100	16.91

Table 3.4 Wave effect in delay

As a summary of this approach, we can highlight that it is an accurate model that includes many innovative features with a realistic behavior of the acoustic signal, the effect of the ocean wave, the importance of the depth of the nodes. The handicaps found in this proposal and that drive us to leave this choice are: first of all, the authors offer us the results of a scenario example; in order to get new coefficients for the formulas that describe the attenuation in another scenario, we have to follow a very complex procedure where we have to manually define all the physical scenario parameters (depth, bathymetry, sound speed profile), which is a hard task when trying to emulate a real scenario at a specific world location. So, in this proposal we are limited to use the actual scenario to do experiments.

3.3.3 Bellhop Ray Tracing Tool

Although there was no simulator framework that included the Bellhop ray tracing tool (WOSS was released in a later phase of our research, in parallel to our investigation), as mentioned in Section 2.3.3, many studies have already used this acoustic propagation tool to compare the data results from real scenarios and to do several experiments in relation to the behavior of acoustic propagation under different conditions and at locations around the world.

Once the tool was tested, it was included into the OPNET simulator framework, and the process to build the scenarios and the physical parameters was automated, so that by only establishing the world network location and the season of the year, through the connection with world databases, the scenario parameters are obtained and the configuration files that are required by the Bellhop ray tracing tool are automatically configured. This includes the bathymetry, seafloor sediment, sound speed profile, while the only parameters to set are the ocean surface (wave length and height) and the desired signal frequency, and the simulation is ready to be run. This is obviously a step ahead of other proposals as it lets us create and reproduce real scenario conditions in the simulator. In the next section, a full explanation of the implementation of the framework is presented, and subsequently simulation scenarios examples and tests are made with this simulator.

3.4 Simulator Framework Proposal

The simulation framework is based on OPNET, MATLAB and the Bellhop ray tracing tool, and uses information related to underwater scenario characteristics like bathymetry, salinity, and seafloor composition, found at real worldwide locations that are downloaded from NOAA and GEBCO worldwide ocean databases. This information is combined with the OPNET network scenario module in order to create the corresponding environmental files.

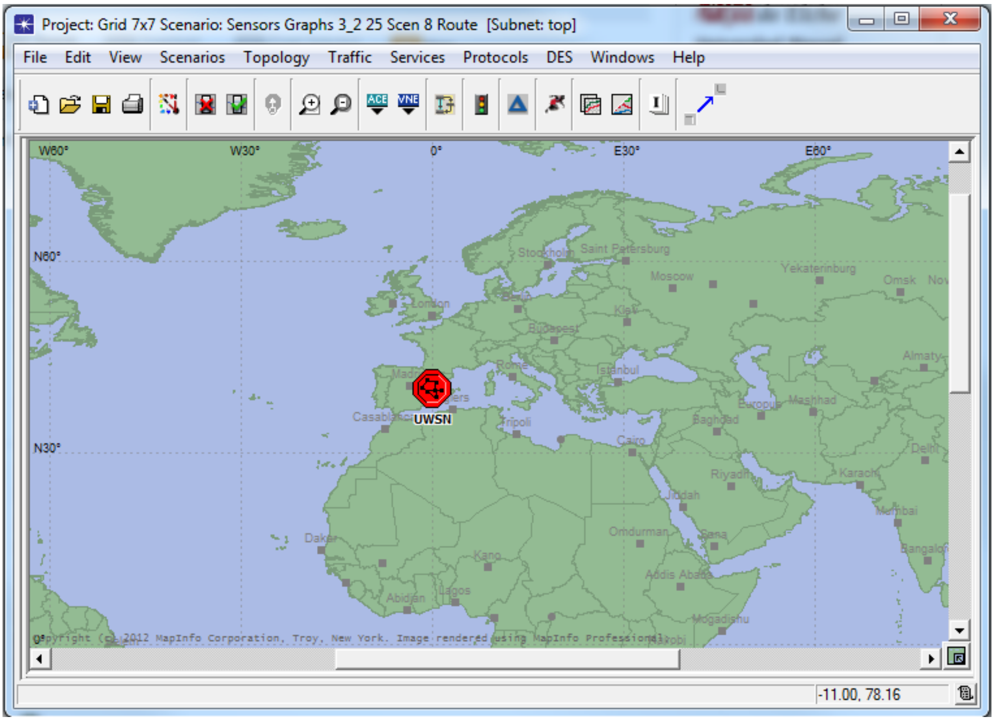

Figure 3.4 OPNET Simulator. World location selection

The objective is to create a simulator able to perform simulations in scenarios located anywhere in the world. In OPNET, it is very easy to set the network world location just by clicking on an area or introducing the GPS coordinates manually.

So the obtained results will be in accordance to the local environmental conditions and will be closer to the ones measured in the real world. Then, inside the network, the nodes can be deployed manually or by introducing their coordinates manually (see Figure 3.5).

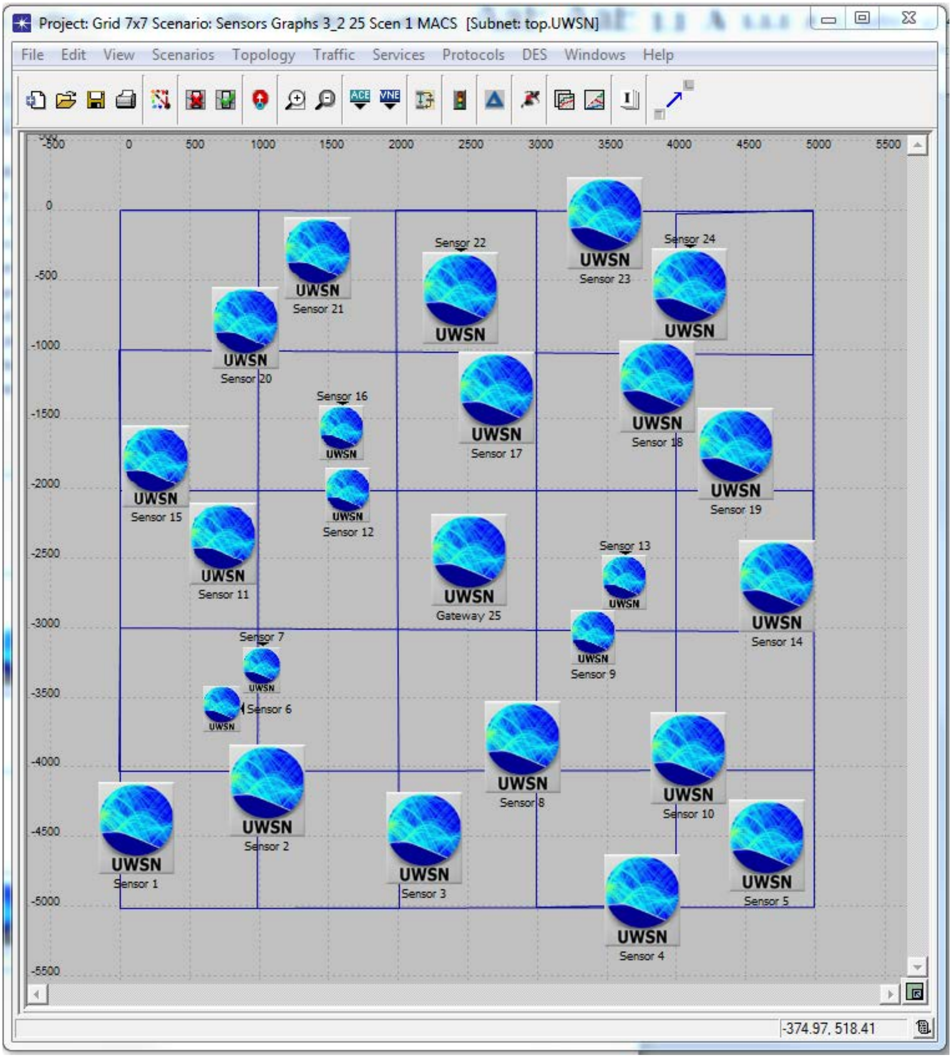

Figure 3.5 Simulator network. Deployment of nodes

Each node has several parameters as shown in Figure 3.6. These parameters are required by the protocols used during the simulation, such as the packet sizes, number of attempts, etc.

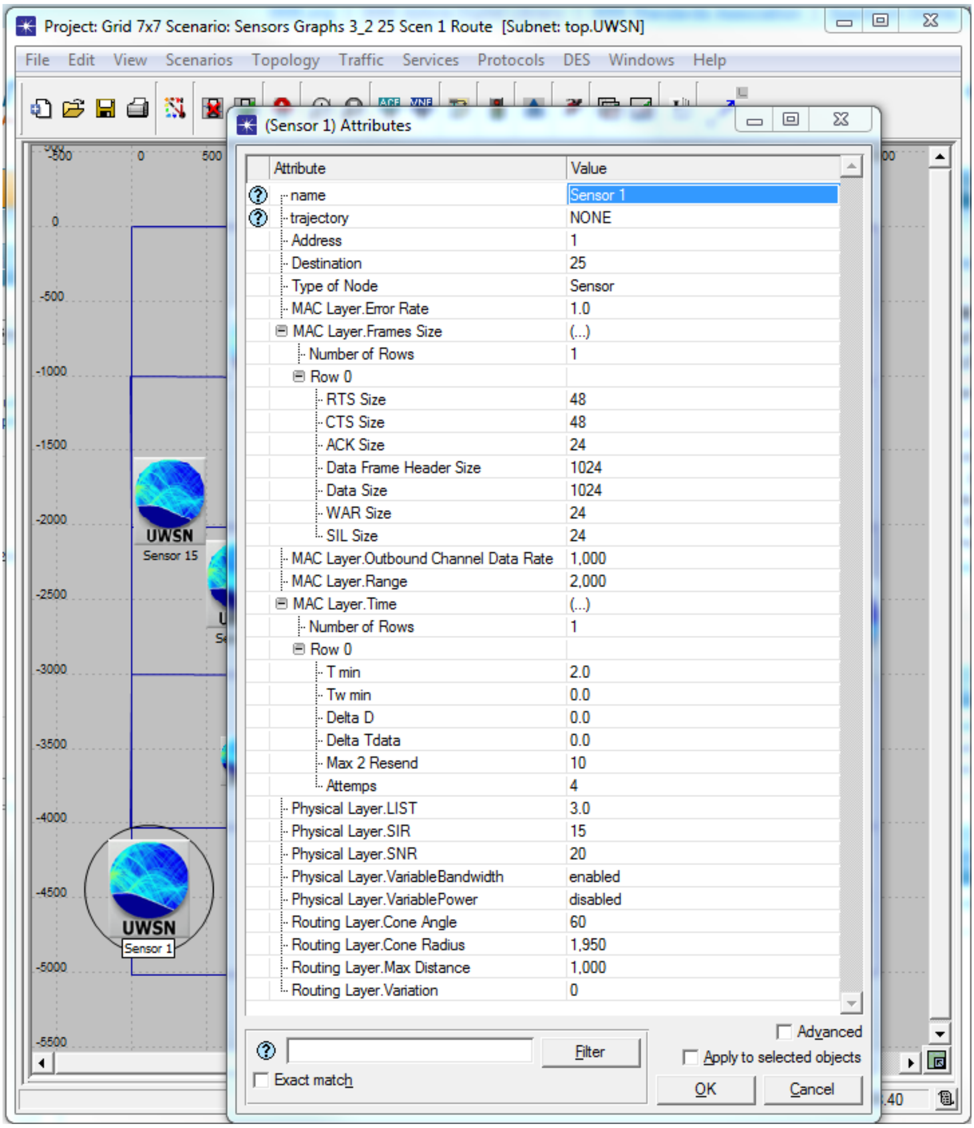

Figure 3.6 Nodes parameters

Also among the specific node parameters, the simulator has many global attributes to define the network environment and the protocols to evaluate as displayed in Figure 3.7. We can set different Bellhop resolutions in depth and range, as well as the ray angle, the definition of the altimetry wave height, length and period, the protocols used in each layer, the packet generation frequency, season of the year, signal frequency, etc.

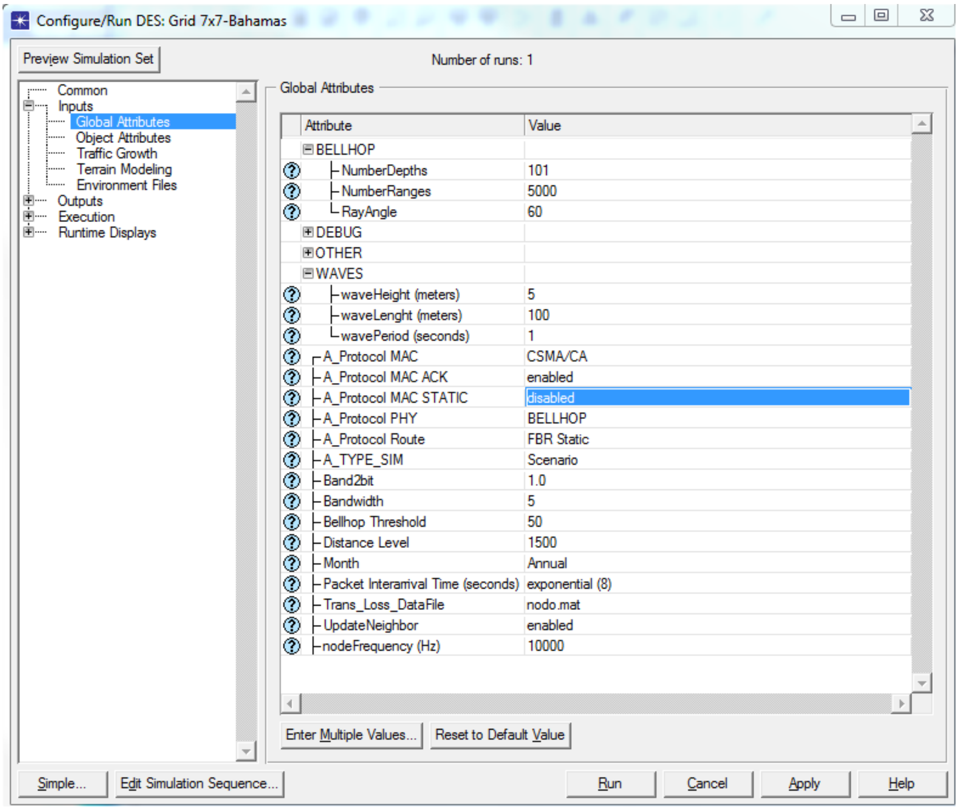

Figure 3.7 Simulation network parameters

Both the node and global attributes can have one or more values. In this way, a set of simulations can quickly configured; for instance, the packet delivery ratio can receive a fixed value (10 packets/sec) or a range of values from 2 to 20 packets/sec in steps of 2. This makes evaluating the effect of the variation of one or more parameters in the simulation easy.

After looking at the interface, we show what is behind it, and how the simulator framework uses this information to build the results. By using the scenario definition and its environmental conditions, the purpose is to pick the world information from databases combined with OPNET scenario information creating the environmental files. With these files, OPNET connects to MATLAB through its interface in an automatic process and runs Bellhop ray tracing tool obtaining the result files as seen in Figure 3.8. This is like a black box for the user who only has to run the simulation.

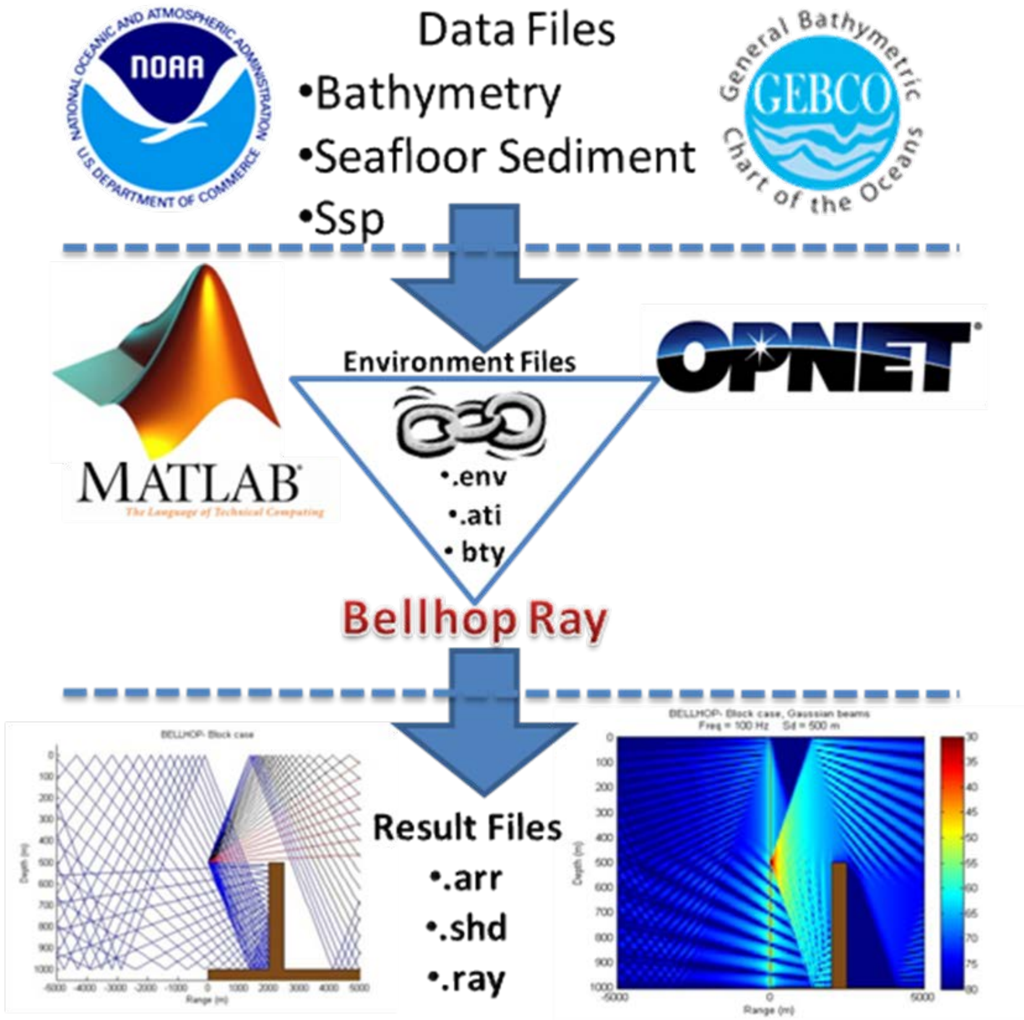

Figure 3.8 Simulator summary

In the following section, the implementation of the background of the simulator is described in detail.

3.5 Propagation Model

As shown in Figure 3.8, there are three steps to complete the process: obtaining the information from the databases, creating the environmental file, and executing the Bellhop to get the result.

3.5.1 World Databases

Three world databases are used to model the environmental files:

- Bathymetry [18]: Is provided by GEBCO, a file containing the world bathymetry data in a global 30 arc-second grid released in January 2009 and updated in November 2009. This information will be used for the bottom scenario relief and for the sound speed profile generation.

- Seafloor Sediment [33]: The National Geophysical Data Center (NGDC) from the NOAA provides a "Deck41" database that contains surface sediment descriptions for over 36,000 seafloor samples worldwide. Mainly we have ten types of floors in the ocean: gravel, sand, silt, clay, ooze, mud, rocks, organic, nodules, hard-bottom; if no one is available, no-data value will be returned.

- Sound Speed Profile (SSP) [64]: Provided by the World Ocean Atlas (WOA) in the NOAA, it contains information of the worldwide sound speed at different times of the year. It is available the average values during the year, a season or a particular month. The sound speed values depend on the latitude and season of the year. The greatest differences are in shallow waters.

All these databases are formatted in netcdf. To read them, we use MATLAB with the mexnc library and the Snctools [51]. We make a connection between OPNET and MATLAB using the interface of MATLAB for executing “c” code. So as to make this possible, the simulation must be compiled including the required libraries for this purpose:

- “libeng.lib, libmat.lib, libmx.lib and libmex.lib”,

the included files in:

- "C:/matlabR2008b/extern/include"

and finally, update the LIBPATH with:

- "C:/matlabR2008b/extern/lib/win32/microsoft"
- "C:/matlabR2008b/bin/win32".

A full explanation of the configuration can be found in [48].

3.5.2 Environmental Files

Once we have all this data in OPNET, it is combined with the information of the nodes (latitude, longitude and depth) and global scenario parameters such as signal frequency, wave information (height and length), month of the year, etc. The results are three environmental files required by Bellhop [41]:

- Environmental file: The general structure of the *.env can be seen in Figure 3.9 Environmental File (left), Bathymetry and Altimetry definition (right). The values of the Sound Speed Block and the Bottom Block are gathered from the databases. The Array block is data from the OPNET nodes global positions, and the Surface line, Output block and Beam block are simulation global parameters.

- Bathymetry file: Two columns, range (km) and depth (m), define the *.bty of the scenarios. This is created from the databases taking into account the global position of the network nodes.

- Altimetry file: Two columns, range (km) and depth (m), define the *.ati. This file is created with two global parameters, “Wave Height” and “Wave Length”.

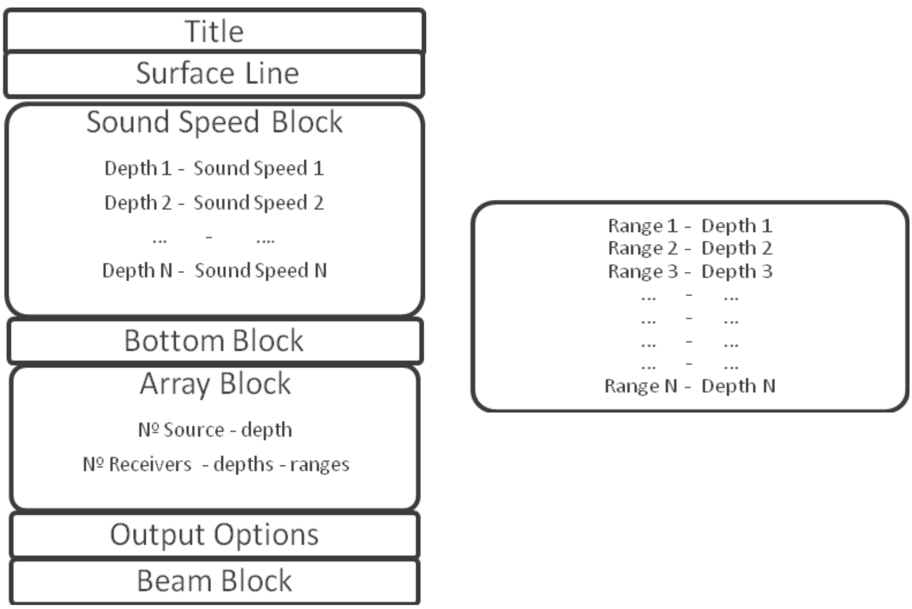

Figure 3.9 Environmental file (left), Bathymetry and Altimetry definition (right)

If we plot the BTY and the ATI files, the result is a 2D vision of the scenario as shown in Figure 3.10, where the wave shape (at the top) and the bottom relief are represented. So, now the network scenario of a simulation can be placed at any part of the world.

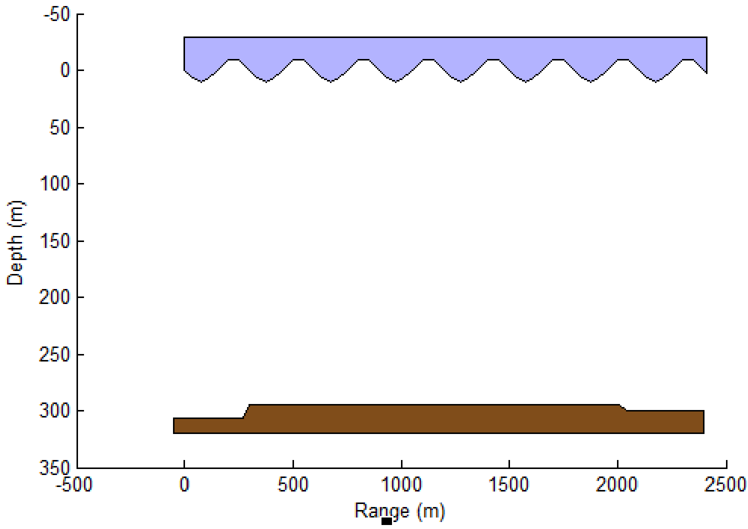

Figure 3.10 Plotting BTY and ATI files

3.5.3 Bellhop Execution

Again, we use the MATLAB [30] interface from OPNET to communicate and execute the Bellhop Ray tracing tool with the files created in the previous step as parameters. Depending on the desired output option, different result files will be created:

- Option R: a *.ray file is created, which includes the ray coordinates.
- Option C: a *.shd file is created, which includes the acoustic pressure.
- Option A: a *.arr file is created, which includes the travel times and amplitude information.

The *.ray file contains the ray coordinates and we can clearly see the behavior of the rays and the reflections along the scenario in Figure 3.11, which will be very different depending on the proximity to the surface of source node, and the height and length of the waves, the shape of the bottom depth and the types of sediment that can be found in the scenario location.

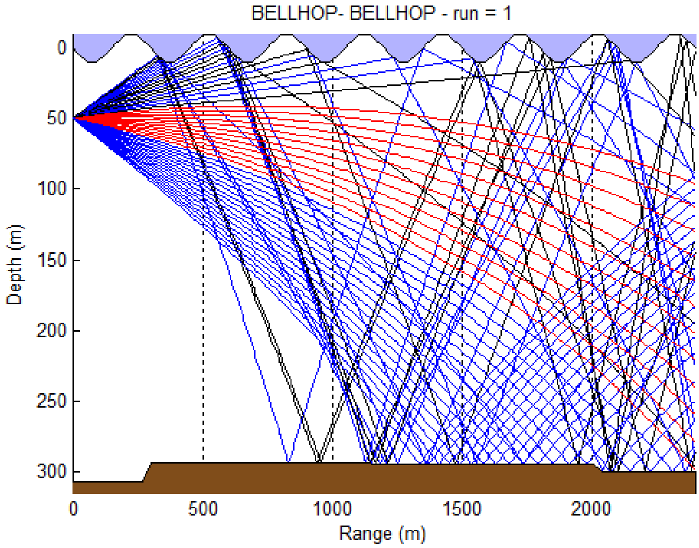

Figure 3.11 Plotting ray files (with ATI and BTY also)

The *.shd file contains the acoustic pressure, which can be calculated in a coherent, incoherent or semi-coherent way. Figure 3.12 shows a coherent execution. The pattern of the pressure fits with the ray plot.

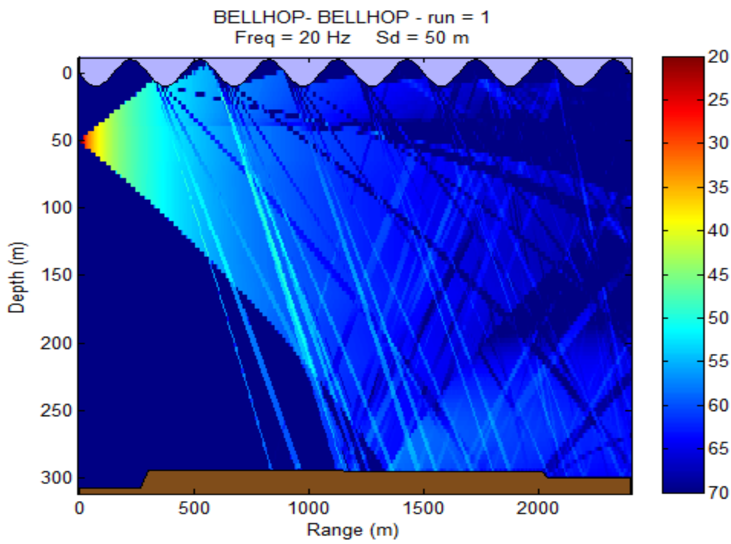

Figure 3.12 Plotting SHD file (with ATI and BTY)

The *.arr file contains the information of the amplitude and travel times of the rays that arrive at the receiver position. In Figure 3.13, we plot the arrival times depending on the node depths.

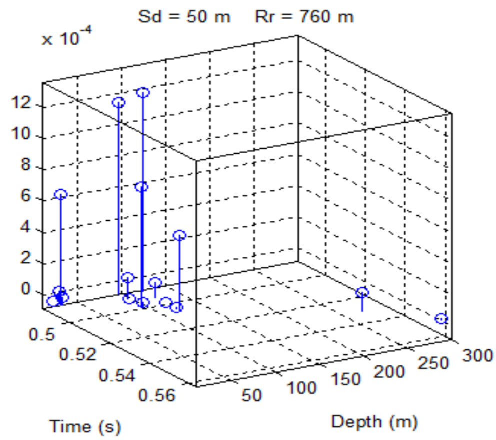

Figure 3.13 Plotting ARR files

As default, OPNET lets export the network to other presentation formats, such as Spreadsheet, Visio or XML; and with a plug-in, the network deployment can also be exported to Google Earth, where a realistic vision of the scenario with the nodes is displayed. Also, where available, Google Earth includes an ocean layer with the ocean bathymetry.

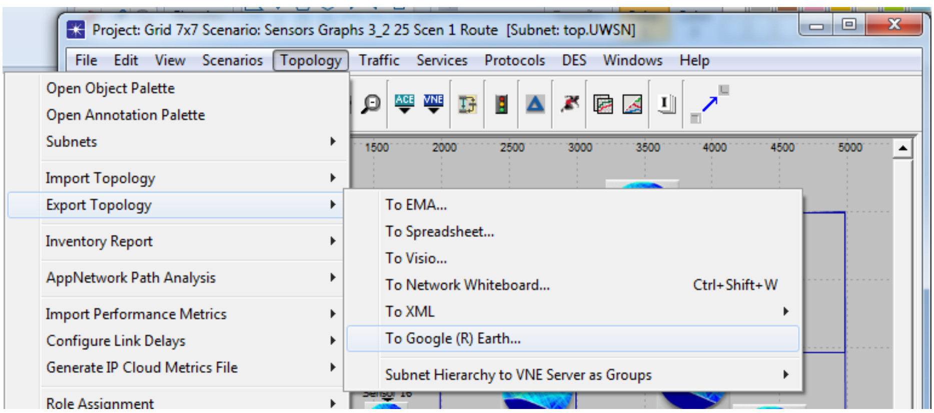

Figure 3.14 Simulator export to Google Earth

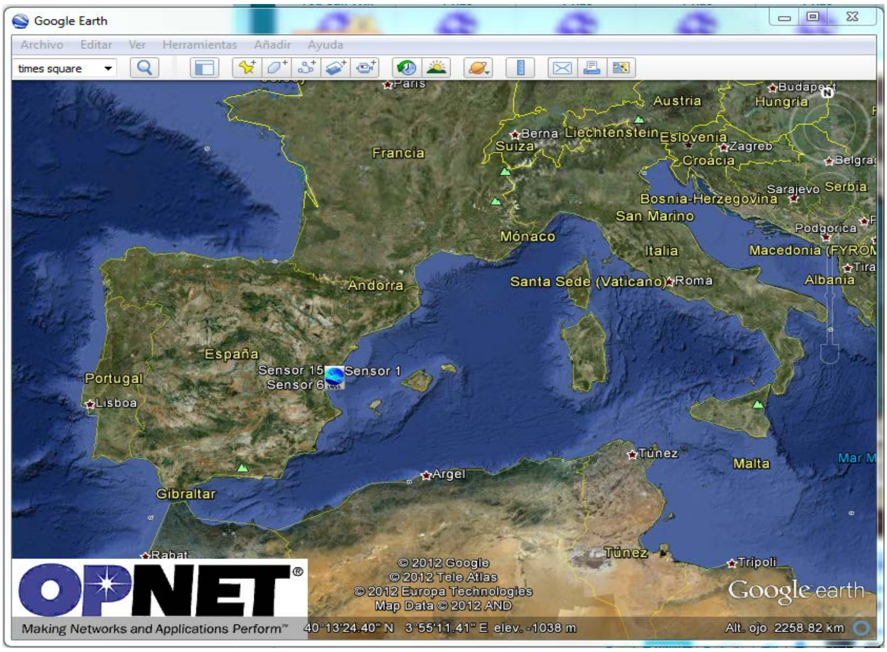

Figure 3.15 Google Earth network location

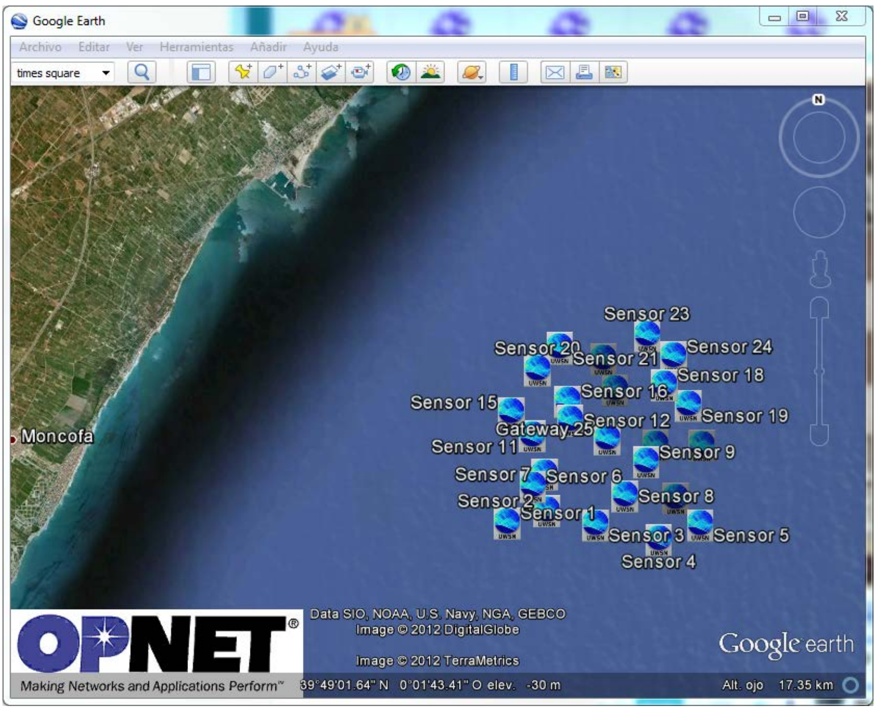

Figure 3.16 Google Earth network deployment

Figure 3.15 and Figure 3.16 show the OPNET deployment in Google Earth where a real 3D vision of the network topology may be displayed, so the real distance of the nodes to the sea floor can be checked and a better node deployment could be done.

3.6 Simulation Scenarios

For testing the simulator, the same node deployment network (shown in Figure 3.16) within a range 5000 meters has been placed at several world locations. The depths of the nodes will vary depending on the scenario we simulate, depending if we are in a shallow or deep part of the ocean.

Here we show the results for three different locations. In each one of them, the environmental conditions differ for the bathymetry, the sound speed profile, the sediment floor, and the altimetry base on the wave parameters. They try to differ as much as possible to see the different results that can be obtained with different circumstances.

3.6.1 Valencia – Spain

The first one is placed at coordinates 39°48'13.14"N and 0° 4'34.53"W. The node depth varies from 5 to 20 meters, with the wave height of 0.5 meters and wave length of 80 meters.

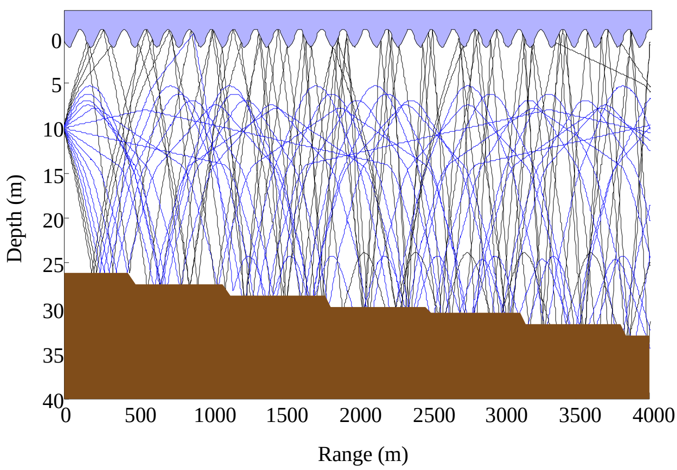

Figure 3.17 Bellhop ray result in Valencia

This is an example of shallow waters with a low altimetry shape. The sediment floor of the bottom of the scenario is gravel. We can see the node deployment in Google Earth and the result for the Bellhop ray execution.

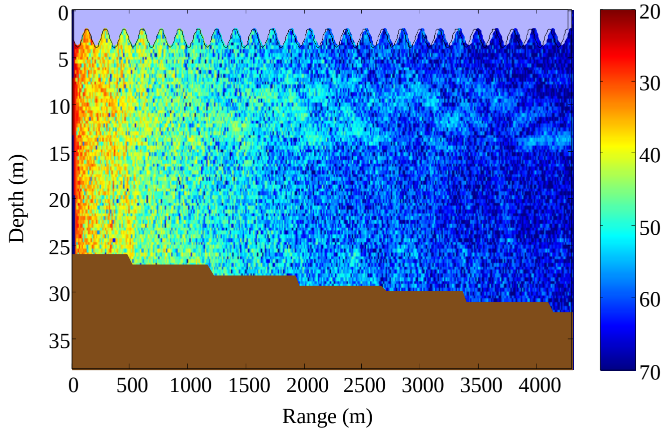

Figure 3.18 Transmission loss (dB) in Valencia

The result is a slow variation of the depth in the scenario as the nodes are father from the coast and how the rays reflect a great number of times in the bottom and the ceiling. It is very important to appreciate that the attenuation values in Figure 3.18 vary not only with the distance but also with the depth. This is valuable information that has been deprecated in many simulator proposals.

The nodes in Valencia are shown in Figure 3.16. This example could represent a typical network scenario close to the coast.

3.6.2 Hawaii – USA

This is at coordinates 20°39'13.10"N and 156°44'39.84"W. The node depth varies from 10 to 300 meters with a wave height 20 meters and wave length 200 meters. This is an example of middle case water with a high altimetry shape. The sediment floor in this region is ooze. We can see the map location and the results in what follows.

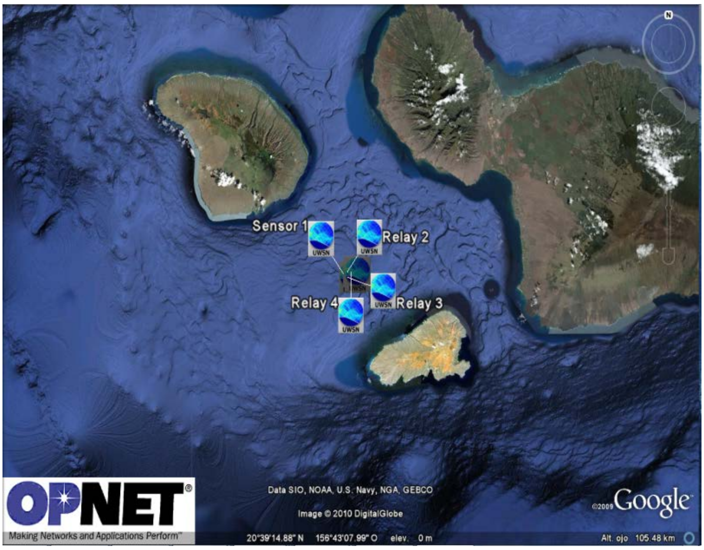

Figure 3.19 Nodes in Hawaii

With this pattern scenario, the rays travel having fewer reflections against the waves and the floor than in the previous one, just because the seafloor is farther than in the previous scenario. It is interesting to see in both Figure 3.20 and Figure 3.21 the shadow zone below the node that transmits the signal, the attenuation difference at different depths again, and the effect of the ocean waves.

This scenario is representative for a network deployed within the surroundings of a group of islands.

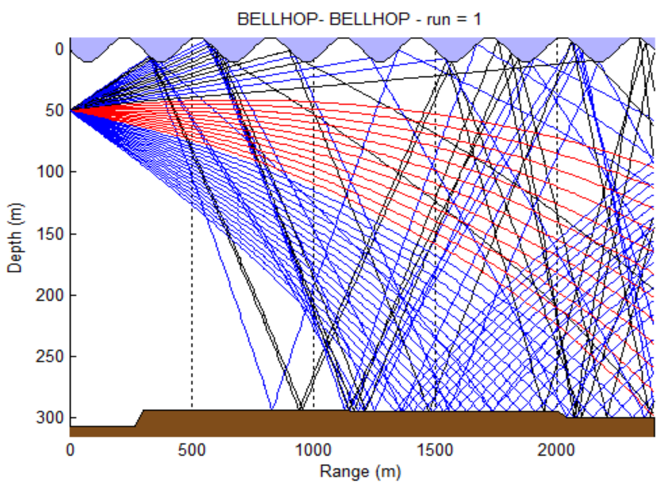

Figure 3.20 Bellhop ray result in Hawaii

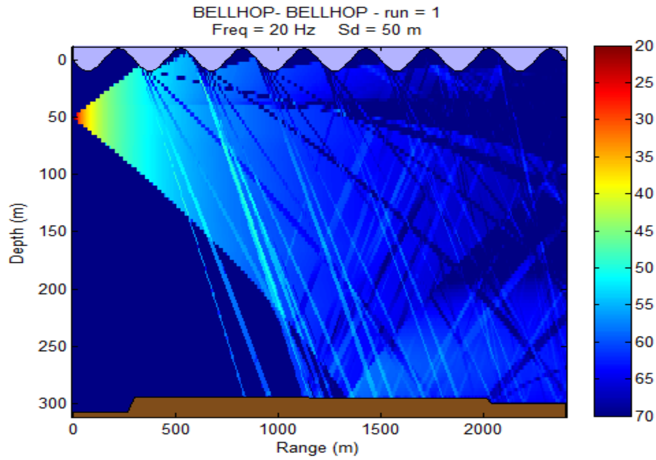

Figure 3.21 Transmission loss (dB) in Hawaii

3.6.3 Random Location – Atlantic Ocean

Finally, a random location to test a deep water location is shown at coordinates 4°52'4.80"N and 34°57'0.00"W. The node depth varies between 250 and 2000 meters. The waves shape is 10 meters for the wave height and 100 meters for the wave length. The sediment floor in this region is mud and organic. In the map in Figure 3.22, we see the Atlantic Ocean between South America and Africa.

Figure 3.22 Nodes in the Atlantic Ocean

This scenario tries to show a network far away from the coast, without obstacles at either at the front or on the seafloor.

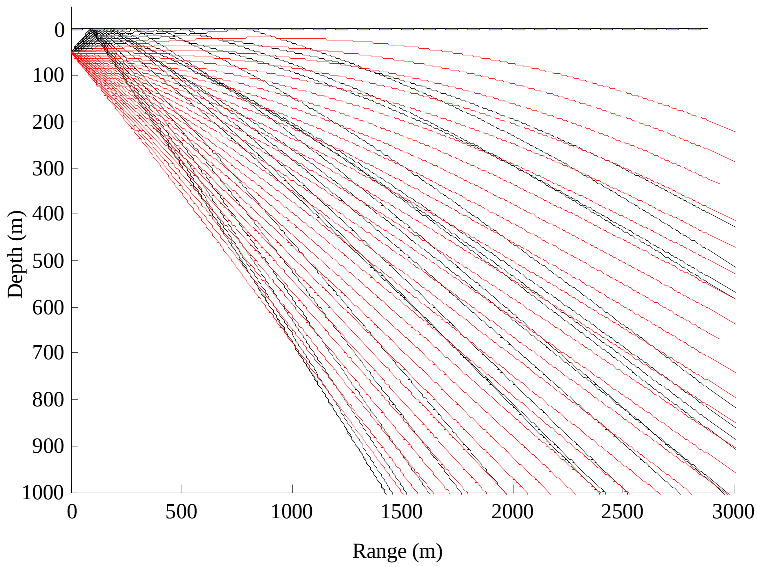

Figure 3.23 Bellhop Ray result in the Atlantic Ocean

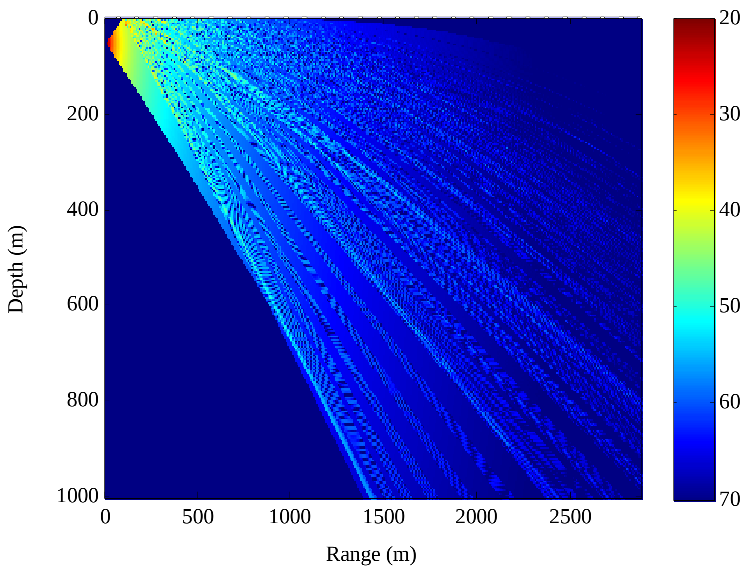

Figure 3.24 Transmission loss (dB) in the Atlantic Ocean

This time the source and receivers are far from the bottom and waves and so they do not have a great effect on the way the rays behave as there are no reflections. Once more, while the signal advances in distance, a different attenuation is observed depending on the receiver depth.

3.7 Simulation Test

In [35], the taxonomy of UWSN regimes is outlined. They classify different UWSNs in terms of both spatial coverage and node density. For every kind of network topology, different architectural approaches have to be considered in order to improve the network performance (throughput, delay, power consumption, packet loss, etc.). Therefore, it is important to design the network architecture taking into account the intended network topology.

Figure 3.25 Network deployment

The same simple network deployment (Figure 3.25), picked from the test realized with MMPE in [66] is placed in the different scenarios, chosen for the previous simulation test. Five sensor nodes generate the network traffic load, two relay nodes only forward packets and there is one sink node that receives the information from the sensors. The distances between nodes vary between 1300 and 1500 meters.

The purpose of the simulation tests is to run a simple MAC protocol such as ALOHA in all the different scenarios with different conditions in order to analyze the simulation tool behavior. This will lead us to the conclusion of how important it is to have a realistic simulator to test new protocols and validate them under multiple conditions where it can be involved.

Parameter	Valencia	Hawaii	Atlantic
Propagation Model		BELLHOP	
Wave Height (meters)	0.5	2	6
Wave Length (meters)	25	100	150
Node Depth (meters)	15	50	50
Scenario Depth (depth)	26	300	5000
Seafloor Sediment	Gravel	Ooze	Mud / Organic
Frequency (kHz)		10	
Pkt Interarrival Time (s)		5 to 1000	
Month		Annual Average	
Data Packet Size (bits)		1024	
Bandwidth (kbps)		5	
Simulation Time (min)		180	

Table 3.5 Parameters in simulations

The simulation duration is 3 hours, which last between 4 and 6 minutes in computational time in an Intel ® Core™ 2 Duo T8100 2.10 GHz with 3 GB of RAM memory. The main performance metrics we will show are network collisions and gateway throughput. The water temperature values are an annual average for each network escenario. The most significant parameters used for the simulations appear in Table 3.5.

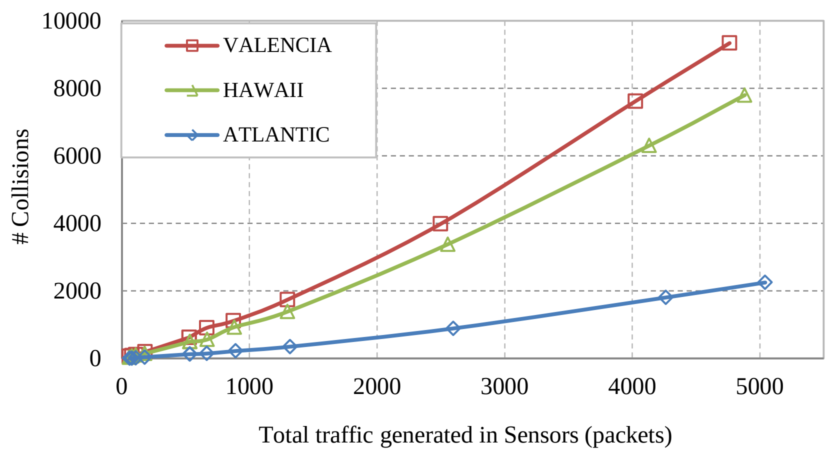

Figure 3.26 Collisions in different scenarios

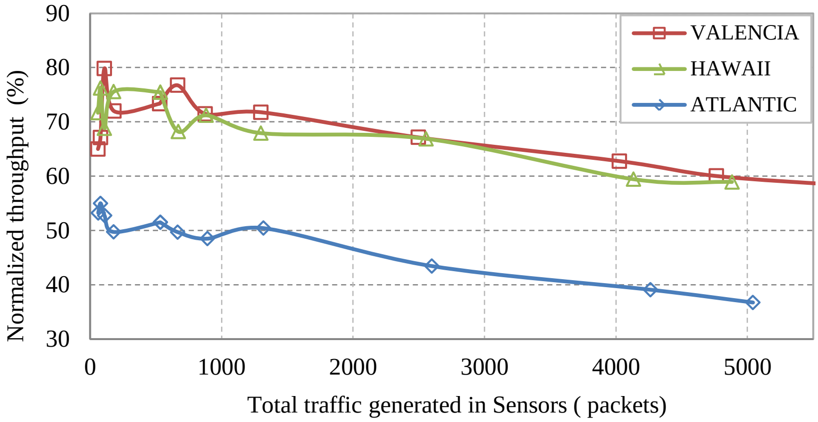

Figure 3.27 Normalized throughput in different scenarios

As expected, even though the same network deployment is used, the simulation results will differ from one scenario to another, as can be seen in Figure 3.26 and Figure 3.27. Apart from using different locations, the protocol has been tested under different conditions (for instance, the wave shape is different for each scenario).

We capture the total number of collisions in all the scenarios; 15 simulations per traffic load have been conducted for each scenario. In the first case (Valencia), where the ocean wave surface has low values, it has less effect on the transmission loss and thus the reachability is bigger. This behavior has a direct influence in the collisions, as more nodes are reached, more collisions appear. We also evaluate the normalized throughput in the gateway (packets received in gateway node divided by all packets generated in the five sensor nodes).

As a result of using the Aloha protocol, the normalized throughput falls as the generation of packets increases. It is noteworthy that the scenario with fewer collisions is also the one with less throughput. This happens because the node signal can reach less neighbors and despite generating the same number of packets, there are fewer packets traveling in the medium and thus less overall traffic. For instance, during a single simulation, the average number of reachable neighbors for Relay 6 for Valencia is around four; in Hawaii this is between four and three, and in the Atlantic Ocean around two. Nevertheless, the important point from these graphs is not the behavior of the MAC protocol but rather the difference of using the same MAC protocol with the same network parameters under different environmental conditions and thus there are different results.

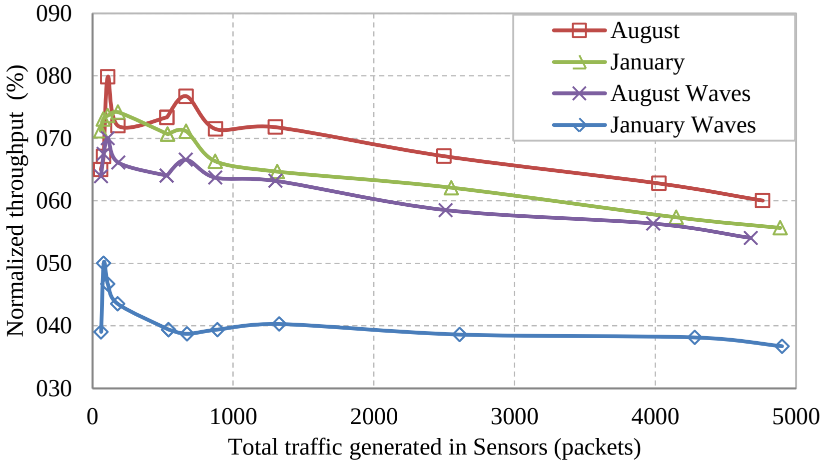

Figure 3.28 Normalized throughput in Valencia (Season & Waves)

Now to emphasize the environmental effects, we choose one single scenario and run different simulations with changing conditions. We have done simulations for every month of the year and with multiple wave shapes for a total of 900 simulations (12 months and 5 ocean wave shapes and 15 traffic loads). In the graph shown in Figure 3.28, we only show two months (January and August) and each one with and without wave effect to highlight both characteristics and their influence. The shape of the ocean waves in the scenarios that include this effect are 2 meters in height and 80 meters in length.

From Figure 3.28, we can infer that there is a small difference between the simulations of January and August without the wave effect. There is also a slightly higher variation in the results when comparing the normal August scenario against the same month with waves. However, we can observe that throughput results get considerably worse when combining the month of January and the wave effect. So we can conclude that in this particular case of shallow water where the temperature variation is greater than in deeper scenarios (see Figure 2.1), the effect of the season is appreciable and its combination with the ocean waves can completely change the network performance.

3.8 Conclusions

We have presented a powerful simulator tool to model underwater network scenarios all around the world. Simply using the simulator to place the network will automatically generate the whole scenario, extracting the necessary information to build the environmental conditions as well as the wave pattern from the databases. The interface can be used by non-developer users, as it is easy to configure all the parameters and possibilities offered; this is an advantage over other proposals where in order to run a simulation there is a need to introduce the simulator and its implementation to the users.

Although the simulator is accurate enough with the acoustic signal behavior, as we can define a huge amount of parameters, it is necessary to achieve a trade-off between accuracy and simulation complexity in order to find a middle point where simulation results are precise enough for our purposes and the required time to obtain them is reasonably short. This is one of the greatest challenges for future work and subsequent simulator improvements. Reducing the simulation times will let us extensively do benchmarks in reasonable times and, as a consequence, the simulator scalability will increase.

As previously mentioned, the importance of testing new protocol proposals not only under ideal conditions, but also when the physical parameters have a great impact on the performance is an essential point for validating our proposals in scenarios very close to real ones.

Chapter 4
Statistical Prediction Model

4.1 Introduction

The growing need for ocean observation and remote sensing has recently motivated a surge in research publications as well as several experimental efforts (e.g. [43]) in the area of underwater acoustic networks (UANs).

Crucial to UAN development is the understanding of propagation conditions that define the time-varying and location-sensitive acoustic environment, not only from the viewpoint of small-scale, rapid signal fluctuations that affect the performance of the physical layer techniques, but also from the viewpoint of large-scale, slow fluctuations of the received signal power that affect the performance of higher network layers.

This fact has been gaining recognition in the research community, leading to increased awareness about the need for network simulators that take into account the physics of acoustic propagation [43], [19] and [66]. As a result, the first publicly available acoustic network simulators have emerged [20], and more are likely to come.

One of the challenges in the design of underwater acoustic networks is the allocation of power across different network nodes. This task is exacerbated by the spatial and temporal variation of the large-scale transmission loss (TL), and the lack of statistical models that capture these apparently random phenomena.

While it is well known from field experiments that the received power varies in time around the nominal value predicted by a deterministic propagation model, little is known about the statistical nature of these variations. Literature on this topic is scarce; however, several recent references indicate that the received signal strength obeys a log-normal distribution (e.g. [59] [67] [29]). A good system design has to budget for signal strength variations in order to ensure a desired level of network performance (e.g. connectivity), and the budgeting task can be made much easier if the statistics of the underlying process are known.

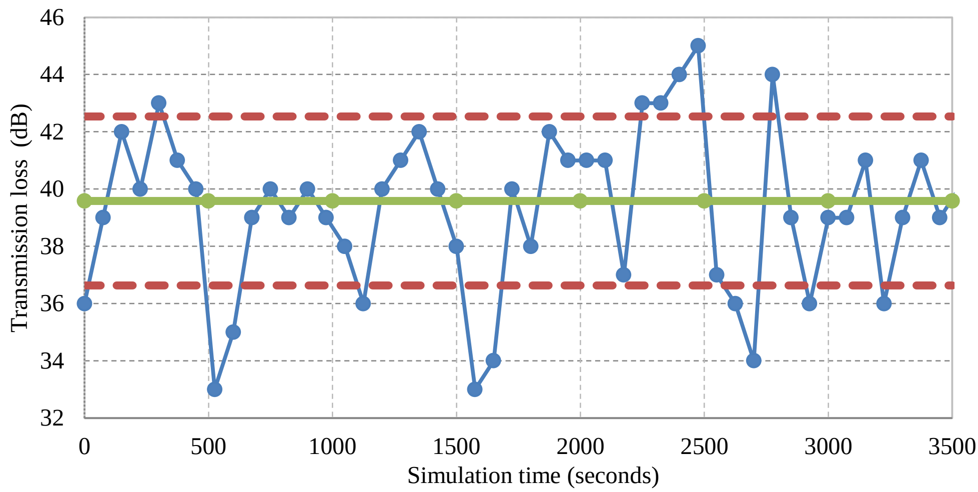

Figure 4.1 An ensemble of transmission losses calculated by the Bellhop model. The solid line indicates the average calculated over the total run time. Dashed lines indicate the values of one standard deviation σ

In this thesis, we analyze those random variations in the large-scale transmission loss that are mainly governed by environmental factors, such as surface activity (waves) for a particular network scenario. We begin by employing a prediction model based on the Bellhop ray tracing tool [41]. Such a deterministic model provides accurate results for a specific geometry of the system, but does not reflect the changes that occur as the geometry changes slightly due to either surface motion or transmitter/receiver motion. Figure 4.1 illustrates this situation for a point-to-point link. It shows an ensemble of transmission losses calculated by the Bellhop model for a set of varying surface conditions, each slightly different from the nominal.

While it is possible in principle to run a deterministic propagation model for a large number of different surface conditions, the underlying computational demands are high. In a large network, it is ineffective, and possibly not even feasible, to run a complex prediction model for each packet transmission. A statistical prediction model then becomes necessary.

The goal of our work is to employ an existing deterministic prediction model (DPM) such as the ray tracer [40] to generate an ensemble of channel responses corresponding to varying propagation conditions in a given network scenario. Using the so-obtained values, we then conduct a statistical analysis to obtain the probability density function (pdf) of the large-scale transmission loss. The result is a statistical prediction model (SPM) that is easy to employ for network design and analysis.

Then, the SPM model would be easily integrated in the network simulation tool to reproduce the acoustic signal attenuation map of the network scenario, resulting in a significant reduction in the overall simulation complexity with acceptable prediction accuracy when comparing with the one obtained through the deterministic prediction model. As a consequence, the SPM model enables computationally-efficient inclusion of fading effects into the network simulator. Namely, to assess the average system performance, network operation has to be simulated over a large set of channel realizations (e.g. varying surface conditions).

Whereas repeated computation of the ray trace for different hops that each of the data packets traverses in a given network may be computationally prohibitive, statistical modeling requires only a single call to the Gaussian random generator for each packet transmission.

Thus, the overall simulation time is considerably reduced, allowing a system designer to freely experiment with different network protocols and resource allocation strategies in an efficient manner.

The ultimate goal of such computational experiments is to choose the best upper-layer protocol suite and to relate the necessary system resources (power, bandwidth) to the propagation conditions, i.e. to the statistical parameters of the transmission loss.

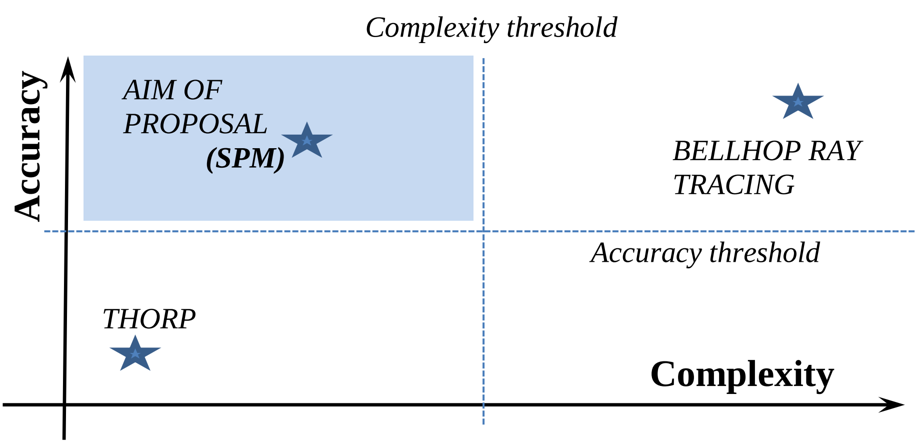

Figure 4.2 Tradeoff between model propagation accuracy and computational complexity

Tradeoff between model complexity and accuracy is shown in Figure 4.2. In this figure, we also define the thresholds for the minimum desirable accuracy and complexity. So, the shaded area covers those propagation models with the minimum acceptable model propagation accuracy that leads to reliable prediction results and, at the same time, low computational complexity overhead to perform detailed and scalable network simulations.

4.2 System Set Up

Now, we are going to define the overall system where we have developed our study. First, we will define the geographical location and dimensions of the network scenario, including the environmental parameters like bathymetry, floor sediment composition, sound speed profile, water temperature and surface wave activity, among others, that could be found in global ocean databases [33], [18] and [64]. Then network specific parameters are defined like network topology, number of nodes, signal frequency and transmission range. Also, we have described a simple model representing the random movement of network nodes anchored to the floor mainly due to marine currents or tides. And finally, we describe the computational resources used to obtain all the results we have employed to build the statistical model approach.

The network of interest is located in coastal waters near Valencia, Spain at coordinates 39°48'13.14"N and 0°4'34.53"W. It consists of eight nodes arranged in a linear topology, as illustrated in Figure 4.3.

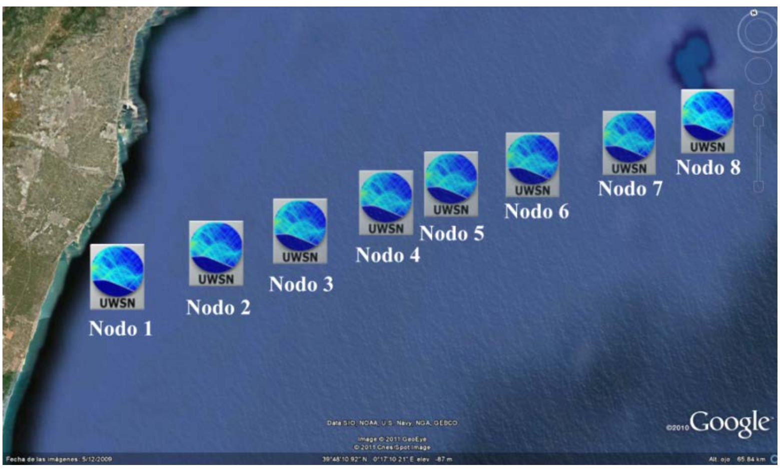

Figure 4.3 Network deployment in Valencia, Spain

For our purposes, the source is assumed to be at one end, and the rest of the nodes are placed at different distances ranging from 500 m to 3700 m. All nodes are anchored to the ocean floor in such a way that their depth is 10 meters, while the water depth varies from 25 m to 35 m within the network scenario of 5000 x 5000 m^2. If we desire to employ a different network scenario, the procedure would be the same, since all network scenario and environmental parameters could be obtained from on-line global databases and the rest of parameters may be fixed in our simulation framework. We assume a fixed network topology, and vary the parameters related to the surface wave activity (wave height and wave length). The surface parameters are taken from historical and prediction values from National Geophysical Data Center databases [31] and [42].

We also account for the fact that an acoustic communication signal does not consist of a single frequency, but occupies a (possibly wide) certain bandwidth as a result of the acoustic signal modulation employed. The overall transmission loss is computed along the whole network scenario by running the DPM with the Bellhop. Each DPM simulation run produces the acoustic field values in a 5 km x 5 km x 30 m volume, with a resolution of 0.33 m^3. The values corresponding to selected receiving node locations are then extracted, and a statistical analysis is performed for each position.

To compute the transmission loss, we have used two different approaches: (1) assuming single frequency acoustic signals, where several experiments were performed with frequency ranging from 5 to 80 kHz; and (2) assuming a more realistic approach taking as reference the Evologics Modems technical data sheet [14] to choose the center frequency and the bandwidth of three different frequency bands, a low-frequency band of 5-15 kHz (S2C R 8/16 modem), a mid-frequency band of 20-34 kHz (S2C R 18/34) and the high-frequency one of 50-75 kHz.

Although the network topology is fixed, i.e. node position is always the same, we have considered, as explained before, that all the network nodes have a random oscillatory mobility (typically larger in horizontal than in vertical direction) due to the nature of the underwater environment and the anchor system. The movement is typically slow and constrained to a specific water volume around the reference placement location. In order to simplify the proposed node mobility model, we will consider that the anchored node may be at whatever point inside the virtual box of dimensions Range x Range x Depth as shown in Figure 4.4.

Node movement virtual boxes
(range x range x depth)

Range	Depth
3 m	0.9 m
5 m	1.5 m
7 m	2.1 m

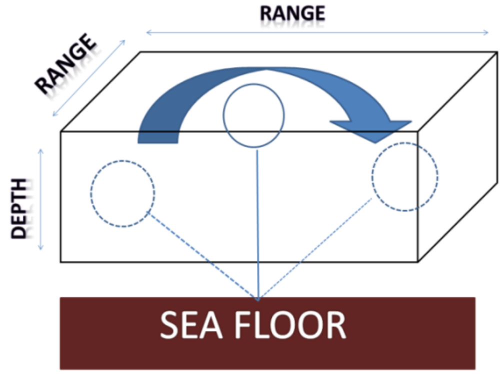

Figure 4.4 Network node movement model

For each experiment, all network nodes employ the same power transmission. Table 4.1 summarizes the fixed and variable system parameters used in the simulation experiment.

Parameter	Value
Transmission range	500 m to 3700 m (in steps of ~500 m)
Area	5000 m x 5000 m
Sediment floor	Gravel
Month	August
Wave height (m)	1 m to 3 m (in steps of 0.15 m)
Wave length (m)	100 m to 150 m (in steps of 3.5 m)
Frequency (kHz)	5 to 80 kHz (in steps of 5 kHz) [5-15][20-34][50-75] kHz (in steps of 1 kHz)
Scenario depth (m)	25-35
Global load (packets/s)	5
Data packet size (bits)	1024
Control packet size (bits)	24
Simulation time (s)	3600

Table 4.1 System parameters

The hardware used to run all the simulations is a cluster of computers that consist of 6 nodes, each one with 4 CPUs of 1 GHz and 8 GB of RAM, a total of 24 cores, all governed by Rocks Cluster OS version 4.3 [44] and using Condor Project software version 6.8.5 [63] to manage the parallel DPM model simulations.

Each execution of the Bellhop tool [41] takes about 5 minutes on a single CPU. Considering 14 different wave heights and 14 different wave lengths, i.e. 196 different scenarios, and 56 different frequencies (5-15, 20-34, 50-75, 35, 40, 45 and 80 kHz), a total of more than 10,000 simulations were performed, about 40 hours, to obtain all the data we used for our statistical analysis.

4.3 Statistical Prediction Model

We have introduced the fact that an ensemble of transmission loss values calculated varying the physical conditions along a range of frequencies obeys a log-normal distribution. The statistical model proposal is an attempt to replace this heavy computational process with a simple expression that offers transmission loss predictions as reliable as the propagation model. The study of the log-normal requires focusing on both of the parameters required to build the distribution, the mean (μ) and standard deviation (σ). Both parameters will depend on the distance, *d*, and the acoustic signal frequency, *f*.

$$SPM(d,f) = \mu(d,f) + \sigma(d,f) \tag{4-1}$$

4.3.1 Mean Value

The study of the mean value of the expression requires following an accurate process to calculate the expression as it is going to be the base value within the whole formula. We start with a quick comparison between the two present alternatives, Thorp's formula and the Bellhop ray tracing tool (DPM) in the selected scenario with the parameters found in Table 4.1.

It may be observed that the Bellhop model offers a much more realistic description of the acoustic signal propagation than the simple Thorp's model. In order to statistically predict the results of the DPM model into a new formula, we have chosen a range of frequencies from 5 to 80 kHz in steps of 5, each of them combined with 196 different surfaces.

In Figure 4.5, we have shown the attenuation map of both propagation models at different frequencies of 10, 20, 30, 50 and 70 kHz.

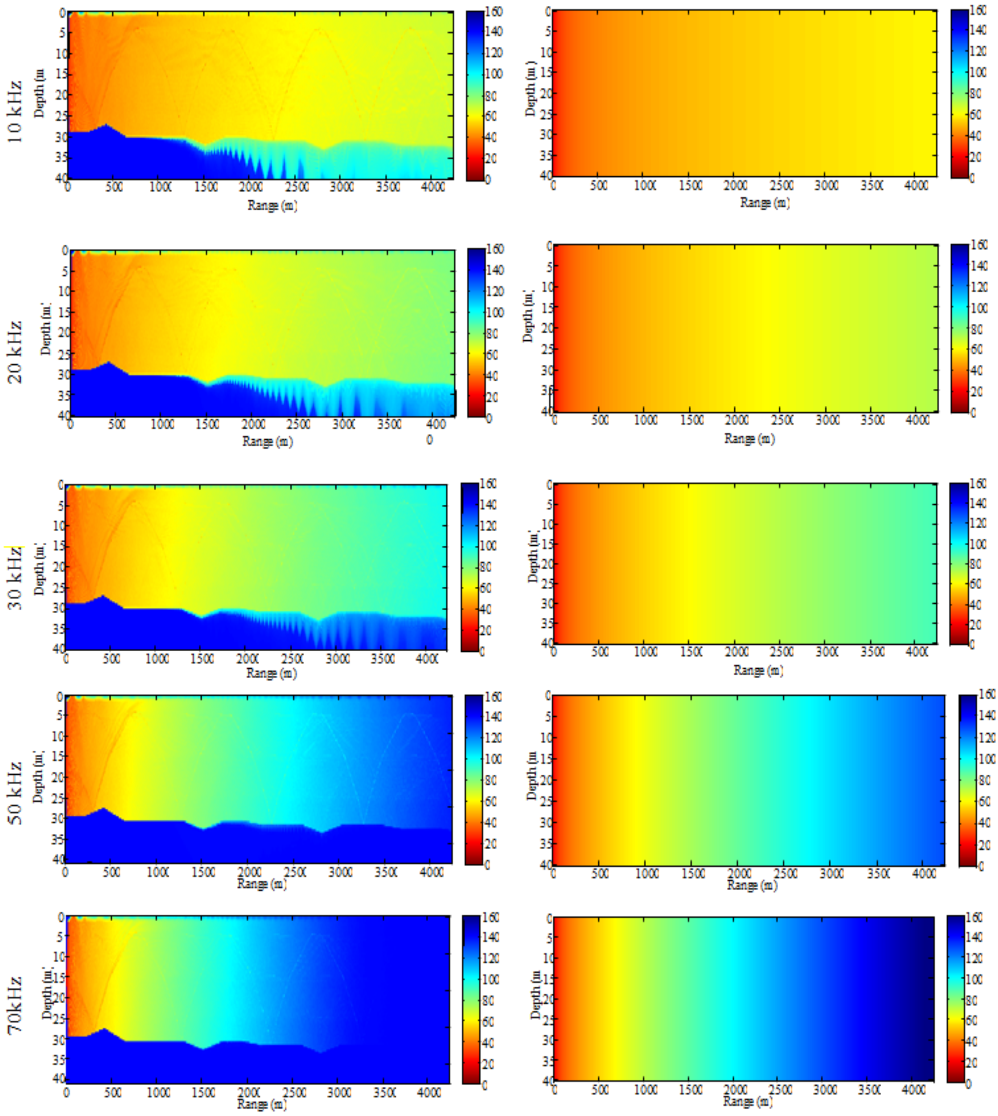

Figure 4.5 Attenuation map at different frequencies, Bellhop (left column), Thorp’s (right column)

In order to perform the mean transmission loss estimation, we have employed the Surface Fitting Tool from MATLAB R2011a [30]. The parameters employed to perform the surface fitting with a polynomial approximation are distance and frequency. In order to get a good fitting with a low complexity formula, we established the distance (*d*) variable to degree 2 and frequency (*f*) to lineal degree.

Achieving a coefficient of determination (R^2) of 0.96, the single frequency mean, *sfμ(d,f)*, is obtained with the formula in the next formula:

$$sf\mu(d,f) = k_1 d^2 + k_2 d + k_3 df + k_4 f + k_5 \quad (4\text{-}2)$$

$k_1 = -0.0000012,\ k_2 = 0.007766,\ k_3 = 0.0002786,\ k_4 = 0.0332,\ k_5 = 36.6$

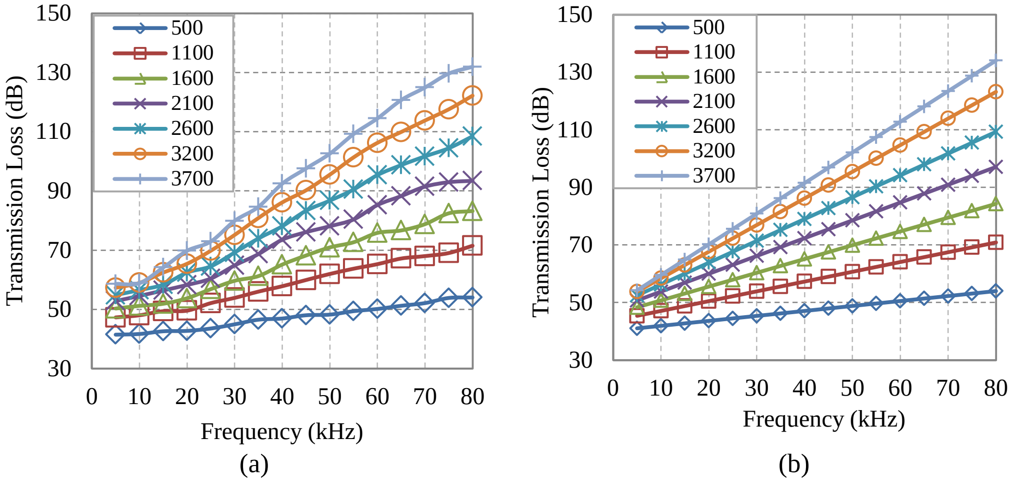

Figure 4.6 Average transmission loss evolution through frequency: (a) Bellhop, (b) SPM mean

In Figure 4.6, we show the plots representing the average transmission loss (*sfμ*) at different values of frequency and distance supplied by (a) the Bellhop model, and (b) the statistical prediction model (SPM) defined in expression(4-2). In order to determine the introduced error, we calculate the average error of all frequencies at a particular distance. In Figure 4.7, the average error introduced by SPM, in dBs, is shown. As can be observed the SPM precision is reduced as distance increases, as expected, the committed error always being under 1.6 dB.

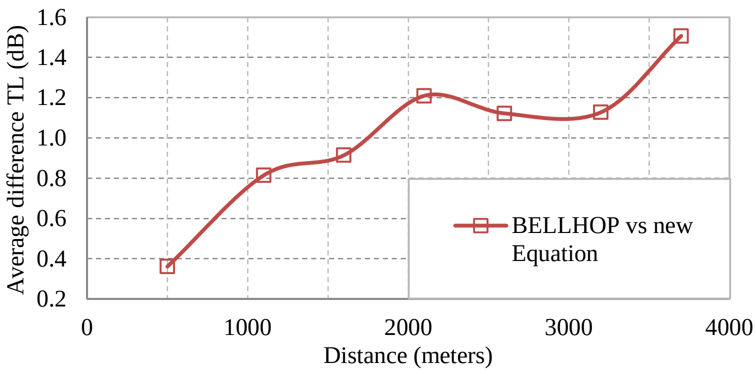

Figure 4.7 SPM average error with respect to the Bellhop model as a function of distance

Now, we are going to extend the single frequency SPM model to acoustic signals with a particular bandwidth, a more realistic approach since real implementations perform signal modulations that produce a specific bandwidth, not a single frequency response.

The process to obtain the average transmission loss (signal attenuation values) out of a range of frequencies is done as follows: for each spatial position in the network scenario, we calculate the inverse of the attenuation values for each single frequency composing the desired bandwidth, and then we obtain their average, the final attenuation being its inverse. In expression (3) we define the general expression and an example for a bandwidth of 5-15 kHz (composed by 11 single frequencies 1 kHz spaced) to calculate the overall attenuation (*A*).

$$\frac{1}{A_R} = \left[\frac{1}{A_1} + \frac{1}{A_2} + \frac{1}{A_3} + \frac{1}{A_4} + \cdots + \frac{1}{A_N}\right] / N$$
$$\frac{1}{A_{5-15}} = \left[\frac{1}{A_5} + \frac{1}{A_6} + \frac{1}{A_7} + \frac{1}{A_8} + \cdots + \frac{1}{A_{15}}\right] / 11 \qquad (4\text{-}3)$$

Now, the transmission loss corresponding with the three frequency bands are plotted together with the transmission loss of their central frequencies calculated with the expression (4-2). At 5-15 kHz we have a bandwidth of 11 frequencies, at 20-34 kHz there are 14 frequencies and 25 in the 50-75 kHz band. So, for each one we select their corresponding central frequencies of 10, 27 and 62.5, respectively.

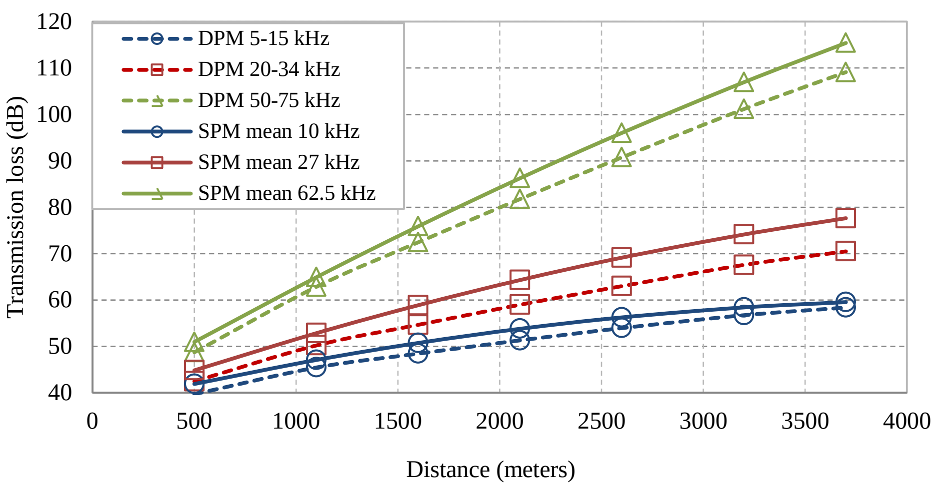

Figure 4.8 Attenuation in set of frequencies at DPM vs. SPM proposal

As expected, Figure 4.8 lets us find out that the proposal is not valid when we use a range of frequencies to establish the attenuation values using the proposed formula in (4-2). The set of 5-15, 20-34 and 50-75 kHz frequency values are always below the ones obtained by the SPM mean formula with the single frequencies of 10, 27 and 62.5 kHz, and difference increases with the bandwidth.

So we add a bandwidth correction factor, *bcf(d,b)*, to the original formula using the distance (d) and bandwidth (b) as parameters. The fitting of the bandwidth correction factor is divided in two expressions: one is a Fourier fitting for bandwidth below 14 kHz with an R^2 of 0.74, and a polynomial fitting of degree one for bandwidth over 14 kHz, leaving the final formula also divided in two parts, one for a single frequency and the other for a center frequency with a bandwidth:

$$bcf(d,b) = \begin{cases} k_6 + k_7 \cos(d * k_8) + k_9 \sin(d * k_8), & b < 14 \\ k_{10} + k_{11}\, b + k_{12}\, d, & b \geq 14 \end{cases}$$

$$k_6 = 2.076,\ k_7 = 0.4811,\ k_8 = 0.002528,\ k_9 = -0.2722, \quad (4\text{-}4)$$
$$k_{10} = 2.547,\ k_{11} = -0.06234,\ k_{12} = 0.001532$$

$$\mu(d,f) = \begin{cases} sfu(d,f), & b = 1 \\ sfu(d,f) - bcf(b), & b > 1 \end{cases}$$

We can plot the results again with the correction factor included in Figure 4.9.

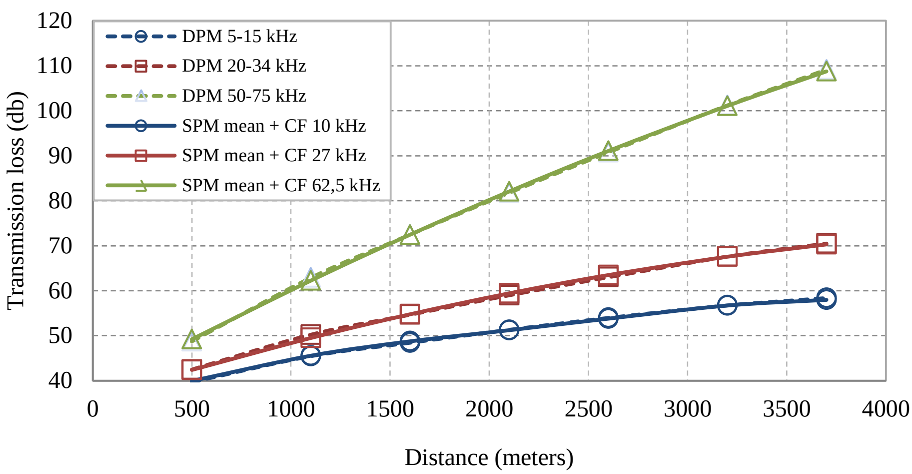

Figure 4.9 Attenuation in a set of DPM frequencies versus the SPM proposal

Now we have a formula that can fit both cases, single frequency and sets of frequencies (frequency bands) with a different bandwidth range. It is time now to introduce a new parameter in the equation, the node movement explained in Section 4.2 and Figure 4.4.

We apply the three types of node movement that have been defined in depth and range to 5-15 kHz (center frequency 10 and bandwidth 11 kHz) at every position in the scenario, and we compare the static results versus the ones including the movement displayed in Figure 4.10.

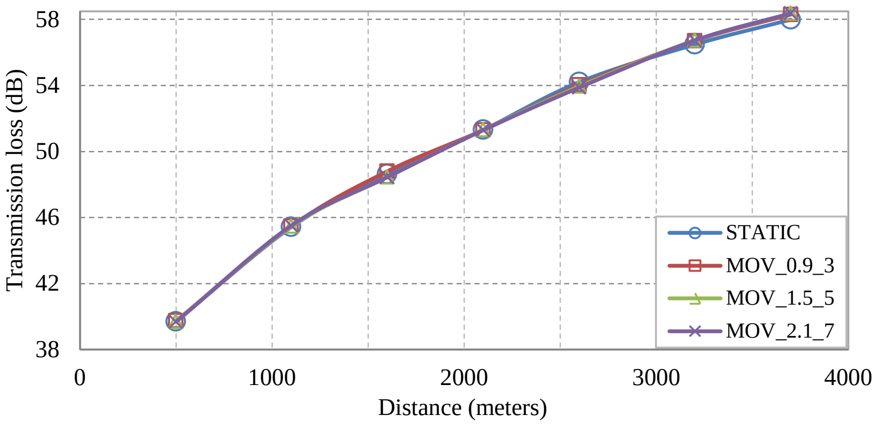

Figure 4.10 Attenuation versus distance with different node movement 5-15 kHz

It is clearly shown that the node movement has no effect on the mean value, where the average and maximum differences are 0.07 and 0.38 dB, respectively. The same behavior happens at the other frequencies; at 20-34 kHz, the average and maximum differences are 0.08 and 0.53, respectively; and at 50-75 kHz, the average difference is 0.1 dB and the maximum 0.49 dB, something we consider a non-significant error in the computation of the mean attenuation value, so the formula remains as in (4-4).

4.3.2 Standard Deviation Value

The study of the Standard Deviation Value (σ) is essential for obtaining a statistical expression that would accurately describe the behavior shown in Figure 4.1. The objective is that the expression experience the same variability around the nominal (mean) attenuation value found at a particular spatial location inside network scenario. This would lead to more realistic attenuation predictions that are caused by environmental parameters like surface wave activity. In Figure

4.11, a network scenario with 25 network nodes is shown. If a static prediction model is used, like Thorp's model, the transmission range for node #1 will be always the same - represented by the solid-line circle in Figure 4.11 (a) and, as a consequence, the reachable neighbors will be the same during the entire simulation time. However, in Figure 4.11 (b) when the Bellhop propagation model is used, the effective transmission range is variable – represented by the disjointed area of the two dashed-line circles – so the reachable neighborhood is also variable during the entire simulation time. So, our statistical approach needs to represent the same variability found in the Bellhop model, being very important to estimate the proper standard deviation value, σ, so the reachability to other nodes will change during the simulation with a similar distribution like the one found with the Bellhop model.

In order to study *σ*, we will use the same set of frequencies as the ones used in the previous section, 5-15 kHz, 20-34 kHz and 50-75 kHz, as well as the same node movement model described in Figure 4.4.

We have run the Bellhop model with the same network scenario, the parameters found in Table 4.1, and the simulation of node movement model described earlier, to obtain the evolution of standard deviation values as a function of the distance. The different curves represented in Figure 4.12 (a), (b), and (c) correspond with the static node approach and the three node movement configurations described earlier for acoustic signal bands of 5-15 kHz, 20-34 kHz, and 50-75 kHz, respectively.

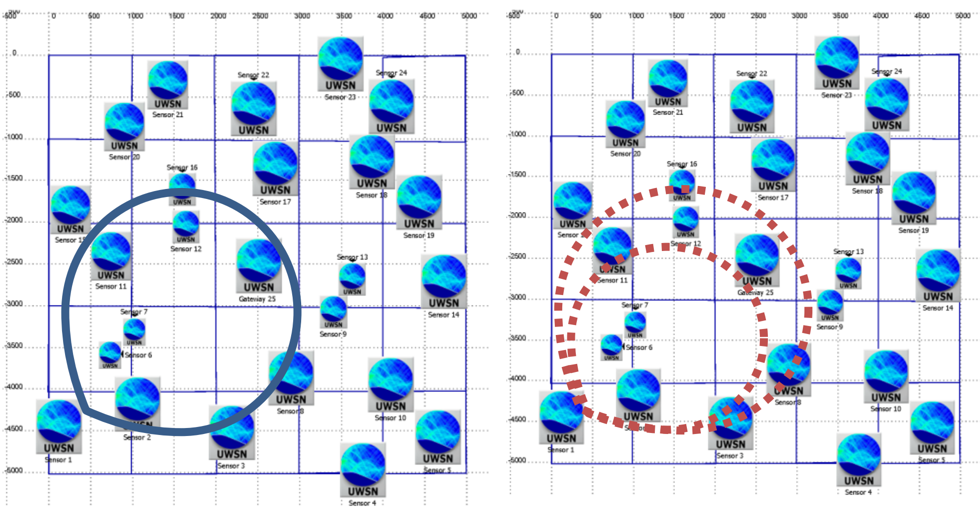

(**a**) Thorp (**b**) Bellhop

Figure 4.11 Gateway reachability (central node) from Node #1 (farthest left on the bottom)

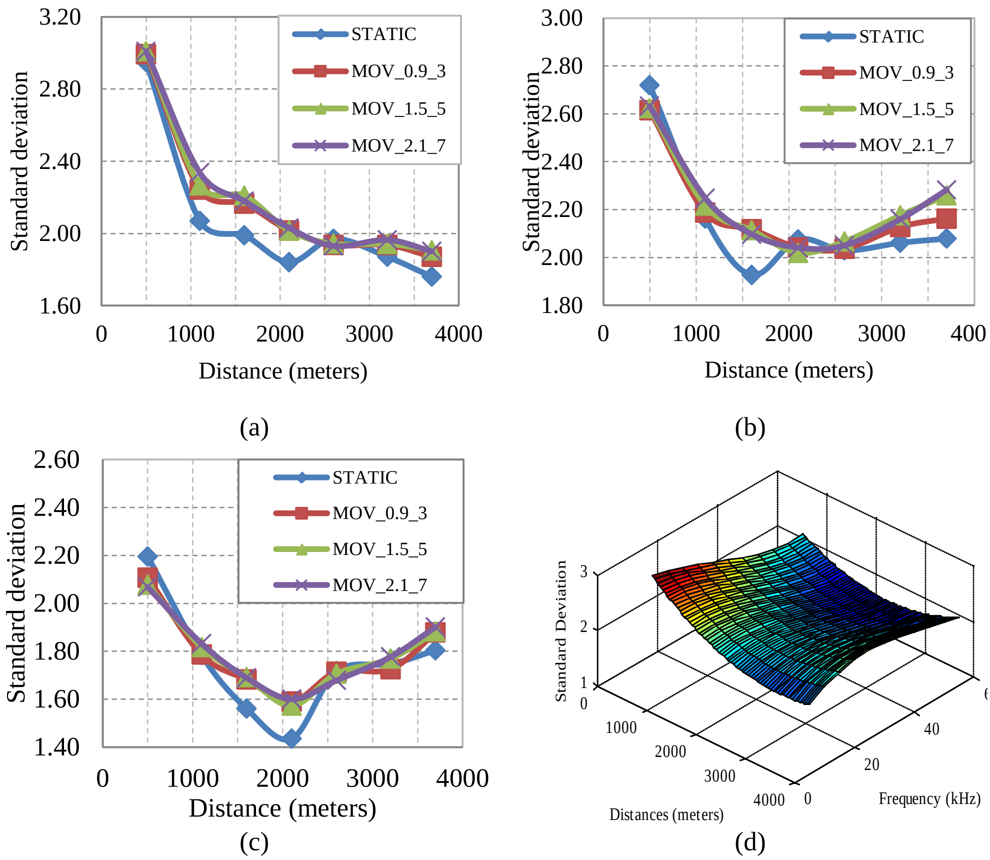

Figure 4.12 Standard deviation of attenuation vs. distance with different node movement and frequency ranges. (a) 5-15kHz, (b) 20-34 kHz, (c) 50-75 kHz, (d) Node movement 1.5 meter height, 5 meter range

As it can be seen at Figure 4.12, All the node movement configurations exhibits near identical behavior, where a bigger σ value is found at distances below 1000 m, and for farther distances the σ oscillates from 1.76 to 2.3. In Figure 4.12 (d) we show a 3D graph of one of the node movement configurations (MOV_1.5_5: 1.5 m depth and 5 m range) that represents the standard deviation as a function of distance and frequency. There is a higher difference at 500 meters, and as commented earlier, the remaining values are within a 1.7 and 2.3 (a difference of 0.6) range.

After testing several regression approaches to obtain the corresponding surface fitting that estimates the standard deviation value, we have performed the polynomial approach represented in expression (5) where d and f represent distance and frequency values, respectively.

The fitting accuracy is represented with an R^2 of 0.9804.

$$\sigma(d,f) = k_1 d^3 + k_2 d^2 f + k_3 f^2 d + k_4 d^2 + k_5 df + k_6 f^2 + k_7 d + k_8 f + k_9 \tag{4-5}$$

$$k_1 = -0.06468, k_2 = -0.01726, k_3 = -0.1214, k_4 = 0.1794,$$
$$k_5 = 0.1477, k_6 = -0.1277, k_7 = 0.07606, k_8 = -0.116, k_9 = 2.013.$$

So, finally, we have determined the mean and standard deviation values of a log-normal distribution that properly represents the same behavior as the Bellhop acoustic propagation model, taking into account the transmission loss variability induced by environmental scenario parameters, and the node movement typically found in underwater deployments.

4.4 Implications for Network Planning

The apparent match between the results of deterministic and statistical models motivates SPM use for network design and analysis via simulation. Consider, for example, network simulation over a prolonged interval of time that spans varying propagation conditions and involves the transmission of a large number of data packets over multiple hops. If deterministic modeling is used, each packet transmission requires one execution of the Bellhop ray tracer, which soon becomes excessively long for a growing number of data packets (assuming 5 minutes for each Bellhop run and a single frequency, simulation of 100000 packets would take about a year). Although the DPM offers an exact solution for the particular geometry observed at any given moment in time, its execution makes the simulation times unaffordable for benchmarking and testing of the upper layer protocols.

In contrast, a statistical model can take several hours to compute (40 hours in the example we presented) a particular network scenario, but this would be needed only once for a network scenario. After that, for a particular simulation run, each packet transmission only requires a single call to a Gaussian random number generator to determine the transmission loss. Moreover, if the network topology changes slightly, or if a new node is added, the statistical model needs to be augmented only by the corresponding set of nominal parameters (mean and standard deviation for the newly created links).

Most importantly, the statistical model can easily be used to assess transmit power allocation that will guarantee successful data packet reception with a desired level of performance (e.g. link reliability). Namely, the SPM can easily be used to calculate the transmission loss values that are not exceeded with a given probability. For example, a 90% transmission loss is that value which is not exceeded for 90% of the time, i.e. in 90% of channel realizations. In Figure 4.13 we show three link reliability levels, corresponding to channel realization probabilities of 50%, 75%, and 90%, that will assess the transmission power required to guarantee the destination node reachability with a specific probability.

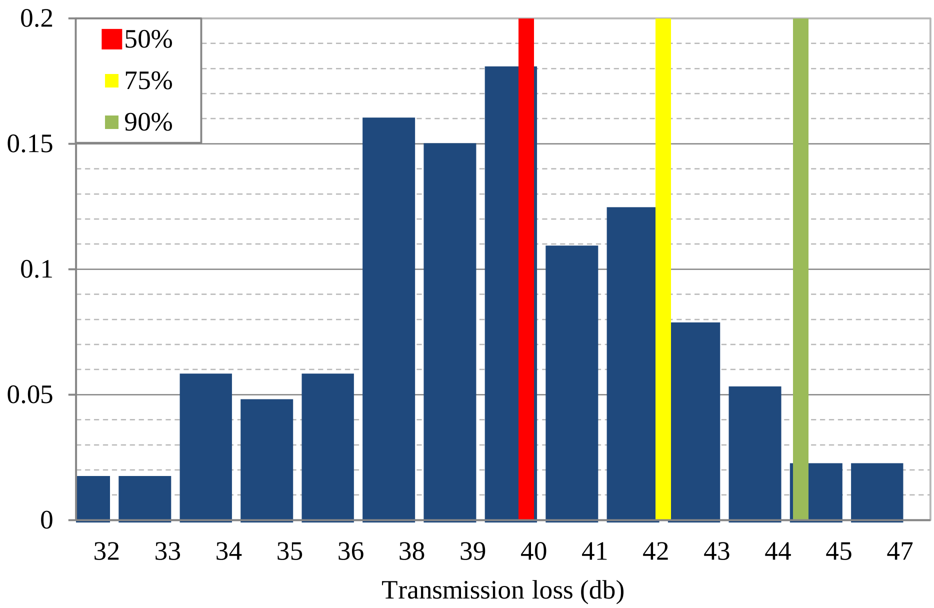

Figure 4.13 The transmission loss value that is not exceeded with a given percentage probability (50%, 75%, 90%)

Figure 4.14, shows 50% and 90% transmission loss for our example system. We observe a good match between the values predicted by the deterministic model and those of the statistical model. Note that the X% values of the SPM are computed analytically, based only on the knowledge of the mean and standard deviation.

The availability of X% values is significant for determining the transmit power necessary to achieve a certain level of performance. Typically, network planning is based on the nominal ray trace, i.e. on the 50% transmission loss to which some margin may be added. If transmit power allocation is based on a different value, say 90% transmission loss instead of the nominal 50%, data packets will be more likely to reach their destinations. More power will be needed at the same time, but the overall network performance may improve. We say may improve, because a higher transmit power also implies higher levels of interference. The resulting performance trade-offs are generally hard to address analytically, and are instead assessed via simulation. A statistical propagation model that directly links the transmit power to the X% transmission loss then becomes a meaningful and useful tool for system design.

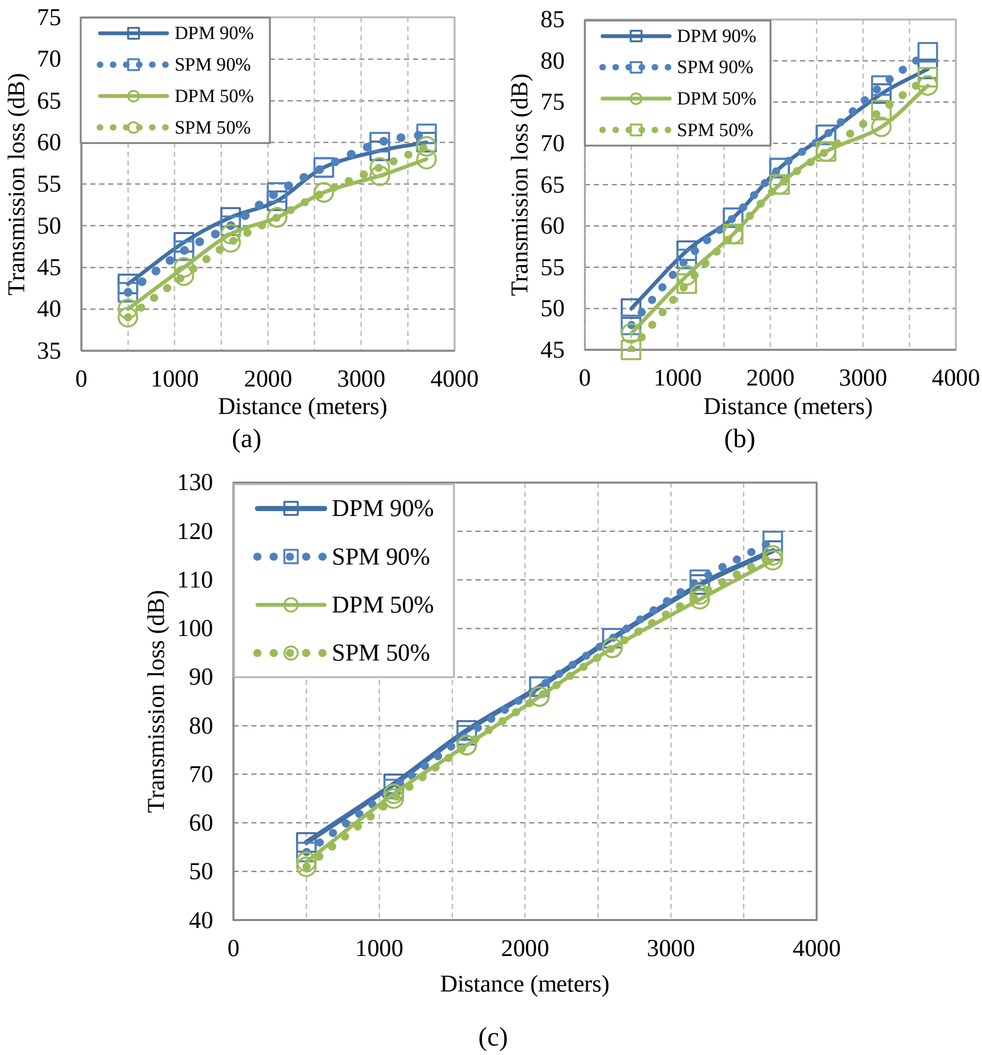

Figure 4.14 The Transmission loss value that is not exceeded with a given probability (50%, 90%) is shown vs. distance

4.5 Conclusions

Large-scale design of an underwater acoustic network requires a judicious allocation of the transmit power across different links to ensure a desired level of system performance (connectivity, throughput, reliability, etc.). Because of the inherent system complexity, simulation analyses are normally conducted to assess the performance of candidate protocols under different resource allocation policies. These analyses are often restricted to using deterministic propagation models, which, although accurate, do not reflect the random time-varying nature of the channel.

While in principle it is possible to examine the network performance for a large set of perturbed propagation conditions, the computational complexity involved in doing so is extremely high. To facilitate network simulation in the presence of channel fading, we investigated a statistical modeling approach. Our approach is based on establishing the nominal system parameters for a desired deployment location (water depth, sediment composition, operational frequency range) and using ray tracing to compute an ensemble of transmission losses for typical inter-node distances. An ensemble is generated by considering a set of perturbed surface conditions, defined by varying wave activity (height, period). The so-obtained ensemble is then used to determine the statistical parameters of a hypothesized log-normal distribution of the transmission loss. For a representative example of a small network operating in a 5 km x 5 km area with inter-node distances ranging between 500 m and 4 km, it was found that the mean can be well approximated as a linear function of the logarithm of distance, while the variance can be modeled as constant over given ranges of distances. Models that are more elaborate and more accurate than the lognormal one can also be developed using this approach.

A statistical model of this type enables computationally-efficient inclusion of fading effects into a network simulator. Namely, to assess the average system performance, network operation has to be simulated over a large set of channel realizations (e.g. varying surface conditions). Whereas repeated computation of the ray trace for different hops that each of the data packets traverses in a given network may be computationally prohibitive, statistical modeling requires only a single call to the Gaussian random generator for each packet transmission. The overall simulation time is thus considerably reduced, allowing a system designer to freely experiment with varying protocols and resource allocation strategies in an efficient manner. The ultimate goal of such computational experiments is to choose the best upper-layer protocol suite and relate the necessary system resources (power, bandwidth) to the propagation conditions, i.e. to the statistical parameters of the transmission loss (e.g. X% value), which can in turn be easily generated using the proposed method of statistical modeling.

Chapter 5
Impact of Propagation Models on Higher Layer Protocol Performance

5.1 Introduction

In order to alleviate the complexity constraint, in the previous chapter we proposed a statistical prediction model based on the Bellhop ray tracing tool that reduces its complexity and achieves similar levels of prediction accuracy. So, we will be able to perform network modeling with a reasonably high accuracy level and low computational overhead.

Modeling tools and a lot of variations around them lead to the hard task of comparing two different proposals unless they are implemented on the same platform. And, even in this case, the simulator should be as realistic as possible to the real environmental conditions. Otherwise, the results will lack accuracy, and empirical testing, at least in scale-down experiments, should be done before releasing the final implementation of the underwater nodes, reducing the power of simulation tools for predicting real network behavior.

At simulation time, when we define the parameters of a network scenario and the location where network nodes would be deployed, we may use a simple assumption through general scenario parameters or define those scenario parameters that will have a direct influence in the acoustic propagation behavior. For example, we may decide to use a simple scenario where the sound speed propagation is considered as a fixed value of 1500 m/s, with a two-dimensional deployment area (depth is not considered) and a simple acoustic propagation approach like the one proposed by Thorp [6] to evaluate the performance of a point-to-point link between two nodes. On the contrary, we could define a more detailed network scenario by including, among others, the scenario world location with bathymetry and floor sediment composition that will affect the way sound propagation is reflected/absorbed on the ocean floor. Also, the water temperature will depend on both the latitude and longitude of network scenario and the season of the year. This fact, together with the water salinity and the depth, may change the sound speed between 1450 and 1540 m/s. There are other important factors that may change sound propagation behavior, such as the well-known ocean wave influence which is different for shallow and deep waters, or the noise produced by ships, biological activity or shoals. All of these scenario parameters should be taken into account in order to develop detailed acoustic propagation models for UWSN, so modeling higher-level network protocols will be aware of network scenario conditions, and the obtained simulation results would be closer to the ones obtained in the experimental previous chapter.

In this work, we will review several acoustic propagation models from simple approaches to the more accurate ones, and observe their behavior when different network scenario parameters are changed (i.e., wave activity), so we can determine their sensibility to environmental network scenario parameters. Then, we will choose the most appropriate acoustic propagation model in terms of accuracy and low-complexity in order to analyze the performance behavior of different MAC protocols, and also check how the scenario environmental changes impact their network performance in terms of throughput, delay and collisions. From the results obtained in this study, we will appreciate (a) the importance of defining an accurate and low complexity propagation model, and (b) the sensibility of higher layer protocols to the time-varying environmental scenario conditions.

5.2 Propagation Model Evaluation

In this section, we will analyze the behavior of different propagation models when simulating an underwater wireless sensor network deployed in a specific network scenario location. We will study both performance results and sensibility under different network scenario parameters. For this purpose, we will describe the characteristics and parameters associated to the network scenario, the MAC protocol we will employ, and the traffic load characterization.

5.2.1 Scenario Deployment

Although a network deployment can be done inserting and configuring node by node into the OPNET Simulator, it can be a monotonous task where connectivity is hard to check. An auxiliary tool has been developed to deploy a network with certain kinds of properties.

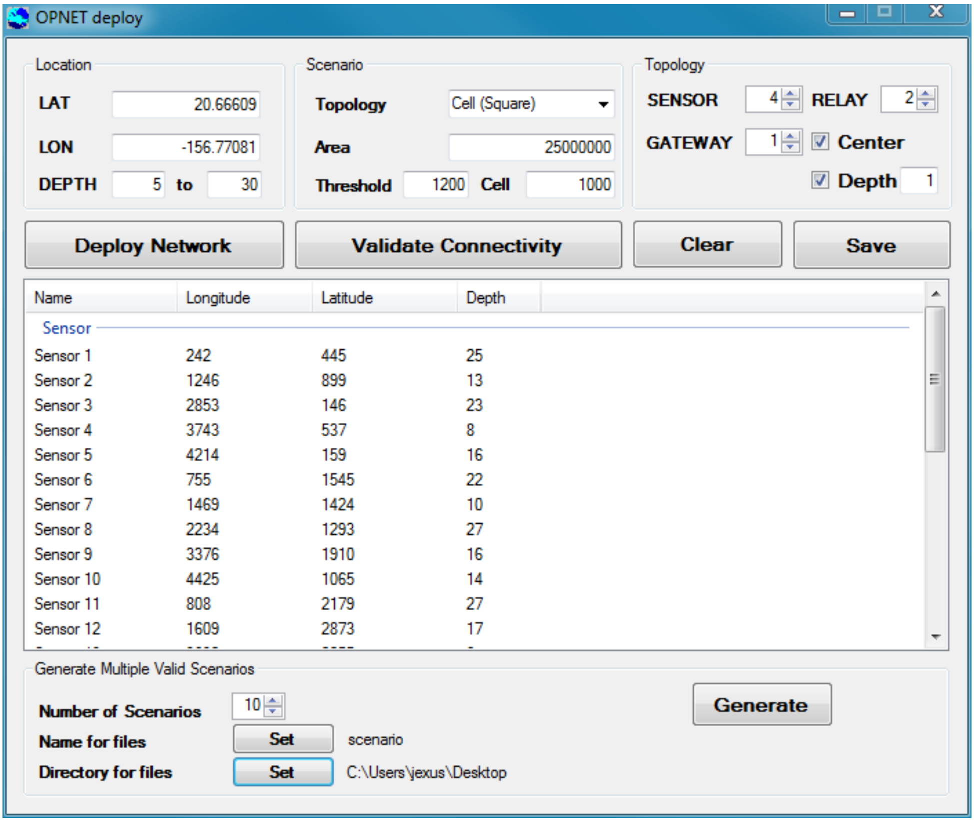

Figure 5.1 Network deployment tool

In this tool called “OPNET deploy” (Figure 5.1) we can choose and select from several parameters explained next:

- The location where the network is deployed in GPS coordinates: latitude, longitude and depth range of the network nodes.
- The size of the “Area” of the network, the size of each “Cell” (if this option is selected) and the maximum distance “Threshold” that two nodes can be apart from the other.
- The quantity of nodes of each type: “Sensor” (nodes that generate data and transmit it, and retransmit data from other Sensors), “Relay” (nodes that only retransmit data) and “Gateway” (the network sink that receives data). If there is only one Gateway, we can choose to set its position in the “Center” of the Area and set a fixed “Depth”.

- The “Random” or “Cell Square” topology: in the first one, the nodes are deployed randomly in the entire Area. If we choose “cell”, the area is divided in the square cells (with the cell size selected) and deploys a node with a random position within each cell.

- Once the network is deployed, we have the chance to validate the network’s connectivity using the selected Threshold value (signal coverage distance)so that there are no isolated nodes or a divided network without a connection between all the nodes. In this way, every node will have a path toGateway.

- Depending on the Area size introduced, the size of the Cell and the distance Threshold, many deployments must be created before achieving one with a valid connectivity. This is an option to generate one or more scenarios with just one click.

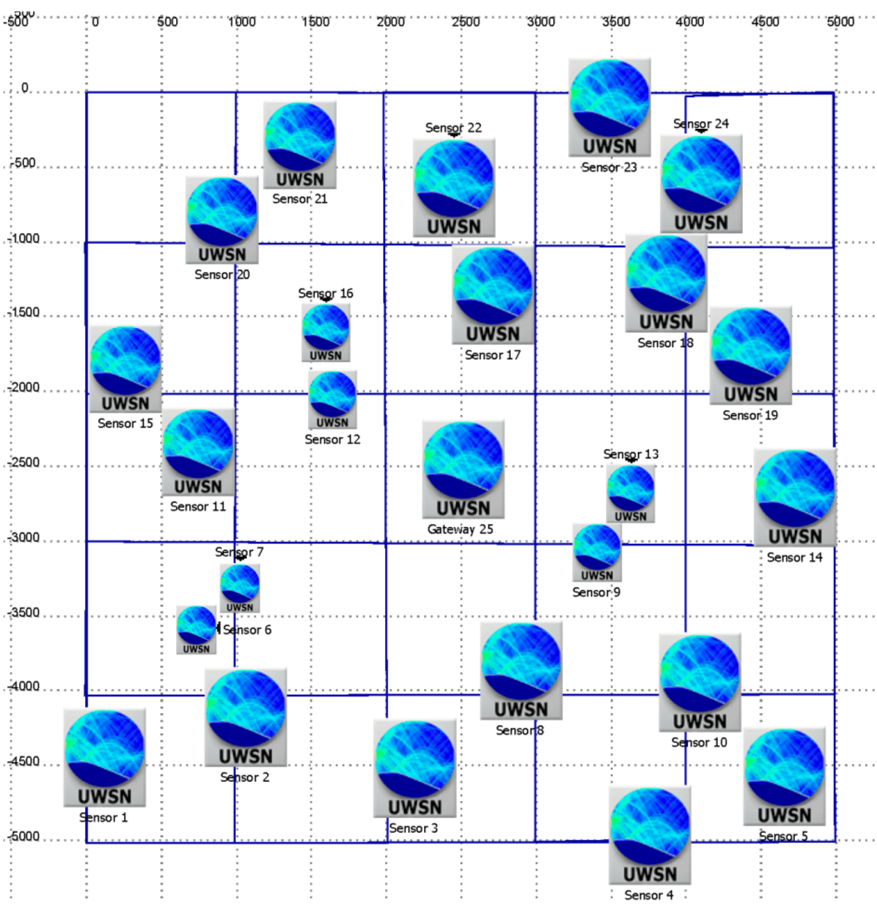

Figure 5.2 Network deployment 2D

Using this tool, the network scenario deployment in this simulation is created in Figure 5.2 (surface view). The volume size is defined as a cube of 5000 × 5000 × 50 m (Length × Width × Depth); the covered area is divided in cells of 1000 × 1000 m. The gateway (sink node) is always placed in the middle cell at a fixed depth of 10 m. Then we put one node per cell at a random position inside the cell, as well as a random depth (this parameter will be bounded by the scenario bathymetry). Once all the nodes are deployed, network connectivity is checked by guaranteeing that every node has a path to the gateway (one-hop or multi-hop paths) and that there are no isolated subnetworks or nodes. Using the same area and cell size, ten different random scenarios have been built and validated for their use in simulation tests.

In Figure 5.3, a 3D representation of the network scenario is shown. It is located at coordinates 39°48'13.14"N and 0°4'34.53"W (Valencia, Spain). This view lets us appreciate the different node depths, close to the surface, medium depth and at the scenario bottom. We have fixed the wave activity with waves of 2 m height and 80 m length. The network scenario floor is composed of gravel. All of the scenario and environmental parameters were taken from National Geophysical Data Center databases in [18] and [33] related to the specific global coordinates of our network. This example could represent a typical network scenario of shallow waters with a low altimetry shape where the bottom relief is deeper as it moves away from the coast.

Table 5.1 shows the main parameters used in the simulations.

Parameter	Value
Propagation models	THORP, MMPE, BELLHOP
# Sensors	24
# Gateways	1
Month	Annual Average
Wave height (m)	2
Wave length (m)	80
Frequency (kHz)	10
Scenario depth (m)	50
Global load (packets/s)	0.16 to 4
Data packet size (bits)	1024
Control packet size (bits)	24
Bandwidth (kbps)	5
# Scenarios	10
Simulation time (s)	3600

Table 5.1 Simulation and network scenario parameters

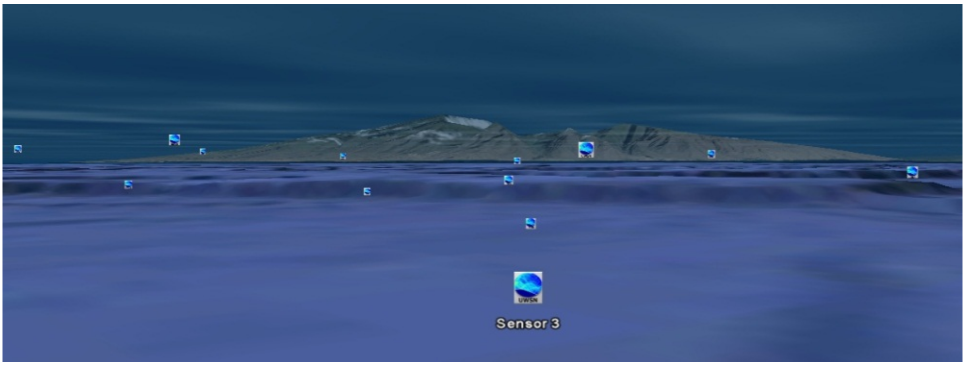

Figure 5.3 Network deployment 3D (Google EarthTM)

With respect to the network traffic load, we proposed a constant bitrate approach where every sensor node generates fixed length data packets at a generation rate defined with an exponential distribution. All sensor nodes in the network will send packets towards the gateway node, so we will obtain a hot-spot traffic pattern, where all the packets are delivered to the same destination.

In this section, we will consider a One-Hop (OH) network topology, where all network nodes are able to reach the gateway in one hop, using the CSMA/CA MAC protocol. The power transmission is constant in all nodes and it is calculated as the energy required by the farthest nodes (the ones in the perimeter) to reach the gateway, considering Thorp’s attenuation model. That means that in Thorp’s simulation, these nodes will always reach the gateway, but in both MMPE and Bellhop, reachability it is not always guaranteed, mainly due to the more realistic assumptions about the acoustic propagation. So, the time-varying acoustic signal attenuation may produce packet losses due to the lack of signal strength at the gateway, which is supposed to have an impact on network performance.

In Chapter 4, Figure 4.11 (a) the transmission range of node #1 is fixed (are covered by the circle) during the entire simulation, indicating the set of nodes that always receives the transmissions from node #1 (in particular the gateway node) using Thorp’s propagation model. However, in Figure 4.11 (b), the MMPE and Bellhop models define the transmission range with two dashed circles. The smaller circle represents the nodes that always receive node #1 transmissions; meanwhile, the other nodes included in the bigger circle (those that are out of the smaller one) may receive the transmissions with a certain probability defined by the propagation model.

5.2.2 Evaluation Results

The simulation framework used is the one describe in Chapter 3. The performance metrics we will show are the Goodput and the Average Packet Delay:

Goodput is defined as the throughput found at the application layer (note that at the top of MAC layer we have no other network layers, only the application), so only data packets that successfully arrive at the gateway node are taken into account. This also means that control packets like RTS, CTS, and ACK are not considered in the goodput computation.

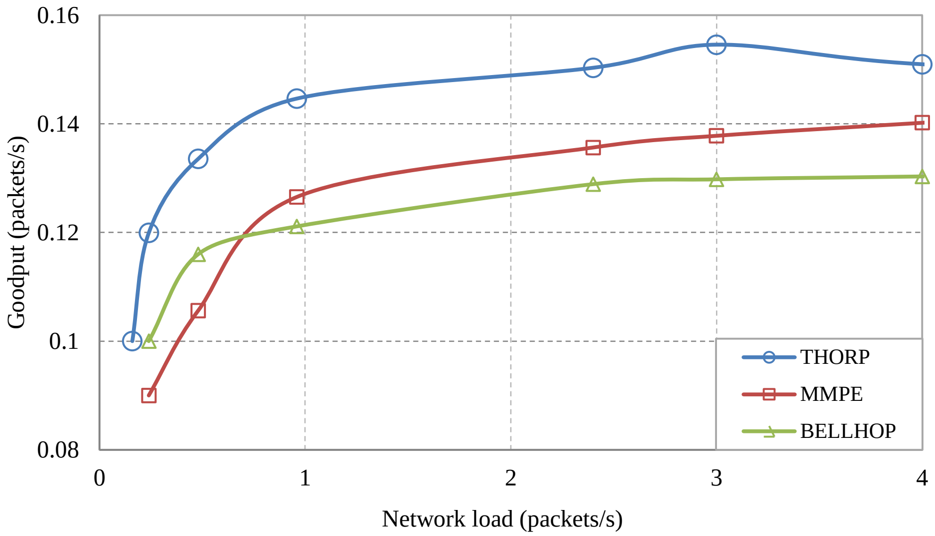

Figure 5.4 Average goodput with different acoustic propagation models

In Figure 5.4, the average goodput from 10 random scenarios (as defined in the previous subsection) is shown. As can be observed, the results appear to follow the same pattern with clearly different goodput values depending on the propagation model used. The Thorp propagation model gets the best performance, MMPE is estimably worse and finally Bellhop is the one with the worst behavior. This behavior agrees with the prediction stated before as the connection links between the nodes that are farther from the gateway suffer the consequences of using more accurate propagation models like MMPE and Bellhop. In other words, Thorp's model always provides link reachability to network nodes during the simulation; however MMPE loses communication due to the wave effect and this leads to reduced goodput performance. This behavior is even more pronounced with the Bellhop model, where signal attenuation is calculated in a more accurate way, resulting in a higher number of dropped packets during the n-way handshaking process of the CSMA/CA protocol.

Average Packet Delay is defined as the average delay incurred by a packet in reaching its destination. This delay is calculated from the time when the MAC layer gets the packet at the source node to start delivery until the instant when this packet is correctly received at the gateway node. The average packet delay will strongly depend on the channel propagation delay. So, the propagation delay (T_{prop}) depends on the distance (d) between sensor and gateway nodes, the specified inter frame delay (SIF), and the sound speed propagation (T_{ssp}) that may change with node depth and water temperature, as shown in Figure 5.5 obtained through databases [31] and [42].

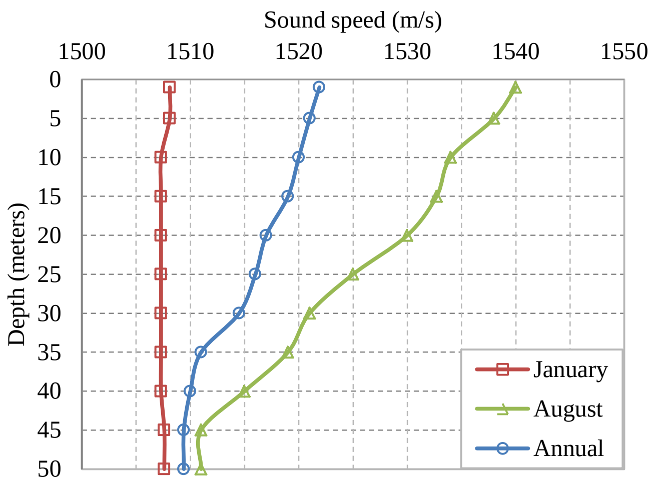

Figure 5.5 Valencia's (scenario location) annual average sound speed as a function of node depth

In expression (5-1), we define the delay experienced by a packet delivery in one-hop transmission without network contention/interference, taking into account the CSMA/CA protocol handshake and the distance and sound speed parameters.

$$T_{prop} = d\,/\,T_{ssp},\ T_{pkt} = packet\_size\,/\,data\_rate,\ SIF = Inter\_Frame\_Delay$$
$$Delay = T_{prop}\,(RTS) + T_{pkt}\,(RTS) + SIF + T_{prop}\,(CTS) + T_{pkt}\,(CTS) + SIF + T_{prop}\,(DATA) + T_{pkt}\,(DATA) \quad (5\text{-}1)$$

Therefore, the experienced packet delay sent by a sensor located 1500 m away from the gateway node and with 10 m depth would be:

$$T_{prop}\,(RTS) = T_{prop}\,(CTS) = T_{prop}\,(DATA) = 1{,}500\ /1{,}520\ = 0.9868\ s$$
$$T_{pkt}\,(RTS) = T_{pkt}\,(CTS) = 24/5{,}000 = 0.0048\ s$$
$$T_{pkt}\,(DATA) = 1{,}024/5{,}000 = 0.2048\ s \qquad (5\text{-}2)$$
$$SIF = 0.02048\ s$$
$$Delay = 3 * 0.9868 + 2 * 0.0048 + 0.2048 + 2 * 0.02048 = 3.21576\ s$$

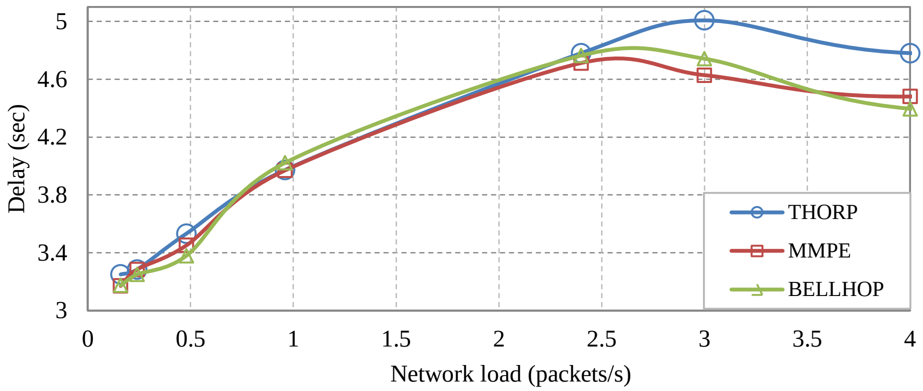

Figure 5.6 Average packet delay with different acoustic propagation models

The results shown in Figure 5.6 reveal almost the same delay for all propagation models until the network enters a saturation state, where MMPE and Bellhop seem to have better results. At first sight, this may lack coherence, but if we take a closer look at the distribution of packets received at the gateway from the different source nodes, we will appreciate that with MMPE and Bellhop, the gateway receives less packets from the farther nodes as they are more affected by the attenuation variability introduced by these propagation models, as shown before in Figure 4.11. Therefore, this is the main cause of the lower overall packet delay with the use of more accurate acoustic propagation models, since the average packet delay decreases.

In the early first tests, it is clear that the propagation model is an important issue to take into account, but now we go a bit further by changing the environmental parameters of the network scenario in order to assess their influence. For that purpose, we will use one of the scenarios used before, fix the network load at 2 packets/s to the point just before network saturation, and introduce two different months, January and August (with different ocean average temperatures), plus six different levels of wave heights (varying surface conditions) from 1 to 11 m heights. The remaining network and environmental parameters are the same as in Table 5.1.

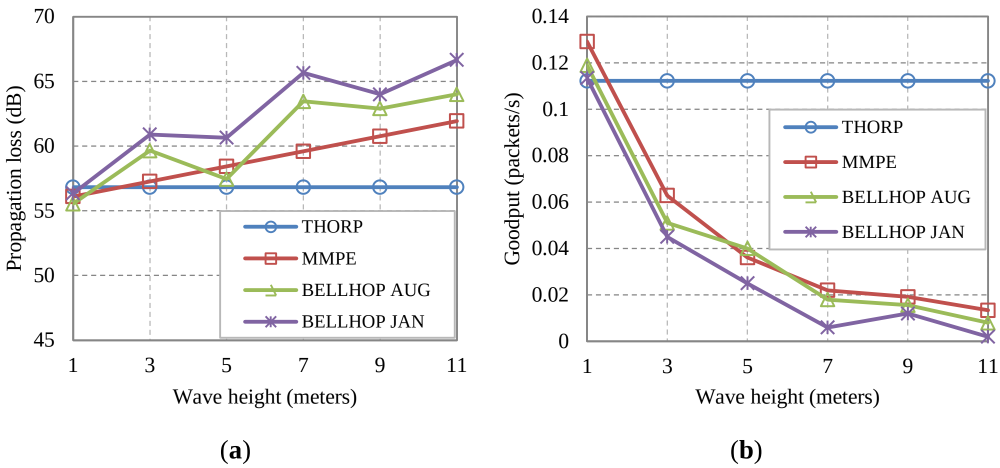

Figure 5.7 Propagation loss (a) and goodput (b) values varying the physical scenario parameters

In Figure 5.7 (a), the acoustic attenuation found between two network nodes, sensor 1 and the gateway, is shown. As expected, Thorp's results remain constant since its equation does not include the effect of the physical parameters. Meanwhile, the MMPE and Bellhop propagation models significantly reduce the obtained goodput, in Figure 5.7 (b), as the wave height increases, i.e., they suffer from the wave motion effect. Also, neither Thorp nor MMPE are affected by the change of season whereas Bellhop shows different results for the months selected. We can appreciate worse performance in January than in August due to the different propagation conditions deriving from the average ocean temperature. The average delay results, including variable physical parameters, are not included here as they exhibit almost the same behavior as in Figure 5.6.

Summarizing this section, we can observe that in addition to having a detailed propagation model, different environmental conditions have a great impact on network performance. This leads us to seriously consider both (a) an accurate acoustic propagation model, and (b) environmental and scenario parameters to obtain reliable simulation results that efficiently predict the real behavior of the sound propagation in a particular network scenario.

5.3 Higher Layer Protocol Evaluation

In the previous section, we found interesting conclusions about the influence of the propagation models. In this section, we are going to evaluate their impact on different higher layer protocols, MAC and routing protocols, using an accurate propagation model like the one defined by Bellhop, and taking into account several physical parameters related to the network scenario and environmental conditions.

In the following evaluation, we will reuse the same network scenarios defined in previous sections but in two different operational modes: One-Hop (OH) and Multi-Hop (MH). In the former, OH, all network nodes are able to directly reach the gateway node (packet destination); whereas the latter mode, MH, some network nodes require relaying their packets through other nodes to reach the gateway.

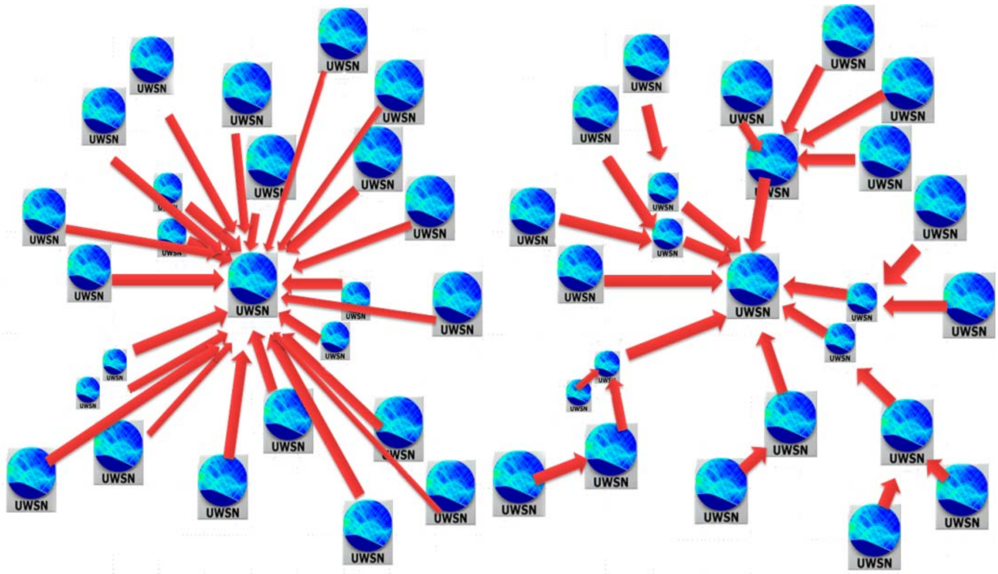

(**a**) (**b**)

Figure 5.8 Network operational modes (a) One-hop, (b) Multi-hop

The difference between the OH and MH modes is focused on the allocated transmission power level to the network nodes, which define their coverage area. So, in OH network scenarios we adjust transmission power level to reach the gateway node from the farthest nodes (the same as in the previous section's simulation experiments). However, for MH network scenarios, we will reduce the power transmission of nodes in such a way that they will be able to only reach the nodes of the adjacent cells. In MH network scenarios, a routing protocol is required to let the packets travel across the network towards their destination (gateway node). By default, in MH network scenarios, we define a static routing protocol. In Figure 5.8, we can see the connections between nodes in both operational modes.

5.3.1 Mac Protocols

In the first test we choose two MAC protocols: CSMA and CSMA/CA. Although they seem to be very similar approaches, CSMA is a simple version with no signaling to handle a packet transmission, meanwhile CSMA/CA is a 4-way handshake protocol as defined in Chapter 2.5.

Our purpose is to analyze how these MAC protocols tackle a network deployment with different power transmission policies, clearing up where it is worth focusing the efforts in terms of power consumption, throughput, packet delay, etc. The simulation parameters are the same as in Table 5.1, increasing the global load up to 12 packets/s.

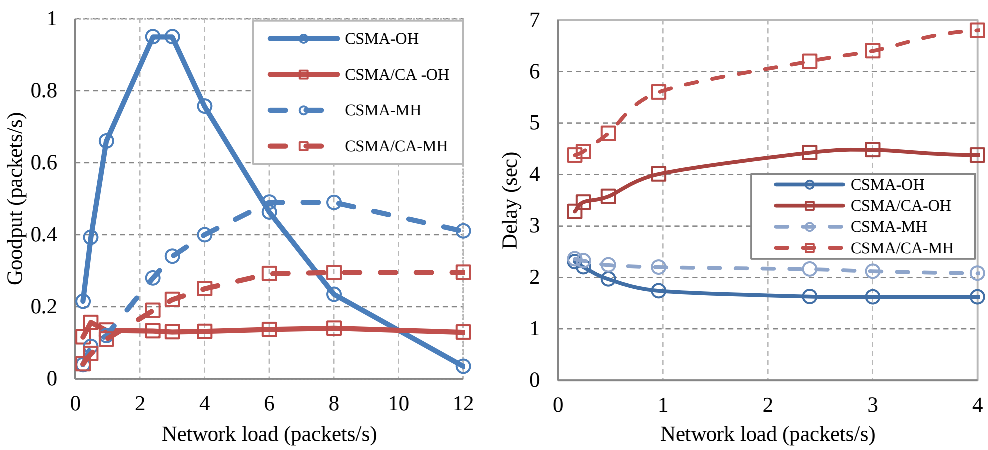

(a) **(b)**

Figure 5.9 Goodput (a) and delay (b) of selected MAC protocols in OH and MH modes

In Figure 5.9 (a), we can see that CSMA-OH soon reaches its highest performance, and after the saturation point it degrades goodput performance very quickly, reaching near the network starvation state. However, CSMA-MH follows the same pattern with a smoother curve. This behavior in the OH scenario can be easily explained because at lower loads the gateway receives more or less the same number of packets from all the network nodes, while in MH scenarios the effect of hot-spot traffic pattern leads to unbalance this behavior, and as a consequence, reduces network load in the gateway neighborhood.

In turn, the CSMA/CA evolution is similar in both strategies, quickly reaching its best performance and maintaining it despite increasing the load; and it has a better overall result in the MH strategy due to the same reasons mentioned before. It is important to remark that at higher network loads, in all cases but especially in MH, sensors closer to the gateway have more chances of achieving successful data packet transmissions than farther nodes (no fair resource sharing due to a hot-spot traffic pattern and the inherent large propagation delay).

From these results, we can state that the MH strategy has overall better performance, and at the same time it is more energy efficient since it is able to reduce energy demands to half of those required by OH. Also, it was observed that those nodes located at the scenario surroundings will have less probability to successfully deliver packets to the gateway. Therefore, this issue opens the way to define routing protocols that will balance the overall packet delivery rate between all the sensor nodes independently of their location.

Now, we take a look at the delay behavior shown in Figure 5.9 (b). As stated in Equation (5-1), the CSMA/CA delay is the result of the acoustic propagation time and the transmission time of the different packets involved in the handshaking, meanwhile in CSMA we only send DATA packets so it is expected that it gets smaller delays. As shown in Figure 5.9 (b), CSMA delays are slightly higher in MH than in OH. This result obeys the fact that the signal propagation delay between a source node and the gateway is typically smaller than the sum of the propagation delays of the paths followed to reach the gateway node, plus the time required to send at least *n* data packets (where *n* is the number of hops to reach the gateway) instead of one.

$$\begin{gathered} OH\text{-}Delay = T_{prop}(O) + T_{pkt}(DATA) \\ MH\text{-}Delay = T_{prop}(M1) + T_{prop}(M2) + 2 * T_{pkt}(DATA) \\ T_{prop}(O) \leq T_{prop}(M1) + T_{prop}(M2) \end{gathered} \tag{5-3}$$

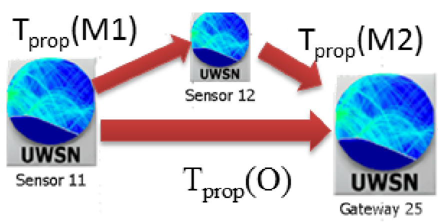

Figure 5.10 Signal propagation times: OH vs. MH

In Figure 5.10, we show an example involving two network nodes and the gateway. The propagation time from sensor 11 to the gateway used to be smaller than the propagation from sensor 11 to 12 plus the propagation from sensor 12 to the gateway. In the event where the OH and MH strategies suffer the same propagation delay, the MH mode would require two data transmission cycles, so the overall packet delay is always longer than in the OH strategy. This fact has greater influence in n-way handshaking protocols, like CSMA/CA, where for each data packet transmission (each hop), *n* packet propagation delays are required, increasing the overall packet delay a lot.

The CSMA/CA protocol shows more stable behavior in terms of goodput performance in OH network scenarios, but environmental conditions and the influence of propagation time on the overall packet delay dramatically affect handshaking protocols. On the other hand, the CSMA protocol maintains the average packet delay low and stable in both OH and MH strategies, since no handshaking is performed to complete one packet delivery. In Figure 5.9 (b), CSMA protocols exhibit higher average packet delay at very low network loads, decreasing as the network load increases. This behavior is due to the hot-spot traffic pattern, since as the network load increases the nodes closer to the gateway are the ones with higher delivery rates and, at the same time, lower packet delays (signal propagation delay), resulting in a reduction of the average packet delay.

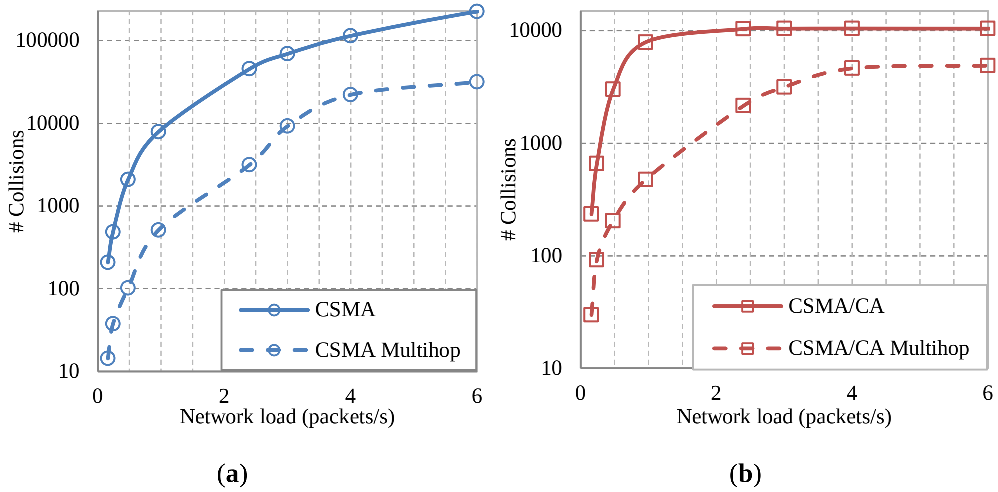

Figure 5.11 Collisions one hop vs. multihop (a) CSMA, (b) CSMA/CA

Finally, another gauge to measure the power consumption in the network is the packet collision statistic. In Figure 5.11, we show CSMA and CSMA/CA protocols with both OH and MH network configurations. As expected, CSMA shows a much higher number of collisions, leading to an increasing number of packets lost, increasing the overall wasted energy. However, CSMA/CA shows better performance, arriving at a constant number of collisions just after the network entered in saturation. In both cases, the number of collisions is highly reduced with the MH approach.

5.3.2 Routing Protocols

In this subsection, we perform a simple simulation experiment with a particular MAC Protocol in combination with different routing policies, in order to assess their behavior under different scenario environmental conditions. We propose the DACAP MAC protocol since it defines some crosslayer support for routing protocols, and we want to quantify the benefits of crosslayer approaches when the scenario environmental conditions change. So we will test the behavior of the DACAP MAC protocol with two routing protocols, a static routing protocol (always supplies the neighbor node that is closest to the gateway) and the FBR routing protocol. Also, we will include two different propagation models in our experiments, Thorp's and Bellhop. The simulation parameters will be the ones at Table 5.1 except for: the propagation models, we only use Thorp's and Bellhop, the global network load that is fixed to 3 packets/s, and the MH network scenario configuration.

Figure 5.12 depicts and interesting behavior of the DACAP protocol in terms of goodput performance. In addition, there is a clear indication that at the routing layers, the environmental conditions (wave activity) of the network scenario may also considerably impact the results of network performance.

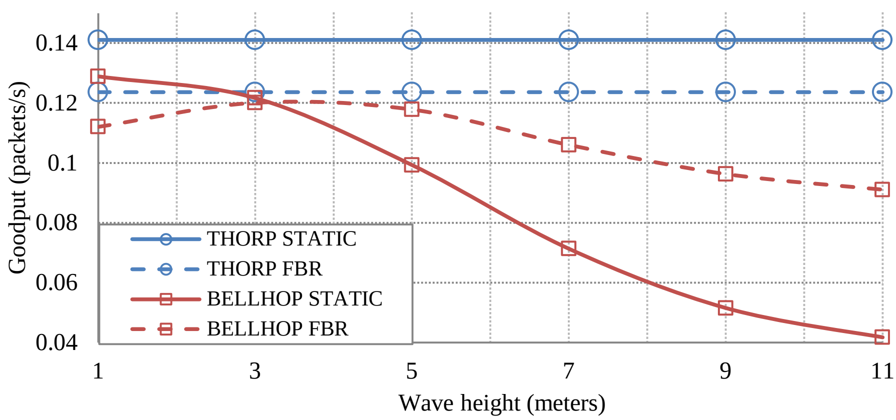

Figure 5.12 Goodput results with DACAP + Routing using two different propagation models

As shown in previous results, the Thorp propagation model does not take into account environmental conditions, so it plots a constant goodput value. As expected, the static routing protocol gets better goodput results because FBR has an extra waiting time in order to accept more than one CTS, but as every node has always the same reachable nodes in its neighborhood, it always chooses the same node to reach the gateway; that is the reason why using static routing under ideal conditions is a better option. If we use Bellhop, the static alternative loses performance as the attenuation grows due to the physical changes. Meanwhile, FBR performance is not so affected under worse conditions as it can dynamically change the routing paths when a connection link is lost.

5.4 Conclusions

One of the main difficulties in comparing and validating the performance of different UWSN proposals is the lack of a common standard to model the acoustic propagation in the underwater environment. In this chapter, we analyzed several underwater acoustic propagation models from a simple approach to more detailed and accurate models in order to study whether differences between them may seriously impact the performance evaluation of higher layer protocols. As a first conclusion, we found that accurate and low-complexity propagation models are required for network simulation in order to obtain reliable results attained to the specific scenario and environmental parameters.

Also, we perform several simulation experiments to determine the sensibility of higher layer protocols (MAC and routing protocols) to propagation models and scenario environmental parameters. From the obtained results, we conclude that: (a) n-way handshake protocols, like CSMA/CA and DACAP suffer from high packet delays, but they show better behavior in terms of goodput and energy consumption; and (b) crosslayer approaches between routing and MAC layers are required to improve network performance, so it is highly recommended to allow routing protocols to get appropriate feedback from the MAC layer about network and environmental conditions found at the physical layer, since in UWSNs we showed the significant impact of physical layer modeling on network performance.

The importance of choosing not only a realistic propagation model but also defining with accuracy the environmental parameters is essential to run the simulation. The first thing to do is to establish the geographic position and the parameters that we can obtain from it to the physical environment conditions, for instance the season of the year or the settled ocean wave motion. It is essential to take into account the role of the physical layer when we design network architectures for UWSNs, to assert that the simulation results will be close to the ones obtained in real network scenarios.

Chapter 6
Conclusions and Publications

6.1 Conclusions

Throughout this thesis, several contributions have been made to the area of Underwater Wireless Sensor Networks. The main purpose of this research was to develop a simulation framework to be able to evaluate Underwater Wireless Sensor Networks with a realistic approach, so that the results can be inferred into real scenario networks with the same performance.

There are some approaches, but there is no standard yet as it is still a novel research field. Therefore, it is time to establish the basis of acoustic signal transmission in underwater networks. An entire study of the state of the art has been done and different propagation models were tested, analyzing the behavior under different environmental conditions, and evaluating MAC and Routing protocols.

We now proceed to summarize the most relevant contributions of this work:

- Study of the state of the art in Underwater Wireless Sensor Networks following a bottom-up review of the network layers. Implementation of several tools and techniques to evaluate UWSN.

- Analyze the behavior of Acoustic Link Models in the underwater environment, including different locations, effect of ocean waves, node movement, depths of the transmitter and receiver nodes.

- Create a simulation framework based on the commercial tool OPNET modeler, and the realistic acoustic prediction tool Bellhop Ray tracing, with an easy to use interface for non-technical users and scalable framework for developers, tested in different world locations to evaluate its capabilities.

- Study of deterministic propagation models to calculate attenuation in the acoustic link (accurate but unaffordable complexity for existing technology), present alternatives (based on simple algorithms and equations but far from real behavior), and the proposal of a statistical propagation model that offers both an easy and fast implementation algorithm and precise results. A statistical propagation model that directly links the transmit power to the X% transmission loss then becomes a meaningful and useful tool for system design.

- Evaluation of higher layer protocols, different MAC and routing methods, were performed addressing the importance of a good definition of the network scenario environment and the usage of an appropriate simulation framework.

Having accomplished all our pre-defined goals, we consider that the final purpose of this thesis has been achieved successfully, and so we conclude this dissertation.

6.2 Publications Related to the Thesis

The research related to this thesis has resulted in twelve publications; we have one journal article (indexed by the Journal Citation Reports (JCR) database), one book chapter, and ten conference papers. We now proceed by presenting a brief description of each of them.

6.2.1 Journals

[LM12] J. Llor, M. P. Malumbres, "Underwater Wireless Sensor Networks: How do Acoustic Propagation Models Impact on Performance of Higher-level Protocols?", SENSORS, January 2012. DOI: 10.3390/s120201312

In this paper we analyze the evolution of underwater acoustic prediction models from a simple approach to more detailed and accurate models. Then, different high layer network protocols are tested with different acoustic propagation models in order to determine the influence of environmental parameters on the obtained results. After several experiments, we can conclude that higher-level protocols are sensitive to both (a) physical layer parameters related to the network scenario and (b) the acoustic propagation model. Conditions like ocean surface activity, scenario location, bathymetry or floor sediment composition, may change signal propagation behavior. So, when designing network architectures for UWSN, the role of the physical layer should be seriously taken into account in order to assert that the obtained simulation results will be close to the ones obtained in real network scenarios.

This journal had an impact factor in 2010 of 1.774, and placed in the first quartile of the Instruments & Instrumentation category.

6.2.2 Book Chapter

[LM10] J. Llor, M. P. Malumbres, “Modelling Underwater Wireless Sensor Networks”, *Wireless Sensor Networks: Application-Centric Design*, Ed. InTech Education and Publishing, Austria 2010.

This chapter will give an overview of underwater wireless networks going-through all the layers with emphasis on the physical layer and how it behaves under different and time-varying environmental conditions.

6.2.3 International Conferences

[LTGM09] J. Llor, E. Torres, P. Garrido, M. P. Malumbres, “Analyzing the Behavior of Acoustic Link Models in Underwater Wireless Sensor Networks”, *4th ACM International Workshop on Performance Monitoring, Measurement and Evaluation of Heterogeneous Wireless and Wired Networks MSWIM*, Tenerife, Spain, October 2009.

In this paper, we evaluate the design of appropriate network architecture for UWSN. These networks are seriously influenced by the specific characteristics of the communication system. In this work, we analyze several acoustic channel models for their use in underwater wireless sensor network architectures. For that purpose, we have implemented them by using the OPNET Modeler tool in order to perform an evaluation of their behavior under different network scenarios.

This conference is indexed as CORE A.

[LMG11] J. Llor, M. P. Malumbres, P. Garrido “Performance Evaluation of Underwater Wireless Sensor Networks with OPNET”, *4th International Conference on Simulation Tools and Techniques Simutools ICST*, Barcelona, Spain, 2011.

In this paper, we proposed a simulator framework for Underwater Wireless Sensor Network modeling based on the OPNET simulation tool. For this purpose, we considered the information provided by global databases (temperature, salinity, etc.) located within the network, which directly affects the sound speed profile. Namely, the bathymetry and floor sediment, the node depth, wave effect, and other factors may affect underwater signal propagation behavior. Taking into account these environmental parameters, the propagation model is calculated using the Bellhop ray tracing tool in order to get the closest representation to the real behavior of the underwater acoustic signal propagation. All these tools are fully integrated with the OPNET Modeler simulator.

[LSM11] J. Llor, Milica Stojanovic, M. P. Malumbres, "A Simulation Analysis of Large Scale Path Loss in an Underwater Acoustic Network", IEEE OCEANS Conference, Santander, Spain, 2011.

In this paper, we study the propagation conditions in an underwater acoustic channel. This propagation is known to vary over time, causing the received signal strength to deviate from the nominal value predicted by a deterministic propagation model. To facilitate large-scale system design under such conditions (e.g. power allocation), we develop a statistical propagation model in which transmission loss is treated as a random variable. We use a ray tracing tool to evaluate varying environmental conditions (surface height, wave activity, small node displacements around nominal locations), an ensemble of transmission losses is compiled which is then used to infer the statistical model parameters. Based on this study, we propose a statistical model useful for higher-level system planning, where simulation is needed to assess the performance of candidate network protocols under various resource allocation policies, i.e. to determine the transmit power and bandwidth allocation necessary to achieve a desired level of performance (connectivity, throughput, reliability, etc.).

This conference is one of the main meetings of scientific and commercial companies on the topic of this Thesis.

6.2.4 National Conferences

[GMLTC09] P. Garrido, M. P. Malumbres, J. Llor, E. Torres, Carlos T. Calafate, "Automating The Modelling And Simulation Life Cycle Of Mobile Ad Hoc Networks", in *XX Jornadas de Paralelismo*, La Coruña, Spain, September 2009.

In this work, a simulation framework is presented supporting both topology modeling and the simulation automation based on the OPNET Modeler simulator. The proposed set of tools is helpful for constructing rigorous MANET scenarios, as well as performing other necessary tasks such as running simulations, extracting the selected data from the simulation results, and generating graphs and reports. These tools have been ported to the most common platforms, and can be executed either sequentially or in parallel with the support of Condor in clusters of workstations.

[LTGM09] J. Llor, E. Torres, P. Garrido, M. P. Malumbres, "Analyzing the Behavior of Acoustic Link Models in Underwater Wireless Sensor Networks", *XX Jornadas de Paralelismo*, La Coruña Spain, September 2009.

In this work, we analyze several model proposals of acoustic channels for their use in underwater wireless sensor network architectures. For this purpose, we have implemented the acoustic channels using the OPNET Modeler tool in order to perform an evaluation of their behavior under different network scenarios. Finally, some conclusions are drawn showing the impact on UWSN performance of different elements of channel model and particular specific environment conditions.

[LSM10] J. Llor, M. Stojanovic, M. P. Malumbres, "An integrated simulation framework for Underwater Acoustic Networks", *XXI Jornadas de Paralelismo - CEDI 2010*, Valencia, Spain, September 2010.

In this paper, we present a simulator proposal integrating the latest discoveries and research. This work includes the information of the location where the network is located (temperature, salinity, etc.) that impacts the sound speed profile changing its value; and also the bathymetry and the floor sediment, in addition to depth, wave effect, etc. To perform the simulator, this whole information provided by global databases is processed using the Bellhop ray tracing tool, all integrated to build a simulation framework based on the OPNET Modeler.

[LM11] J. Llor, M. P. Malumbres, "Statistical Modeling of Transmission Path Loss in Underwater Acoustic Network", *XXI Jornadas de Paralelismo*, La Laguna (Tenerife), Spain, September 2011.

In this paper, we study the propagation conditions in an underwater acoustic channel. This work is based in LSM11 paper presented before.

References

[1] N. Abramson, "Development of the alohanet," *Information Theory, IEEE Transactions on*, vol. 31, no. 2, pp. 119-123, March 1985.

[2] F. Akyildiz, D. Pompili, and T. Melodia, "State of the Art in Protocol Research for Underwater Acoustic Sensor Network," in *Proceedings of the ACM International Workshop on UnderWater Networks (WUWNet)*, Los Angeles, USA, 2006, pp. 7-16.

[3] I. F. Akyildiz, D. Pompili, and T. Melodia, "Underwater acoustic sensor networks: research challenges," *Ad Hoc Networks*, vol. 3, no. 3, pp. 257-279, May 2005.

[4] I. F. Akyildiz, W. Su, Y. Sankarasubramaniam, and E. Cayirci, "Wireless sensor networks: a survey," *Computer Networks*, vol. 38, no. 4, pp. 393-422, March 2002.

[5] S. Azad, P. Casari, C. Petrioli, R. Petroccia, and M. Zorzi, "On the impact of the environment on MAC and routing in shallow water scenarios," in *OCEANS, 2011 IEEE*, Santander, Spain, 2011, pp. 1-8.

[6] L. Berkhovskikh and Y. Laysanov, *Fundamentals of Ocean Acoustics*, 3rd ed. New York, USA: Springer, 1982.

[7] V. Bharghavan, A. Demers, S. Shenker, and L. Zhang, "MACAW: A Media Access Protocol for Wireless LAN's," in *Proceedings of the ACM SIGCOMM Conference*, London, England, 1994, pp. 212-225.

[8] University of Southern California. The Network Simulator 2. [Online]. http://www.isi.edu/nsnam/ns/

[9] N. Chirdchoo, W. Soh, and K. C. Chua, "Aloha-based MAC Protocols with Collision Avoidance for Underwater Acoustic Networks," in *The IEEE Conference on Computer Communications (infocom)*, Singapore , 2007, pp. 2271-2275.

[10] R. Coates, *Underwater Acoustic Systems*. New York, USA: Wiley, 1989.

[11] J. D. Colladon, *Souvenirs et Memoires*. Geneva, Switzerland, 1893.

[12] J. H. Cui, J. Kong, M. Gerla, and S. Zhou, "Challenges: Building scalable mobile underwater wireless sensor networks for aquatic applications," *IEEE Network*, vol. 20, no. 3, pp. 12-18, May-June 2006.

[13] T. B. Curtin, J. G. Bellingham, J. Catipovic, and D. Webb, "Autonomous oceanographic sampling networks," *Oceanography*, vol. 6, no. 3, pp. 86-94, 1993.

[14] Evologics. EVOLOGICS. [Online]. http://www.evologics.de/

[15] L. Freitag, M. Stojanovic, D. Kifoyle, and J. Preisig, "High-Rate Phase-Coherent Acoustic communication: A Review of a Decade of Research and a Perspective on Future Challenges," in *Proceedings of the 7th European Conf. on Underwater Acoustics*, Delft, Netherlands, 2004.

[16] L. Freitag, M. Stojanovic, S. Singh, and M. Jhonson, "Analysis of Channel Effects on Direct-sequence and Frequency-hopped Spread-spectrum Acoustic," *IEEE Journal of Oceanic Engineering*, vol. 26, no. 4, pp. 586-593, October 2001.

[17] C. L. Fullmer and J. J. Garcia-Luna-Acebes, "Floor acquisition multiple access (FAMA) for packet-radio networks," *Computer Communication Review*, vol. 25, no. 4, pp. 262-273, 1995.

[18] GEBCO. General bathymetric chart of the oceans. [Online]. http://www.gebco.net

[19] F. Guerra and P. Casari, "A performance comparison of MAC protocols for underwater networks using a realistic channel simulator," in *OCEANS 2009, MTS/IEEE- Marine Technology for Our Future: Global and Local Challenges*, Biloxi, 2009, pp. 1-8.

[20] F. Guerra and P. Casari, "World Ocean Simulation System (WOSS): A Simulation Tool for Underwater Networks with Realistic Propagation Modeling," in *Proceedings of the ACM International Workshop on UnderWater Networks (WUWNet)*, New York, USA, 2009, pp. 1-8.

[21] A. F. Harris III and M. Zorzi, "Modeling the underwater acoustic channel in ns2," in *Proceedings of the 2nd international conference on Performance evaluation methodologies and tools (ValueTools)*, Brussels, Belgium, 2007, pp. 1-8.

[22] J. Heidemann, Y. Wei, J. Wills, A. Syed, and L. Yuan, "Research challenges and applications for underwater sensor networking," in *Wireless Communications and Networking Conference*, Las Vegas, USA, 2006, pp. 228-235.

[23] S. Ijaz, A. J. Silva, O. C. Rodriguez, and S. M. Jesus, "Doppler domain decomposition of the underwater acoustic channel response," in *OCEANS, 2011 IEEE*, Santander, Spain, 2011, pp. 1-7.

[24] F. Jensen, W. Kuperman, M. Porter, and H. Schmidt, *Computational Ocean Acoustics*. Berlin, Germany: Springer, 1994.

[25] J. M. Jornet. (2008) AUVNetSim: A Simulator for Underwater Acoustic Networks. [Online]. http://sourceforge.net/projects/auvnetsim/

[26] J. M. Jornet and M. Stojanovic, "Focused beam routing protocol for underwater acoustic networks," in *Proceedings of the third ACM international workshop on Underwater Networks*, New York, USA, 2008, pp. 75-82.

[27] D. N. Kalofonos, M. Stojanovic, and J. G. Proakis, "Performance of adaptive MC-CDMA detectors in rapidly fading rayleigh channels," *IEEE Transactions on Wireless Communications*, vol. 2, no. 2, pp. 229-239, March 2003.

[28] P. Karn, "MACA - A new channel access method for packet radio," in *Proceedings of the ARRL 9th Computer Networking Conference*, Ontario, Canada, 1990, pp. 134-140.

[29] S-M. Kim, S-H. Byum, S-G. Kim, and Y-K. Lim, "Characterization of underwater acoustic channel using slowly moving transmitter in shallow water," in *OCEANS, 2011 IEEE*, Santander, Spain, 2011, pp. 1-3.

[30] MathWorks. MATLAB R2009a & MATLAB R2011a. [Online]. http://www.mathworks.com/

[31] METEOSIM. [Online]. http://www.meteosim.com

[32] M. Molins and M. Stojanovic, "Slotted FAMA: A MAC Protocol for Underwater Acoustic Networks," in *Proceedings of the IEEE OCEANS*, Singapore, 2006, pp. 1-7.

[33] NOAA. National geophysical data center, seafloor surficial sediment descriptions. [Online]. http://www.ngdc.noaa.gov/mgg/geology/deck_41.html

[34] OPNET. OPNET Modeler v15.0 Reference Manual OPNET Technologies Inc. OPNET Modeler. [Online]. http:/www.opnet.com/

[35] J. Partan, J. Kurose, and B. Neil Levine, "A Survey of Practical Issues in Underwater Networks," in *Proceedings of the ACM International Workshop on UnderWater Networks*, Los Angeles, USA, 2006, pp. 17-24.

[36] B. Peleato and M. Stojanovic, "Distance aware collision avoidance protocol for ad hoc underwater acoustic sensor networks," *Communications Letters, IEEE*, vol. 11, no. 12, pp. 1025-1027, December 2007.

[37] C. Petrioli, R. Petroccia, and J. Potter, "Performance evaluation of underwater MAC protocols: From simulation to at-sea testing," in *OCEANS, 2011 IEEE*, Santander, Spain, 2011, pp. 1-10.

[38] C. Petrioli, R. Petroccia, J. Shusta, and L. Freitag, "From underwater simulation to at-sea testing using the ns-2 network simulator," in *OCEANS, 2011 IEEE*, Santander, Spain, 2011, pp. 1-9.

[39] D. Pompili, T. Melodia, and I. F. Akyildiz, "A Distributed CDMA Medium Access Control for Underwater Acoustic Sensor Networks," in *Proc. of Mediterranean Ad Hoc Networking Workshop (Med-Hoc-Net)*, Corfu, Greece, 2007.

[40] M. B. Porter and H. P. Bucker, "Gaussian beam tracing for computing ocean acoustic fields," *Journal of the Acoustical Society of America*, vol. 82, no. 4, pp. 1349-1359, October 1987.

[41] M. Porter and Yong-Chun Liu. (2010) Bellhop. [Online]. http://oalib.hlsresearch.com/Rays/index.html

[42] Puertos del Estado. [Online]. http://www.puertos.es

[43] J. A. Rice and W. O. Che, "A Discovery Process for Initializing Underwater Acoustic Networks," in *Sensor Technologies and Applications (SENSORCOMM), 2010 Fourth International Conference on*, Venice, Italy, 2010, pp. 408-415.

[44] ROCKS. Rocks Cluster. [Online]. http://www.rocksclusters.org

[45] S. Rosenbush, R. O. Crockett, and C. Yang, "Sin cables, sin normas y a bajo precio. ," in *Dinero: Inteligencia empresarial.*, 2004, pp. 70-73.

[46] F. Salva-Garau and M. Stojanovic, "Multi-cluster protocol for ad hoc mobile underwater acoustic networks," in *OCEANS*, San Diego, USA, 2003, pp. 91-98.

[47] F. Schill, U. R. Zimmer, and J. Trumpf, "Visible Spectrum Optical Communication and Distance Sensing for Underwater Applications," in *Proceedings of the Australasian Conference on Robotics and Automation*, Canberra, Australia, 2004.

[48] J M. Seppälä, "Simulating Devices With Adaptive Antenna Arrays Using OPNET Integrated With MATLAB," in *Proceedings of the 4th ACM workshop on Performance monitoring and measurement of heterogeneous wireless and wired networks (PM2HW2N)*, New York, USA, 2009, pp. 159-166.

[49] A. Silva, S. M. Jesus, and J. Gomes, "Probe timing optimization for time-reversal underwater communications," in *OCEANS, 2011 IEEE*, Santander, Spain, 2011, pp. 1-8.

[50] K. B. Smith, "Convergence, Stability, and Variability of Shallow Water Acoustic Predictions Using a Split-Step Fourier Parabolic Equation Model," *J. Comp. Acoust. Special Issue of Proceedings of the Shallow Water Acoustic Modeling (SWAM) Workshop, 8* , vol. 9, no. 1, pp. 243-285, September 1999.

[51] Snctools. Snctools for MATLAB. [Online]. http://mexcdf.sourceforge.net

[52] E. Sozer et al., "Direct sequence spread spectrum based modem for under water acoustic communication and channel measurements," in *OCEANS MTS/IEEE*, Seattle, USA, 1999, pp. 228-233.

[53] E. Sozer, M. Stojanovic, and J. Proakis, "Design and Simulation of an Underwater Acoustic Local Area Network, Northeastern University," *Communications and Digital Signal Processing Center*, 1999.

[54] M. Stojanovic, "Underwater Acoustic Communication," in *Wiley Encyclopedia of Electrical and Electronics Engineering*.: John Wiley & Sons, Inc, 2001.

[55] M. Stojanovic, J. Catipovic, and J. G. Proakis, "Phase coherent digital communications for underwater acoustic channels," *IEEE Journal of Oceanic Engineering*, vol. 19, no. 1, pp. 100-110, January 1994.

[56] M. Stojanovic, J. G. Proakis, and J. Catipovic, "Analysis of the impact of channel estimation errors on the performance of a decision feedback equalizer in multipath fading channels," *IEEE Transactions on Communications*, vol. 43, no. 2/3/4, pp. 877-886, February 1995.

[57] A. S. Tanenbaum, *Computer Networks*, 3rd ed. Upper Saddle River NJ, USA: Prentice Hall, 2003.

[58] A. N. Tikhonov and A. A. Samarskii, *Equations of Mathematical Physics*. New York, USA: Courier Dover, 1990.

[59] B. Tomasi, P. Casari, L. Badia, and M. Zorzi, "A study of incremental redundancy hybrid ARQ over Markov channel models derived from experimental data," in *Proceedings of the Fifth ACM International Workshop on UnderWater Networks (WUWNet)*, New York, USA, 2010, p. 8.

[60] R. J. Urick, *Principles of Underwater Sound*, 3rd ed. New York, USA: McGraw-Hill, 1983.

[61] T. J. van der Werff. (2003) 10 Emerging Technologies That Will Change the World. Technology Review (MIT).. [Online]. http://www.technologyreview.com/read_article.aspx?id=13060&ch=infotech

[62] W. van Dorn, *Oceanography and Seamanship*. New York, USA: Cornell Maritime Press, 1974.

[63] University of Wisconsin-Madison. Condor: High Throughput Computing (HTC). [Online]. http://research.cs.wisc.edu/condor/

[64] WOA. World Ocean Atlas. [Online]. http://www.nodc.noaa.gov/OC5/WOA05/pr_woa05.html

[65] P. Xie, J. H. Cui, and L. Lao, "VBF: Vector-Based Forwarding Protocol for Underwater Sensor Networks," in *Proceedings of IFIP Networking*, Coimbra, Portugal, 2006.

[66] G. Xie, J. Gibson, and L. Diaz-Gonzalez, "Incorporating Realistic Acoustic Propagation Models in Simulation of Underwater Acoustic Networks: A Statistical Approach," in *Proceedings of MTS/IEEE Oceans Conference*, Boston, USA, 2006, pp. 1-9.

[67] W. B. Yang and T. C. Yang, "Characterization and Modeling of Underwater Acoustic Communications Channels for Frequency-Shift-Keying Signals," in *OCEANS 2006*, Boston, USA, 2006, pp. 1-6.

[68] H. Yan, Z. Shi, and J. H. Cui, "DBR: Depth-Based Routing for Underwater Sensor Networks," in *Proceedings of the 7th international IFIP-TC6 networking conference on AdHoc and sensor networks, wireless networks, next generation internet (NETWORKING)*, Berlin, Germany, 2008, pp. 72-86.